Printable Low-Cost, Sustained and Dynamic Cell Stretching Apparatus

Thesis Report

Timothy J Wilson

42868068

Bachelor of Engineering

Mechanical Engineering

MACQUARIE
University

Department of Engineering

Macquarie University

November 6, 2017

Supervisor: Dr. Shaokoon Cheng

ACKNOWLEDGMENTS

I would like to acknowledge a number of people who helped me throughout the course of my undergraduate degree and thesis.

First of all my parents who gave me my love of learning and determination to always attempt and finish tasks to the highest standards.

Thank you to Dr. Shaokoon Cheng for giving me flexibility in this thesis. I truly appreciate how much time and attention you have given my research and this project.

Thank you to Joel Raco and Adrian Orellana who provided me with the technical knowledge and insight in to the nuances of 3D printing and the associated processes.

STATEMENT OF CANDIDATE

I, Timothy Wilson, declare that this report, submitted as part of the requirement for the award of Bachelor of Engineering in the Department of Mechanical Engineering, Macquarie University, is entirely my own work unless otherwise referenced or acknowledged. This document has not been submitted for qualification or assessment through any academic institution.

Student's Name: Timothy Wilson

Student's Signature:

Timothy J Wilson (Digital)

Date: November 6, 2017

TABLE OF CONTENTS

INDEX OF GRAPHS

INDEX OF TABLES

INDEX OF IMAGES

INDEX OF FIGURES

ABSTRACT

Cell stretching has been used in modern medicine as a way of treating injury and determining cell properties since the late 1980's. It has always been an expensive and specialised process, performed only in specific laboratories. The high initial set up cost prevents many laboratories from engaging in such research.

This paper explores the development and manufacturing of a low cost bi-directional static and dynamic cell-stretching device. The device was developed to function as a low cost economical solution for modern laboratory equivalents. The device underwent stress and accelerations test with consistent results and strain calculations to show the reliability and consistency of the device.

The device was constructed out of 3D printed PLA and controlled though two stepper motors with open source Arduino programming. This enabled the device to be produced for under AU $400 making it both an economical and sustainable way of producing laboratory equipment. Testing the device has shown that it is more than capable of producing the necessary precision and accuracy to be used in live cell experiments.

The primary objective of this research is to confirm the work done by Samer Toume, Amit Gefen and Daphne Weihs in 2016 research article "Printable Low-Cost, Sustained And Dynamic Cell Stretching Apparatus". This paper has confirmed the accuracy and legitimacy of their research along with some improvement on the original design to allow it to be adapted to new test conditions.

KEY TERMINOLOGY

ABS (Acrylonitrile butadiene styrene)

PLA (Polylactic acid)

PTFE (Polytetrafluoroethylene)

in vitro and *in vivo*

Arduino Hardware

Arduino Software

FOSS (Free and Open-source Software)

RepRap (Self-replicating Rapid Prototype)

FFF (Fused Filament Fabricationn)

ASSUMPTION

The key assumption is that the cell membrane can be connected to a rigid outer supporting structure, which will prevent the cell membrane from deforming during the stretching process.

CHAPTER ONE

INTRODUCTION

It has been know for the better part of three decades that stretching *in vivo* body cells can have a significant positive impact on an individual's health outcomes. Cell stretching has been used since the early 1990's to help patients with osteoarthritis and a range of other injuries (Kaspar et al., 2000).

This methodology functions adequately for cells which can be observed via *in vitro* operations but was inadequate for cells which could not be viewed in their natural state. This led to the development of large-scale laboratory cell stretching devices, which could better simulate an *in vitro* environment in an *in vivo* setting. (Mpkb.org, 2017)

Laboratory cell stretching devices generally fall into three major categories;

- Whether the device stretches the cells bi-laterally or laterally
- If the device has a uniform force distribution or not, and
- If the device is a contact based force or pressure-based force.

Within these major categories there are four primary types of actuating cell-stretching devices, each with their own individual advantages and disadvantages (Shapiro et al., 1994). These are:

- Pneumatic,
- Electromagnetic,
- Piezoelectric
- Optical.

Of these four, Electromagnetic is the most common as it is the simplest to develop and requires the least amount of additional information to operate (Kamble et al., 2016).

The Samer Toume, Amit Gefen and Daphne Weihs cell stretching apparatuses uses motors to drive the upper stretching plate hence Samer Toume, Amit Gefen and Daphne Weihs apparatus is categorized as an Electromagnetic cell stretching device. Samer Toume, Amit

Gefen and Daphne Weihs cell stretching apparatus is categorized as a bilateral, uniform contact based force apparatus.

Modern cell stretching aims at creating the closest to *in vivo* environment in an *in vitor* setting. Currently one of the biggest obstacles to cell testing is the high initial setup cost for obtaining the necessary equipment. In most cases the cost of setting up laboratories designed to monitor cell stretching exceed ten thousand dollars USD (Wang, Yang and Li, 2005).

The high setup cost has slowed the advancement of cell stretching research. Some of these costs are related to the complex biomedical engineering required. The development of a low cost, simple to operate, static and dynamic cell stretching device may help to reduce some of these costs and enable this vital laboratory equipment to become more readily available. (Huang, Mathieu and Helmke, 2010) (Toume, Gefen and Weihs, 2016)

This report investigates the development of printable low cost, static and dynamic cell stretching apparatus, which was developed by Samer Toume, Amit Gefen and Daphne Weihs in 2016 as a viable replacement for the current high cost laboratory equipment. It will explore how the device operates, the properties of the materials used to develop the device, and modification which can be made to the original device developed by Samer Toume, Amit Gefen and Daphne Weihs. (Toume, Gefen and Weihs, 2016)

PROJECT OBJECTIVES

The objective of this research is to validate the initial findings of Samer Toume, Amit Gefen and Daphne Weihs in their 2016 research article "Printable Low-Cost, Sustained And Dynamic Cell Stretching Apparatus" (Toume, Gefen and Weihs, 2016).

This will be achieved though the development and manufacture of the low cost cell stretching apparatus. Cost and materials will then be compared to those used in current industry. Testing though a range of independent and verifiable tests to given results, which are repeatable.

The device will be based off the design provided by Amit Gefen and Daphne Weihs but include the necessary improvement and modifications to allow the device to be more user friendly and operable in an incubator.

It is expected that, if these objectives can be achieved, this device could make cell stretching equipment more accessible for smaller biomedical laboratories in the future.

CHAPTER TWO

BACKGROUND INFORMATION

The use of cell stretching in modern medicine has been known since the early 1990's. Cell stretching apparatus consist primarily of four major components; the stretching wells, the body of the device, the controlling interface and software and the drivers. The following information outlines the considerations taken when selecting and developing these primary components for the Printable Low-Cost, Sustained and Dynamic Cell Stretching Apparatus (Toume, Gefen and Weihs, 2016).

STRETCHING WELLS

Laboratories primarily use high volume stretching equipment to minimize cost and time required. One of the ways that high accuracy is achieved is though the use of a large number of stretching wells. Stretching wells are the area of the device over which the force is applied to the cells. They are generally a dome shaped structure with a uniform upper surface over which the cell membrane can be stretched. The majority of laboratory cell stretching equipment is currently designed and built to function with a minimum of 64 cell-stretching wells (Kamble et al., 2016). This helps to increase accuracy and reduce experiment time.

The stretching well allows for a uniform bilateral force to be applied to the cells. This is achieved though the contact between the stretching wells and the cell membrane. For this reason it is critical that the stretching wells be made of a product with a very low coefficient of friction. The low coefficient of friction of the material helps to reduce the impact of the contact between the cell structure and the stretching wells. To achieve this result Polytetrafluoroethylene (PTFE) or Teflon are often used due to their very low coefficient of friction at around 0.04 μs (Biswas and Vijayan, 1992)(Pouzada, Ferreira and Pontes, 2006). PTFE is a known solid lubricant and has a very low rate of wear and tear. However, for this application the primary reason for using PTFE is its very low coefficient of friction and low thermal conductivity. Due to this low rate of wear PTFE is extremely difficult to machine and because of its high melting point, PTFE cannot be 3D printed. (Burris and Sawyer, 2006)

ABS and PLA are both possible alternatives to PTFE as materials for the stretching wells even though neither of them possesses similar coefficients of friction. When PLA and ABS are examined they are found to have coefficient of friction as high as 0.2 and 0.8 respectively (Bax and Mussig,2008) (Khun and Liu, 2013). This is not ideal. Both PLA and ABS after printing require additional finishing and post processing work. In the case of ABS this is achieved though an acetone bath followed with light sanding, while PLA can be finished with light sanding only. This can result in uneven surface finishes and incorrect sized stretching wells, which could reduce the reliability of the experiment.

3D PRINTING AND PRINTING MATERIALS

Laboratory equipment is primarily built out of steel or aluminium frames, which incur high costs and require extensive engineering. In many cases this is the major expense when developing and building modern cell stretching equipment. To minimize this cost the cell-stretching device developed by Samer Toume, Amit Gefen and Daphne Weihs is 3D printed. This has a range of added benefits including the vast reduction in cost compared to traditional laboratory equipment. An additional benefit of using 3D printers to develop medical equipment is the reduced manufacturing time (Zhang et al., 2013). When 3D printing is compared to the manufacturing time for similar equipment using traditional methods, 3D printing is considerably faster.

3D printing produces much lighter and more portable equipment, suited to desktop use and can be tailored to individual's needs and requirements. The device that was developed for this project was printed with a PLA frame. PLA is a widely used plastic in every day life but is also commonly used in the medical industry. PLA is a biodegradable and simple to print material (Lipsa, Tudorachi and Vasile, 2010). Through annealing, PLA can be modified to have a high Young's Modulus (i.e. high strength) and has a low melting point making it simple to print with a smooth finish. The primary reason PLA is used in medicine is that it has high biocompatibility with humans. PLA is also highly elastic and due to its High Young's modulus it is ideal for implants and medical research (Hamad et al., 2015), (Mathew, Oksman and Sain, 2005).

3D printing has risen in popularity over the last 5 years with the growth of the open source self-replicating rapid prototype (RepRap). This has primarily been seen in the growth of the Fused Filament Fabrication (FFF) RepRap equipment (Goyanes et al., 2014). The result of this has been the localising of mass scale manufacturing and digital production. This has

enable individuals to develop, prototype and produce products, which would have normally required much greater time and resources. 3D has also lead to reduced manufacturing times and environmental impacts of production (Tymrak, Kreiger and Pearce, 2014). It has been estimated that the domestic low cost 3D printing market will reach US$5.1 billion by 2018 (T.Wohlers, 2014)

Currently there is a wide range of materials available for 3D printing when using a Fused Filament Fabrication printer including PLA, ABS, Nylon, HDPE and many others. (Hunt et al., 2015). However the most commonly used materials for domestic and medical applications are ABS and PLA. Both PLA and ABS have low melting points, below 250 DegC, which simplifies printing. Both materials have a high Young's Modules of around 3GPa (Wittbrodt and Pearce, 2015). Recently, PLA has grown in popularity as it has been shown to be safer than ABS. This is because PLA does not produce any dangerous gases during the manufacturing process. (King et al., 2014).

When 3D printing there are a range of variables, which need to be considered and taken into account before printing can occur. The temperature of the extrusion noses is one of the key considerations as this will impact on the extrusion quality and crystallisation of the structure. For PLA the ideal printing temperature is 210 DegC as this allows for optimal crystallisation to occur within the structure, to ensures optimum structural strength. (Wittbrodt and Pearce, 2015) (Senatov et al., 2016)

The filament used is also a key-determining factor when printing and producing a high quality finish. 3D printing filaments are produced in 1.75 mm and 3 mm diameters. The most commonly used is the 1.75 mm this is because it requires less energy to operate and melt the filament. The smaller filament is also better suited to small increment printing resulting in a more uniform finish, and therefore less post processing (Oksman, Skrifvars and Selin, 2003). Filament dye also has an impact on the printability and the quality of PLA printed products. Studies have shown that filament dye impacts on the printing temperature and the crystallisation of 3D printed PLA with some colour groups having lower or high crystallisation which results in varying Young's Modulus. Natural colours were found to have the highest Young's Modulus and ultimate tensile strength but the lowest crystallinity. White was found to have the highest crystallinity with a high Young's Modulus and ultimate tensile strength. Dark colours like black and blue where found to have lower Young's Modulus and ultimate tensile strength, but the difference was less than 5MPa in most cases. (Wittbrodt and Pearce, 2015)

PLA printed products with high levels of crystallisation are known to have increased levels of Young's Modulus's and quicker bio degradability. Biodegradability is becoming a key consideration in the development of new and emerging technologies as it helps to limit their end-of-life and environmental impact during all stages of development (Mathew, Oksman and Sain, 2005).

The fill percentage is another variable that can be adjusted to reduce manufacturing time and help to increase strength. For structural adequacy, it is advised that products have a minimum fill of 25%. The fill is primarily made up of a hexagonal supporting honeycomb. Studies have shown that a honeycomb structure is one of the strongest 3D printable supporting structures. The 3D printed parts have a minimum of five external solid shells to form the flat surfaces of the device.

The primary advantage of using the honeycomb structure when compared to solid walls is the strength to weight ratio. Honeycomb is much lighter, time efficient and cost effective to produce compared to solid sections. Solid sections provide high strength and a durable frame but are often unnecessary, very time consuming and wasteful in production. Honeycomb structures help to mitigate this strength to weight trade off issues (Nilsson. E, Nilsson. A. 2004)

The way honeycomb structures are formed allows them to have increased strength along the horizontal faces while maintaining a lightweight construction between the two flat supporting surfaces. The disadvantage of the honeycomb structure when compared to other structures and construction methods is the lack of strength with point loads and loads which are perpendicular to the main flat supporting surfaces. This is due to the way the structure is formed. The honeycomb lattice is strongest in uniform compression along the face but suffers when compressed along the edges as the internal structure of the lattice can collapse. The way the structure is manufactured also limits the strength of the Honeycomb when the lattice is in direct compression or tension (Foo et al,. 2007).

ARDUINO

The majority of experiments and developed technologies in the modern era use software as a primary means of control. The implementation and development of such technology can be expensive and time consuming. To minimize cost, free and open-source software (FOSS) was developed. FOSS software is developed software, which can be modified and altered to suit the user's requirements. This has been a common method in recent times to reduce cost in the

development of new laboratory equipment and specialty products, especially with the rise of RepRap printing equipment (Pearce, 2012).

One of the primary implementation methods for such technologies has been through the use of Arduino open source programing and hardware. Arduino is a simple to learn, easy to use, microprocessor, which has a variety of attachable hardware additions, which makes it ideal for engineering purposes. Through the use of various shields and transformers, the user is able to control a wide variety of equipment from example simple brushless DC motors though to in-depth DNA analysis and radiation detection equipment (Pearce, 2012). Though the use of Arduino and FOSS technologies, products can in some cases be produced for less than twenty percent of their new original purchase price (Fisher and Gould, 2012).

The Arduino Uno Control board consists of a simple printed circuit board based on ATmega328 8-bit programmable microcontroller with an attached 32 kilobytes (KB) of flash memory for data-storage memory. It has 14 digital pins and 6 analog pins, which allow for analog-to-digital conversion capability. The microcontroller has a range of built-in features, including: timer/counters, programmable, watchdog timer, and low-power, energy-saving modes. The Arduino Uno has an on-board USB connector to interface with personal computers. (Fisher and Gould, 2012)

The Arduino Uno board is fitted with the ability to allow for expansion to auxiliary boards or shields which are connected though a mating pin arrangement. Theses auxiliary boards or shields are simply connected to the headers of the Arduino board and controlled through the original Arduino Uno. The auxiliary boards or shields are programed and integrated though the inbuilt operating library and auxiliary coding for the microprocessor. (Anzalone et al., 2013)

The Arduino hardware is controlled through free software available from the Arduino website (Arduino.cc, 2017). The software controls the devices via C/C++ code which runs pass fail operations to validate the authenticity of code. The software provides a terminal output window for users to observe the code and operations in real time. (Fisher and Gould, 2012)

FOSS software is widely used in modern small-scale laboratory experiments. It is coupled with RepRap printers to reduce cost of production for smaller commercial equipment facilities. In most cases they have been found to yield the same results as commercially available equipment (Anzalone et al., 2013).

Due to Arduino being open source software there is a range of downloadable libraries and controlling code to help in the development of new technologies and operating functions.

Many of the commonly used items of coding including information regarding motors and encoders is found on the Arduino website and are provided free to help further similar research and project (Playground.arduino.cc, 2017).

BRUSHLESS DC MOTORS

Brushless DC motors are direct linear motors with attached gear ratios to reduce the operating speed. The motors are controlled in parallel though the Arduino hard and software. The brushless DC motors have attached encoders to allow for the speed and number of rotation to be counted. An alternative is to use two-stepper motor connected in parallel but has increased cost and programing difficulty when compared to brushless DC motors. DC motors can be geared either up or down to increase or decrease the rotations speed. In this case the DC motors are highly geared down to reduce the speed of the rotations and control the distance the lead screw travels. The low cost cell stretching apparatus developed by Samer Toume, Amit Gefen and Daphne Weihs depicts the use of two DC brushless motors.

STEPPER MOTORS

Stepper motors are a commonly used device for high precision and controlled device movement. They are commonly used in 3D printers and similar high accuracy devices. The motor is controlled though electronic pulses which are correlated to the required number of steps. A step is equal to a fixed number of degrees. This is usually between 1.6 degrees and less than 0.25 degrees. Stepper motors are controlled in a similar way to DC motors with speed and distance controls. But unlike DC motors the speed is controlled though the number of rotations per minute as opposed to a linear scale from 0 to 255. The distance is controlled though a number of steps not a number of encoder counts or time. For this reason stepper motors are preferred to DC and servomotors.

SILICONE AS A PROXY FOR CELL BED

A cell bed was not available for this project and a silicone sheet was developed as a proxy for the cell bed. Silicone is a commonly used material in every day life from producing kitchen utensils to industrial components. Two-part rubber silicone mixtures are commonly used in medical applications. The Elastosil chemical reaction produces a clear rubber silicon, which is

highly flexible and has a neutral pH, which can be used for growing and culturing cells. Two-part rubber silicone can have a shear modulus higher than 250 kPa and be formed into films as thin as 50 microns making it ideal for stretching (Lötters et al., 1997).

CHAPTER THREE

THESIS TIME LINE

The thesis timeline includes information gathered during initial research conducted in the pervious subject Engg460, which has been beneficial for continued research.

The thesis has not followed the original time line developed in Engg460. This is primarily due to the unavailability of funding and changing testing methods from testing live cells to acceleration and stretch testing.

Project Time Line

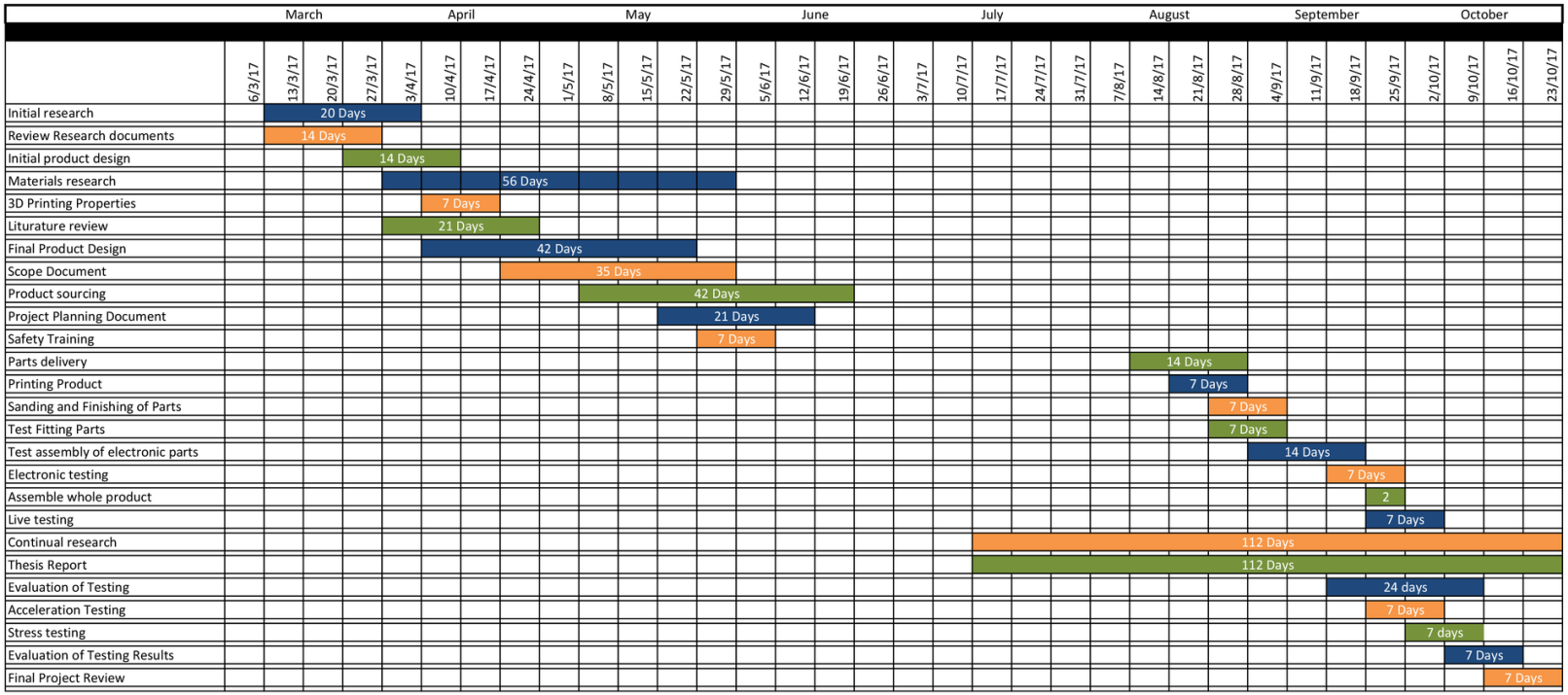

CHAPTER FOUR

PARTS AND COSTING

Included below is the actual costing without labour for the development of Printable Low-Cost, Sustained and Dynamic Cell Stretching Device. $300 of the funding was provided by Macquarie University, all additional funding was from other sources.

Item	Quantity	Price per unit	Development Cost	Expected Cost
PLA Material	1	$40.00	$40.00	$40.00
DC Motors	2	$50.80	$101.60	
Arduino Uno	1	$24.71	$24.71	$24.71
Arduino Servo Controller Shield	1	$8.75	$8.75	$8.75
Wiring	1	$9.86	$9.86	$9.86
Teflon tube	1	$19.00	$19.00	
Lead screw and nut	2	$5.00	$10.00	$10.00
Postage	1	$40.00	$40.00	$40.00
Sand Paper	6	$1.35	$8.10	$8.10
9 volt Clips	2	$0.98	$1.96	$1.96
Adafruit Accelerometer	1	$12.95	$12.95	$12.95
NEMA 14 Stepper Motors	2	$45.00	$90.00	$90.00
Arduino Mega	1	$49.99	$49.99	
	Total		$416.92	$246.33

TABLE 1 COSTING TABLE

CHAPTER FIVE

METHOD

The low cost cell-stretching device was designed at Macquarie University using the 3D modeling CAD software CREO. The designs of the device was initially based on the model and schematics provided by the drawings and accompanying paper from Samer Toume, Amit Gefen and Daphne Weihs for the original low cost stretching device.

The device was designed to the extent of the supplied drawings in CREO, additional parts including the motor support stands and supporting printing structures were designed.

The components were designed in CREO as individual parts for simplicity and then merged together to create the upper and the lower stretching beds. In some cases the merge function did not work and so the parts where exported into a secondary modeling program called Rhinoceros 5, which is another 3D modeling program. In this program the parts where formed as surfaces and booleaned together. This removed the need to secure the multiple stretching parts together using epoxy removing the possible risk of not aligning the parts together correctly. They were exported back to CREO.

The completed product was then assembled using the CREO software, which allowed the device to be viewed as a completed model. This helped to ensure that any possible manufacturing and assembly issues could be resolved at this point. Points of possible assembly difficulty were identified, including the connection between the motor supports and the lower supporting frame. To reduce the possibility that these critical sections connected in the correct way, the tolerance of the printing head was changed from 0.5 mm to 0.3 mm.

Once the identified manufacturing difficulties were resolved a set of technical drawings were produced along with detailed and assembly drawing. These drawing were checked by Dr. Cheng and Mr. R. Wilson and subsequent updates drawing were made. The parts were exported from CREO as STL, which reformed them as surfaces to be printed rather than individual points. STL's allow the parts to be read by the printing software FlashPrint.

Research was conducted into the most appropriate material for the manufacturing of the device. After discussions with Dr. Cheng, Mr Joel Raco and research into the original

materials used to manufacture the device along with the materials used for similar products, PLA was chosen as the most appropriate material. PLA was chosen due to its simple 3D printing properties, its reliable and predictable durability and its high biocompatibility with human cells. Originally the stretching rings for the device were going to be manufactured using PTFE due to its low coefficient of friction but because of time constraints and machining difficulties it was decided that PLA was a suitable substitute for the PTFE.

The Macquarie University Laboratory staff conducted an introduction into the methodology and working of the 3D printer and surrounding safety equipment. This included the operation of the printer, safety features, location of the safety equipment and the most common problems, which occur during the printing process.

The parts were uploaded to FlashPrint and then set to be secured to the middle of the printing bed. During this process the type of printing filament was selected and installed. For this project only the left extrusion head was used because of damage from a previous printing project to the right extrusion head. The required supporting structures and rafts were attached and the bed was cleaned of debris and leveled. The lower stretching bed required supporting structures to be printed. No rafts where required for any of the 3D printing.

The device was printed using Macquarie University's Flash Forge Dreamer 3D printer, which was set to prints in 0.05 mm vertical increments for the body of the device and 0.03 mm increments for the stretching wells to give the highest possible precision.

The device was printed using two different types of PLA, standard PLA and PLA+. The difference between the two products is the printing temperature and the colour of the printing. The PLA was white and printed with a head temperature of 205 DegC with a bed temperature of 60 DegC. The PLA+ was black and printed with a head temperature of 215 DegC and a bed temperature of 60 DegC. Both of the printing materials had printing speeds of 80 mm/s and free run printing speeds of 100 mm/s. This was to aid in limiting the total printing time. The device was printed using the two different types of PLA to provide a colour distinction between the different parts, which helped in adding the user to see the relative movement of the parts.

The printing was completed in four sessions for the body of the device and an additional session for the silicon mould. The printing time ranged from the pair of motor support, which required 6 hours to print to 38 hours.

Once the printing of the parts was complete the parts were inspected for accuracy and fit. The parts were then sanded using 240P sand paper followed by 600P and then 1200P wet and dry

sand paper. The sanding for flat surfaces occurred on a leveled even stone bench top to ensue that the finish was evenly applied to the surface. The finishing removed approximately 0.5 mm of material off all of the surfaces. This post operation finishing provided a smooth and uniform surface to the base of the device. This ensured that the device would sit level.

During the printing phase of the project the Arduino Electronics were tested and assembled. Initial tests where conducted to ensure the correct functioning of the Arduino Uno Pro Board. This was achieved through using a Led light and simple C++ coding using the free open source Arduino software. The code for this test is included in appendix A. The Arduino Uno Board was powered and controlled through a connection between a USB A to USB C cable and the controlling computer.

After the initial setup it was found that it was not possible to control both the motors and encoders with the Arduino Uno. This was because the Arduino Uno only had two free digital pins, 2 and 13 which where covered by the motor shield and so could not be reached. The encoders required power which is a additional digital input pin, which was not available on the Arduino Uno.

For this reason the original Arduino board was upgraded to the Arduino Mega 2560, which has additional, free digital pins and the required power input to run the encoders and fits the original digital shields. The use of the Arduino mega 2560 board enabled for all of the electronic components of the device to be controlled on the same piece of code and operating window.

The device was controlled though C++ coding. C++ allowed the motors to be operated in parallel to a given position. This is governed by a feedback if loop which allow the mega board to determine how any rotations the encoders have taken from their original position. From the number of rotations the distance the bed has moved was calculated. This loop also allows the speed of the motors to be changed. The motors can run at a maximum free run speed of 14 RPM. The speed can be lowered by incrementally from 255 untill the motors are stationary.

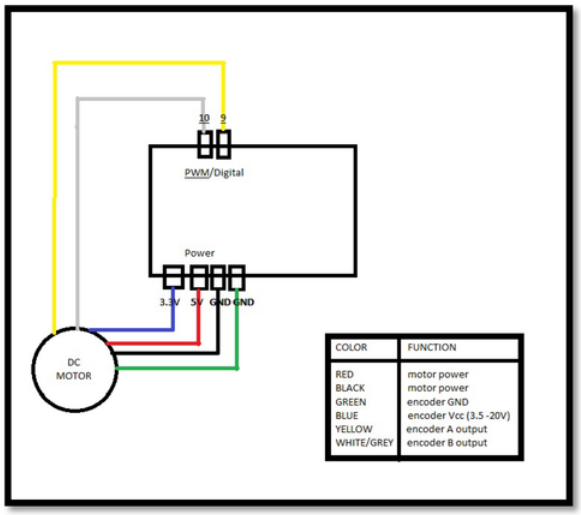

(Arduino.cc, 2017)

FIGURE 1 ENCODER CONNECTIONS

The DC motors have 48 CPR (cycles per revolution) encoders, which require additional power, grounding and controlling sequences. Figure 1 sets out the wiring diagram for the encoders.

The encoders are controlled through the Arduino Mega 2560 board and powered through the original Uno Arduino board. This was due to the encoders requiring additional external power, which was not available though the Mega Board.

After some additional testing it was discovered that the Arduino boards were not capable of keeping up with the required rotation count of the encoders. The DC brushless motors were replaced with two NEMA 14 stepper motors. This would guarantee that the device would turn the required number of steps. To make this change the only part, which needed to be replaced, was the motors because the shield and Arduino where capable of running the two stepper motors.

The motors were attached to the shield in a lock step format, which enable both of the motors to turn in unison in the same direction. This was because in Arduino the function Step is an exclusive function, which prevents other sequences from taking place while it is running. The motors were tested individually and then together. The test code is included in Appendix B.

The device operates through the use of a steel lead screw, which is 1/4 inch in diameter. This lead screw had its head and the lower extremity of the thread machined off. The head was

machined off to ensure that the bolt could fit into 6 mm slot in the lower stretching plate and so that the bolt was secured into place preventing it from coming out of alignment. The upper portion of the thread was removed from the bolt so that it could be inserted into the collar, which connects the motor drive shaft and the lead screw. The lead screw also had a flat machined on it so the collar and the grub screw would have the highest possible contact area. The connecting collar was machined out of PTFE with two internal one-millimeter grub screws, which secure the lead screw and motor shaft.

The motor and lead screw assembly was tested to determine if they would meet the required control standards. The test included;

- A single static movement and return to position
- A stepped movement and returning to its original position
- A continuous movement and return to original position
- A combination test that included both a stepped and a continuous movement test

When the stepper motor function was verified, the motors were attached to the operation test rig. The key consideration when developing the operation test rig was to ensure that all of the parts were level and perpendicular to each other. An image of the operation test rig is as image 1. The lower stretching frame was placed in the test rig and then the dimensions for the motor supports were taken.

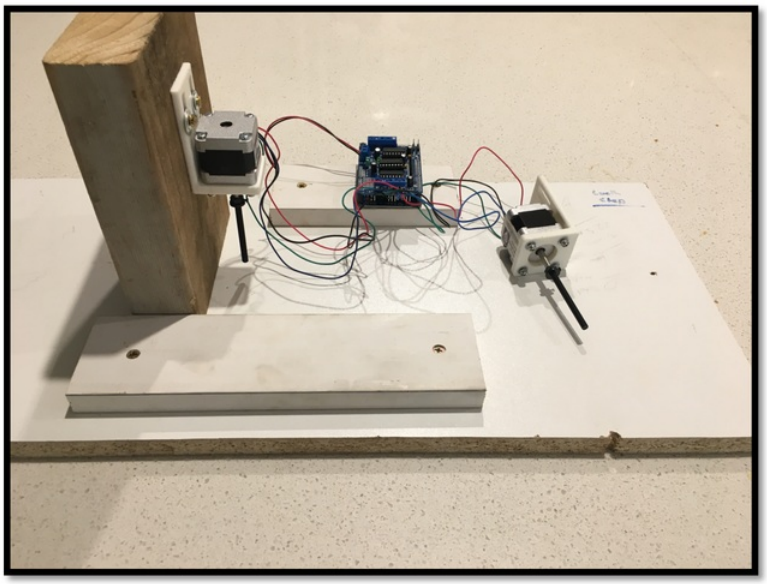

IMAGE 1 OPERATION TEST RIG

During the testing phase a mould was 3D printed for the silicone mixture. The mould was printed using the same parameters as the rest of the device and then painted in a water-based spray paint. The mould was given six coats of paint and kiln dried between each application for one hour. The mould was painted to provide a smooth uniform surface finish, which allowed the silicone film to dry clear. The silicone film is 1 part Elastosil RT 601 B and 9 parts Elastosil RT 601 A by weight. In this case the parts were 2.5 grams of part B and 22.5 grams of part A. The two parts are combined and mixed for two minutes and then placed in a sealed vacuum container to remove any imperfections and bubbles, which form during the chemical reaction. The chemical reaction produces a gas and a vacuum is used to draw the air out of the mixture. To aid in removing the bubbles from the mixture, every 5 minutes fresh air is released back into the vacuum. This helps to break the surface bubbles and draw more gas out of the mixture. The vacuum process can take up to one hour. The silicone mixture has a working time of two hours. The mixture was poured into the set mould and the supporting structure was up ended into the mould with the locking feet (drawing 6 sheet 3) placed in the wet silicone. As the silicone set it left the required holes for the supporting structure. The supporting structure was weighed down to prevent it from moving and ensure it was in contact with the base of the mould. The silicone mixture was left to cure overnight. Latex gloves and bench covers were required to perform this task and any clean up was performed without using water because the chemical reaction between the silicone mixture and water forms hydrogen gas.

The silicone sheet was removed from the mould and trimmed to the required size. The silicone sheet is support in the 3D printed frames, which sandwiches the silicone sheet and cell membrane between the 3D printed frames. The frame provides a strong and stable foundation for the cells to be grown on. The silicone surface also helps to evenly distribute the stretching force over the cell surface. The silicone support was finished with a light sand and air blast to remove any debris.

Covers and cases for the motors and the Arduino electronics were designed and printed. These covers are intended to be airtight as the device is going to be placed in an incubator, which is heated to 37 DegC with 95 percent humidity. With this in mind the covers were designed to go over the entire motor and enclose the whole Arduino unit. The motor covers are secured into place using the securing 4 mm nuts and washers and the Arduino case has an interference fit which provides an airtight seal.

To confirm the consistency of the device an accelerometer controlled though Arduino was attached to the device next to the right hand lead screw. The accelerometer was connected to the upper stretching plate and then leveled in the horizontal plane. The accelerometer was

required to be leveled so only velocity in the vertical direction was recorded. The upper stretching plate was set to take 100 steps at 1 RPM down and then back to its original position. This sequence occurred three times. The results were taken and compared. This test was conducted to measure the speed of the upper plate and verify that the stretching plate speed was uniform and as predicted. Accelerometer was an Adafruit three axis accelerometer, which was connected to an external Arduino microprocessor. The supporting code and libraries for the Adafruit accelerometer were downloaded though the Arduino controlling interface. The sample code was used as a template and then modified to give: time, acceleration, velocity and gravity (see Appendix C). The accelerometer required 5 V power, grounding, SDA and SCL controls that in an Arduino Mega are found in digital ports 20 and 21. SDA and SCL are date line and clock line outputs, which allow the Arduino to determine time and movement and with this to record acceleration in the X, Y and Z planes with gravity. The output from the Arduino was theoretical velocity, actual velocity, time and Z-axis position. Actual velocity is was compared to the theoretical velocity over the course of the experiment. The required velocity was 0.01mm/s while in the stretching range as this is the required stretching speed.

The device was then reconfigured in a temporary strain test apparatus to establish tensile stress. This test confirmed that the force exerted by the upper stretching plate onto the silicone sheet and stretching wells was uniform and predictable. For the testing to occur the motors, upper stretching plate, stretching wells and silicone sheet were placed into the stress apparatus, as shown in image 2. The strain testing apparatus used a set of Acaia Lunar scales to measure the force exerted on the stretching wells by the upper stretching plate though the silicone sheet. Results were measured every 50 steps while inside the 950 steps stretching range. These results were taken and then divided by the surface area of the well bases to give the tensile force. This test was repeated three times and the results were averaged and graphed.

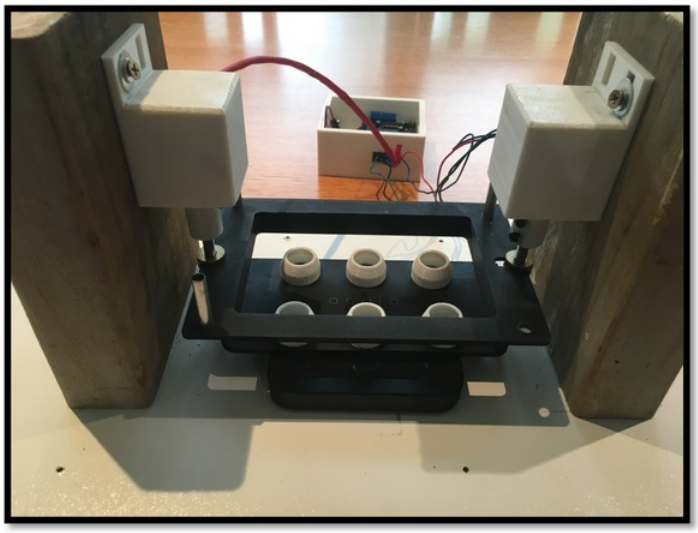

IMAGE 2 STRESS TESTING APPARATUS

The final test was a theoretical strain test to measure the level of deflection of the silicone sheet. This was calculated by determining the change in surface area between the stretching and relaxed surface areas for the silicone sheet while inside the stretching range. These theoretical calculations relied on three assumptions;

1. There is uniform stretch across the whole surface
2. The force is uniformly applied to the silicone surface
3. There is no resistance between the stretching wells and the silicone sheet at the point of contact

Based on these assumptions, the known stretch distance, pitch of the lead screw and the number of steps, the stretch percentage was calculated.

The device was then reassembled and prepare for the final presentation.

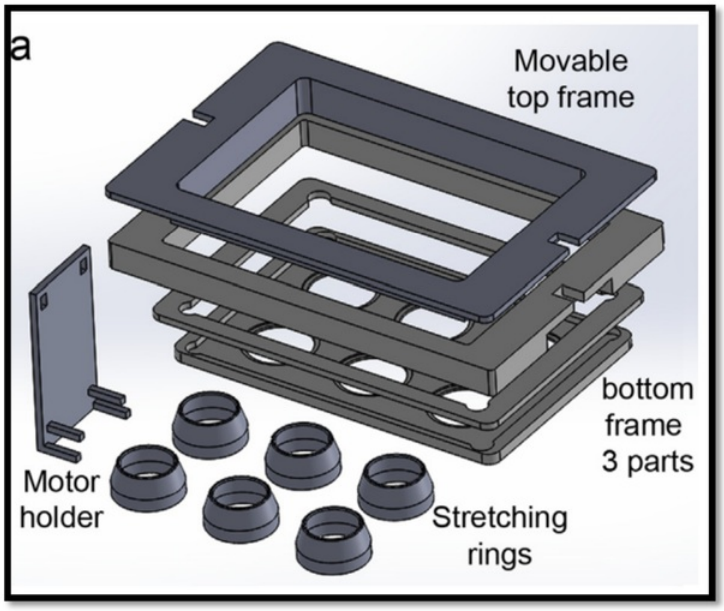

FIGURE 2 TOUME, GEFEN & WEIHS CAD DESIGNS

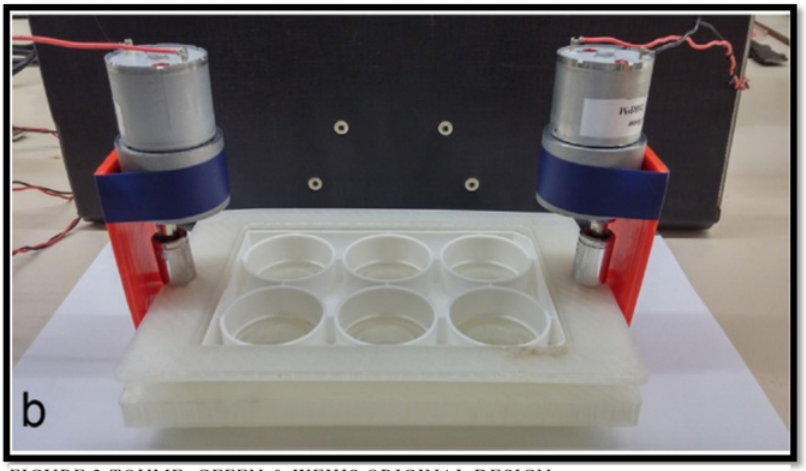

FIGURE 3 TOUME, GEFEN & WEIHS ORIGINAL DESIGN

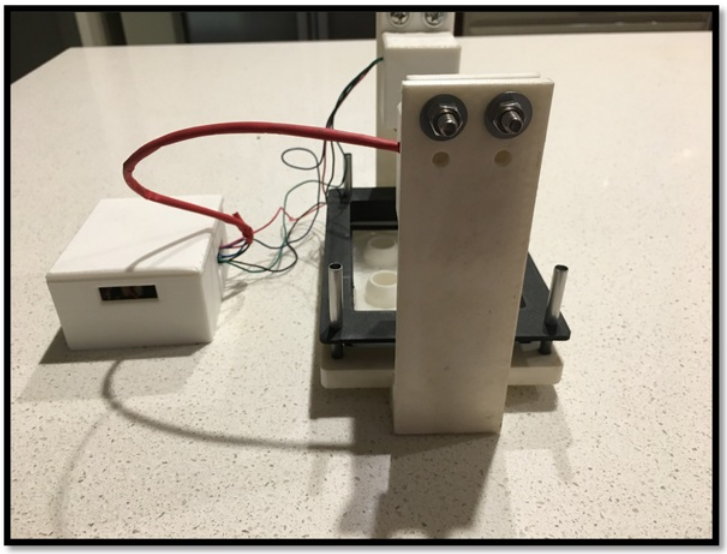

IMAGE 3 CELL STRETCHING DEVICE END VIEW

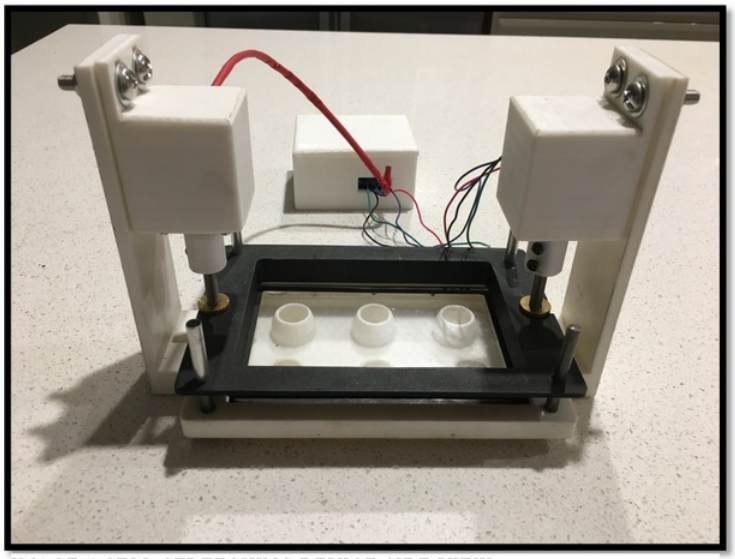

IMAGE 4 CELL STRETCHING DEVICE SIDE VIEW

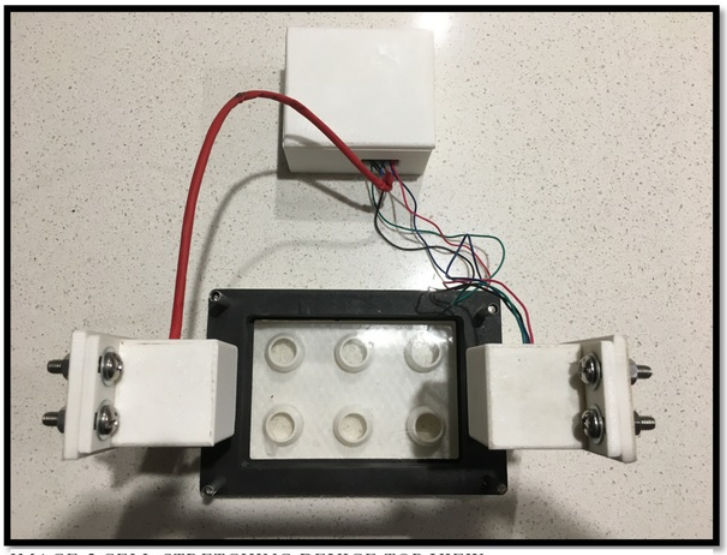

IMAGE 5 CELL STRETCHING DEVICE TOP VIEW

Top View A

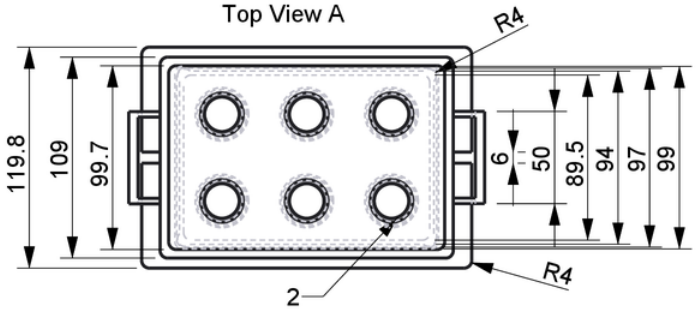

ITEM	DESCRIPTION	QTY
1a	Lower Stretching Plate	1
1b	Middle Spacer Plate Upper Face	1
1c	Middle Spacer Plate	1
2	PLA Stretching Wells	6
3a	Stretching Plate Face	1
3b	Upper Stretching Plate Walls	1
4	Motor Supports	2

Left View A

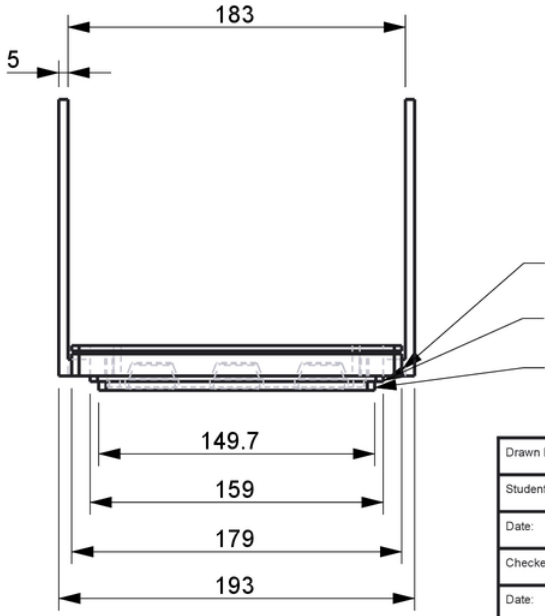

End View A

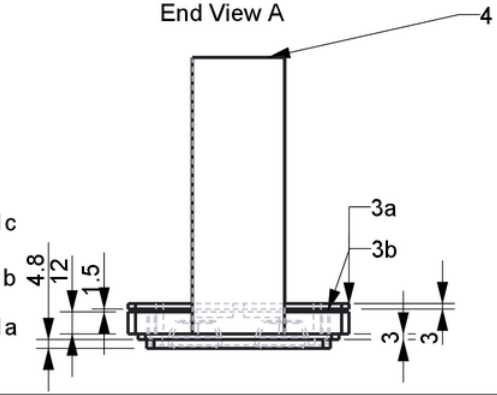

Cross Sectional View

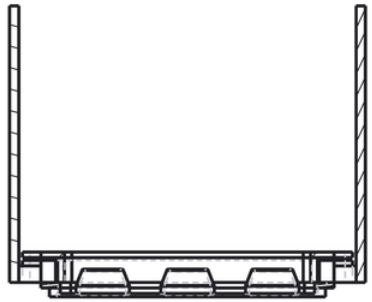

Drawn By: Timothy J Wilson	Material: PLA	MACQUARIE UNIVERSITY	
Student ID: 42868068	General Tolerance: ±0.001		
Date: 28/08/2017	Drafting Standard: AS 1100	Cell Streching Apparatus Assembly	
Checked By: RDW	Projection:	Size: A4	Drawing No.: 4
Date: 31/08/2017		Scale: 1:3.5	Sheet: 1

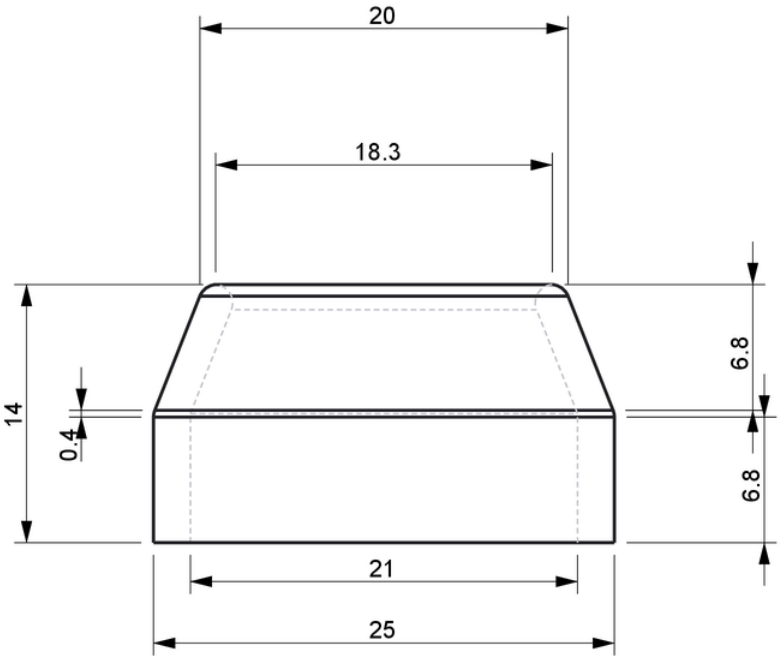

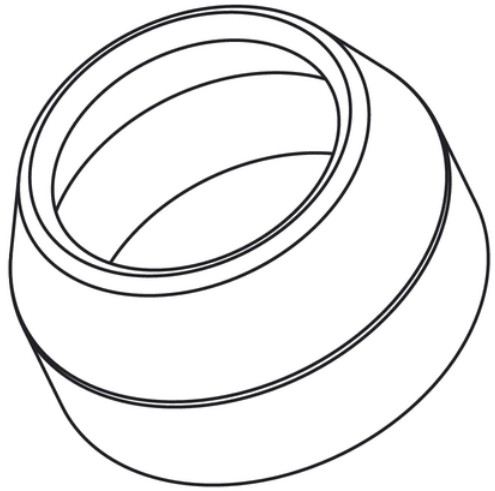

Drawn By:	Timothy J Wilson	Material:	PLA	MACQUARIE UNIVERSITY	
Student ID:	42868068	General Tolerance:	±0.01		
Date:	28/08/2017	Drafting Standard:	AS 1100	Stretching Wells	
Checked By:	RDW	Projection:		Size: A4	Drawing No.: 4
Date:	31/08/2017			Scale: 1:3	Sheet: 2

Top View A

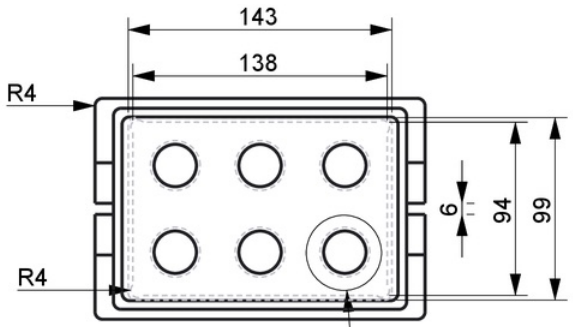

Detail A

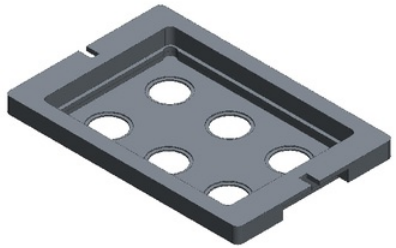

Left View A

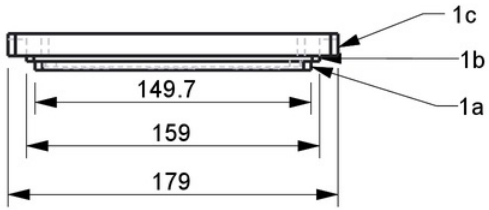

End View A

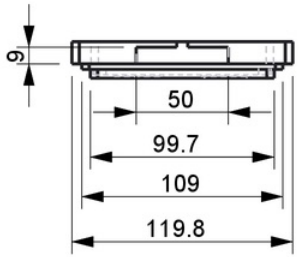

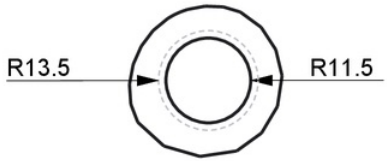

Detail A(3:5)

Drawn By: Timothy J Wilson	Material: PLA	MACQUARIE UNIVERSITY	
Student ID: 42868068	General Tolerance: ±0.001		
Date: 28/08/2017	Drafting Standard: AS 1100	Lower Stretching Plate	
Checked By: RDW	Projection:	Size: A4	Drawing No.: 4
Date: 31/08/2017		Scale: 1:3.5	Sheet: 3

Top View A

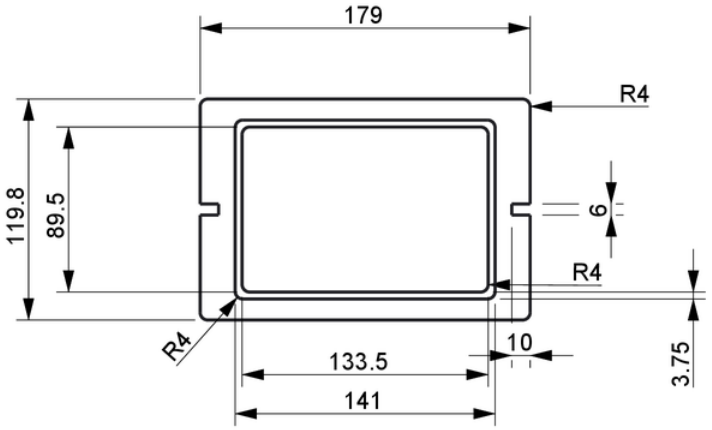

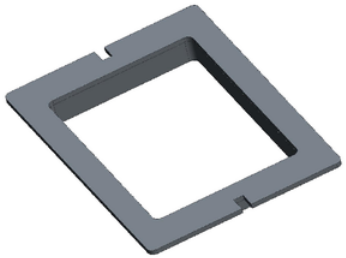

Left View A

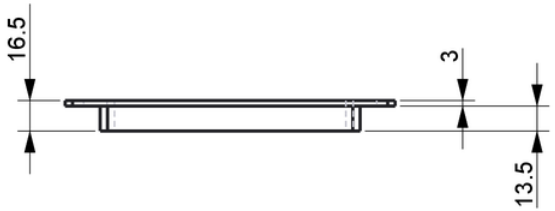

End View A

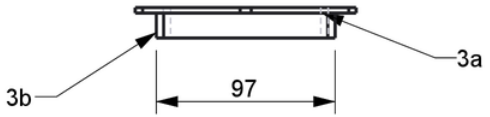

Drawn By: Timothy J Wilson	Material: PLA	MACQUARIE UNIVERSITY	
Student ID: 42868068	General Tolerance: ±0.001		
Date: 28/08/2017	Drafting Standard: AS 1100	Upper Stretching Plate	
Checked By: RDW	Projection:	Size: A4	Drawing No.: 4
Date: 31/08/2017		Scale: 1:3.5	Sheet: 4

Top View A

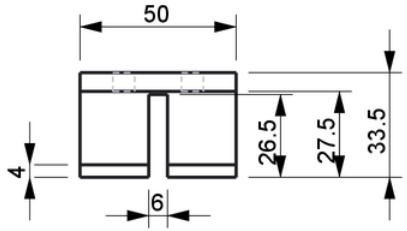

Left View A

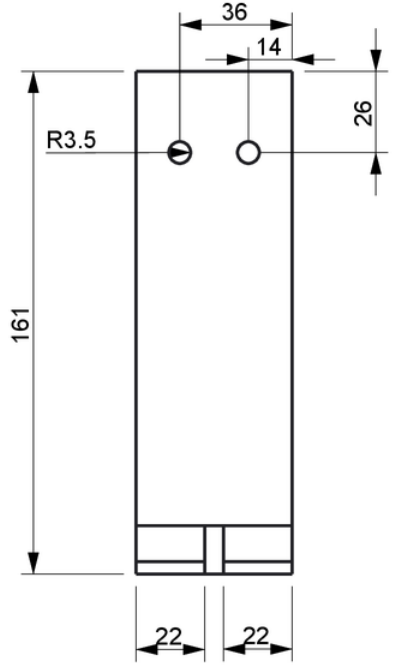

End View A

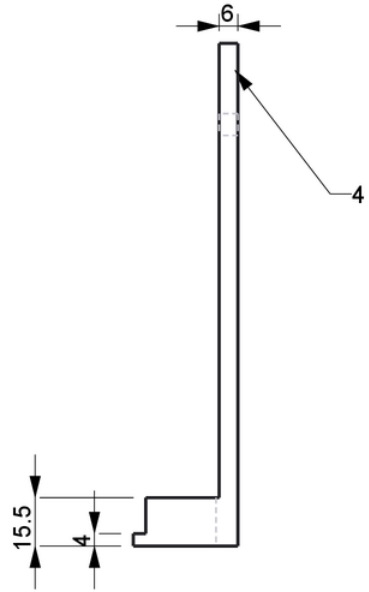

Drawn By: Timothy J Wilson	Material: PLA	MACQUARIE UNIVERSITY	
Student ID: 42868068	General Tolerance: ±0.1		
Date: 28/08/2017	Drafting Standard: AS 1100	Motor Supports	
Checked By: RDW	Projection:	Size: A4	Drawing No.: 4
Date: 31/08/2017		Scale: 1:2	Sheet: 5

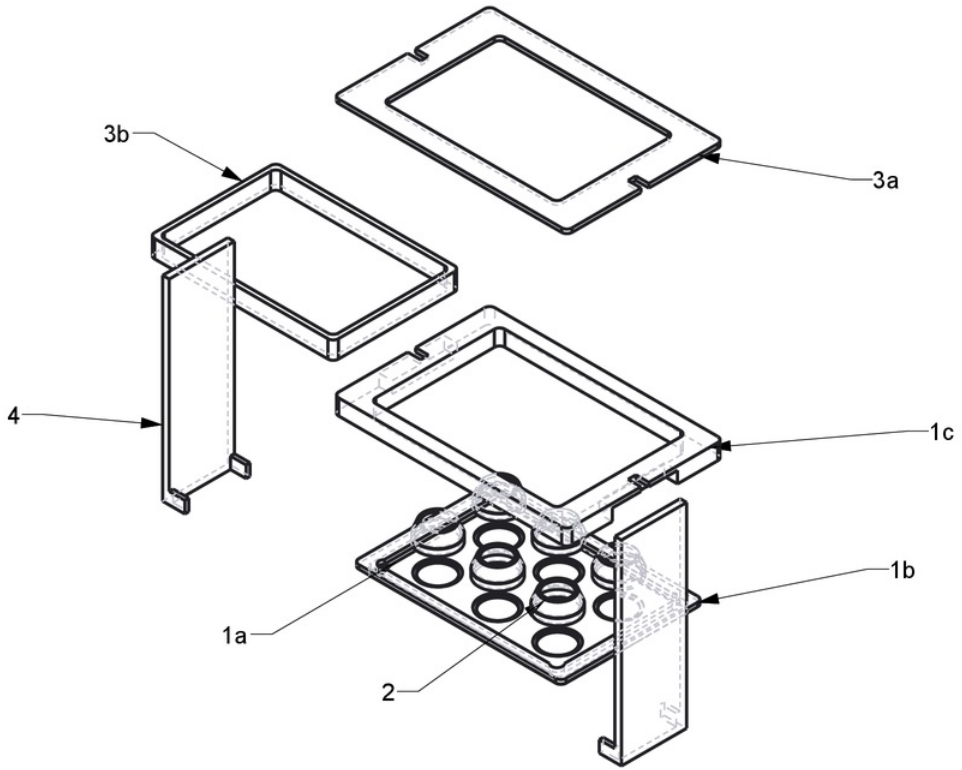

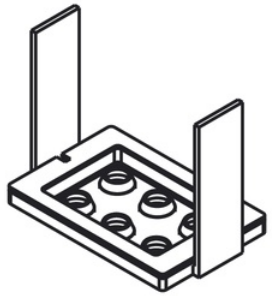

Drawn By: Timothy J Wilson	Material: PLA & PTFE	MACQUARIE UNIVERSITY	
Student ID: 42868068	General Tolerance: ±0.001		
Date: 28/08/2017	Drafting Standard: AS 1100	Whole Assembly Exploded View	
Checked By: RDW	Projection:	Size: A4	Drawing No.: 4
Date: 31/08/2017		Scale: 1:5	Sheet: 6

Top View A

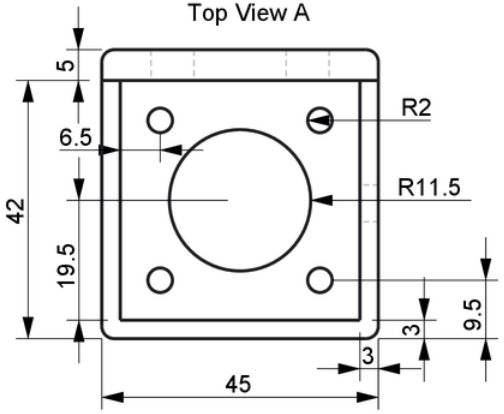

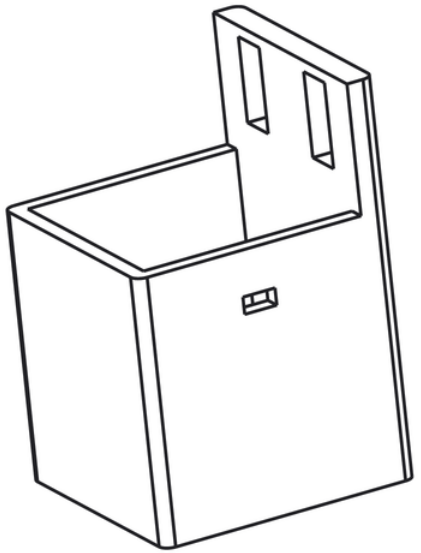

Front View A

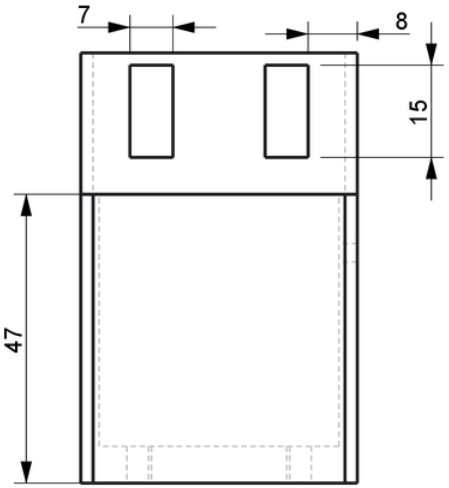

Left View A

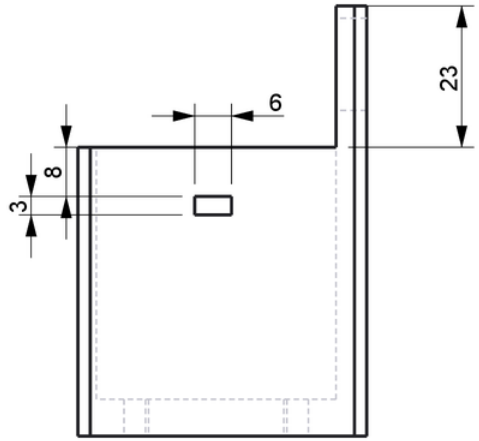

Drawn By:	Timothy J Wilson	Material:	PLA	MACQUARIE UNIVERSITY	
Student ID:	42868068	General Tolerance:	±0.1		
Date:	28/09/2017	Drafting Standard:	AS 1100	Motor Mounts	
Checked By:	RDW	Projection:		Size: A4	Drawing No.: 4
Date:	28/09/2017			Scale: 1:1	Sheet: 7

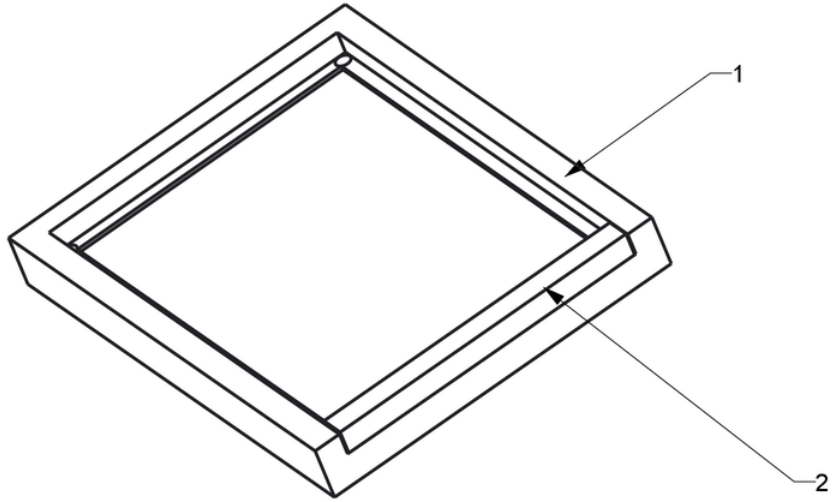

Drawn By: Timothy J Wilson	Material: PLA	MACQUARIE UNIVERSITY	
Student ID: 42868068	General Tolerance: ±0.1		
Date: 28/09/2017	Drafting Standard: AS 1100	Silicone Mould	
Checked By: RDW	Projection:	Size: A4	Drawing No.: 5
Date: 28/09/2017		Scale: 1:2	Sheet: 1

Top View A

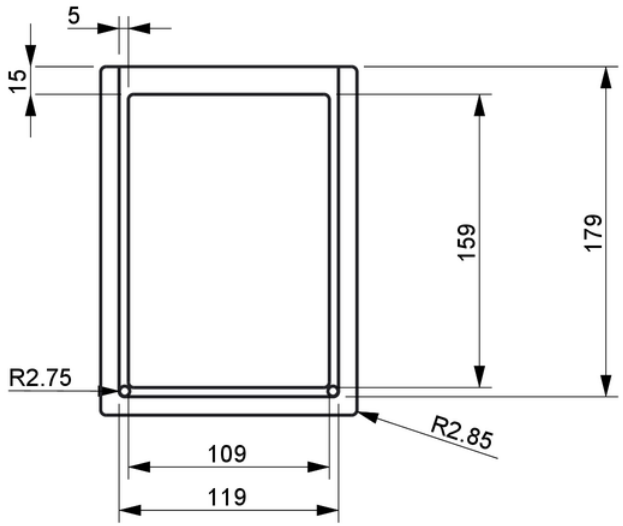

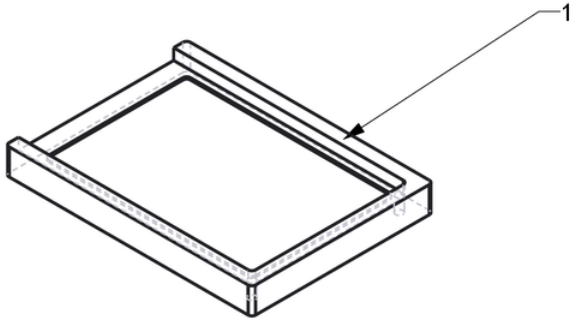

End View A

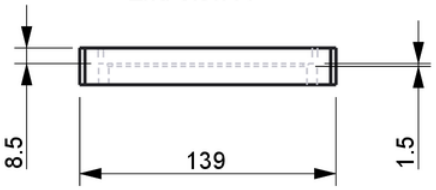

Left View A

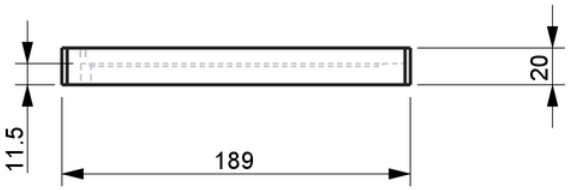

Drawn By: Timothy J Wilson	Material: PLA	MACQUARIE UNIVERSITY	
Student ID: 42868068	General Tolerance: ±0.01		
Date: 28/09/2017	Drafting Standard: AS 1100	Silicone Mould Base	
Checked By: RDW	Projection:	Size: A4	Drawing No.: 5
Date: 28/09/2017		Scale: 3:10	Sheet: 2

Top View A

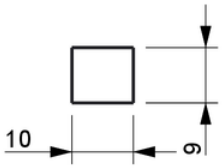

Left View A

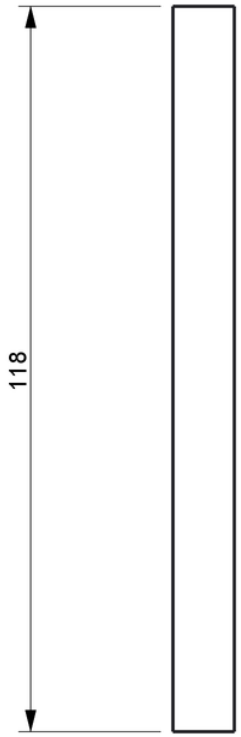

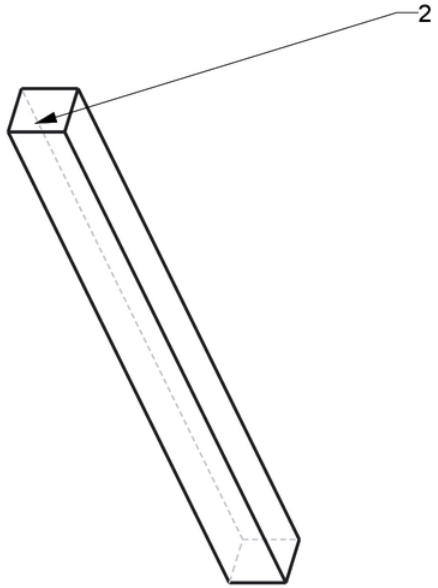

Drawn By: Timothy J Wilson	Material: PLA	MACQUARIE UNIVERSITY	
Student ID: 42868068	General Tolerance: ±0.01	Silicone Mould Wall	
Date: 28/09/2017	Drafting Standard: AS 1100		
Checked By: RDW	Projection:	Size: A4	Drawing No.: 5
Date: 28/09/2017		Scale: 1:1	Sheet: 3

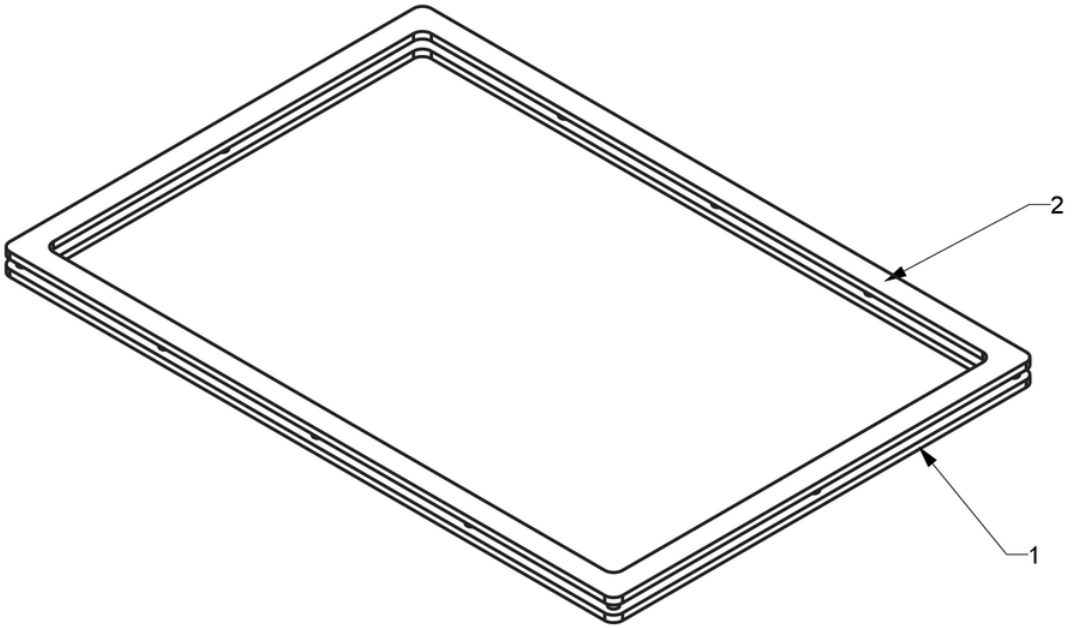

Drawn By: Timothy J Wilson	Material: PLA	MACQUARIE UNIVERSITY	
Student ID: 42868068	General Tolerance: ±0.1		
Date: 28/09/2017	Drafting Standard: AS 1100	Silicone Support	
Checked By: RDW	Projection:	Size: A4	Drawing No.: 6
Date: 28/09/2017		Scale: 1:1	Sheet: 1

Top View A

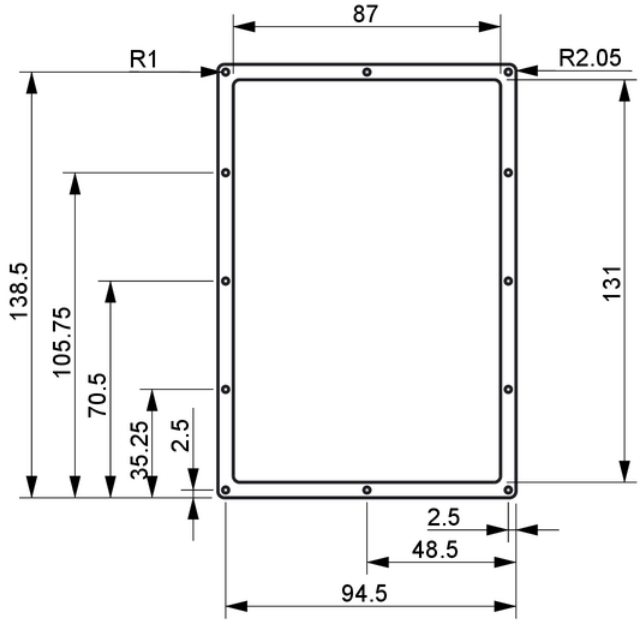

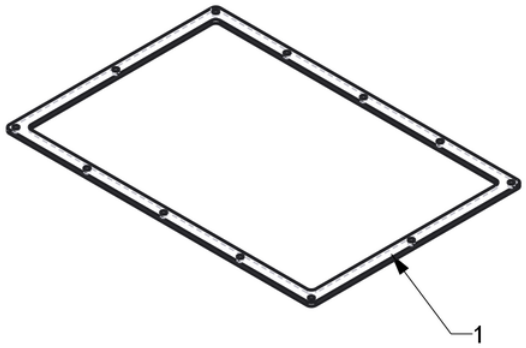

End View A

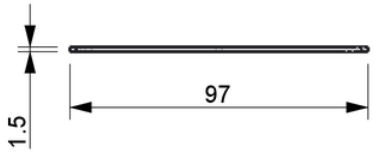

Left View A

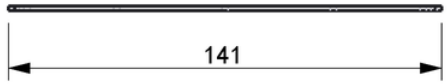

Drawn By: Timothy J Wilson	Material: PLA	MACQUARIE UNIVERSITY	
Student ID: 42868068	General Tolerance: ±0.1		
Date: 28/09/2017	Drafting Standard: AS 1100	Upper Silicone Support	
Checked By: RDW	Projection:	Size: A4	Drawing No.: 6
Date: 28/09/2017		Scale: 1:2	Sheet: 2

Top View A

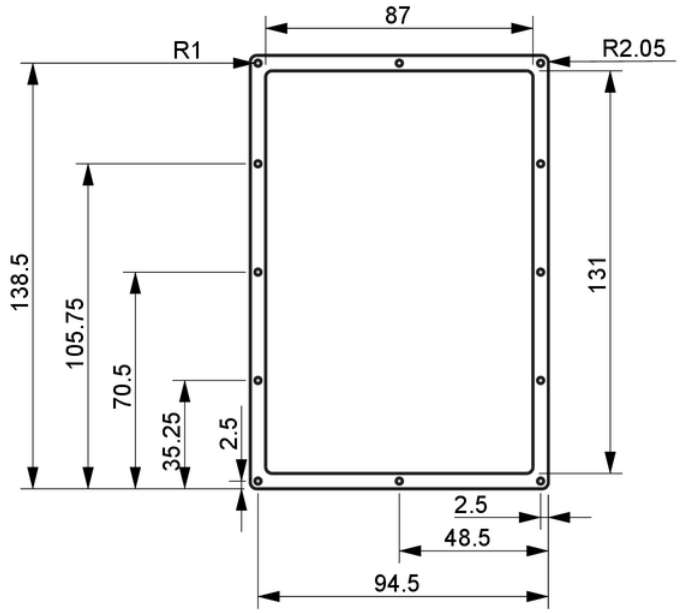

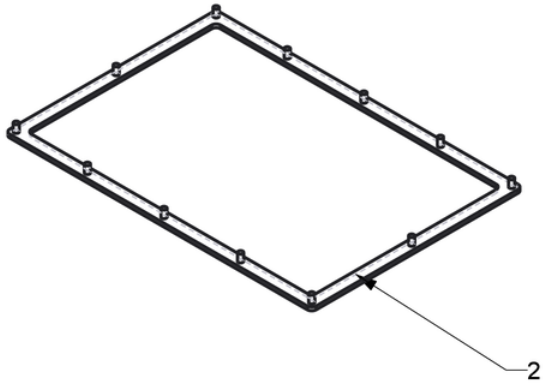

End View A

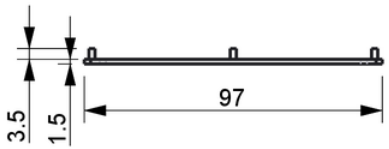

Left View A

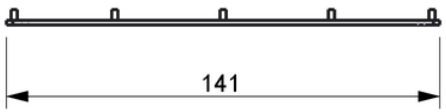

Drawn By:	Timothy J Wilson	Material:	PLA	MACQUARIE UNIVERSITY	
Student ID:	42868068	General Tolerance:	±0.1		
Date:	28/09/2017	Drafting Standard:	AS 1100	Lower Silicone Support	
Checked By:	RDW	Projection:		Size: A4	Drawing No.: 6
Date:	28/09/2017			Scale: 1:2	Sheet: 3

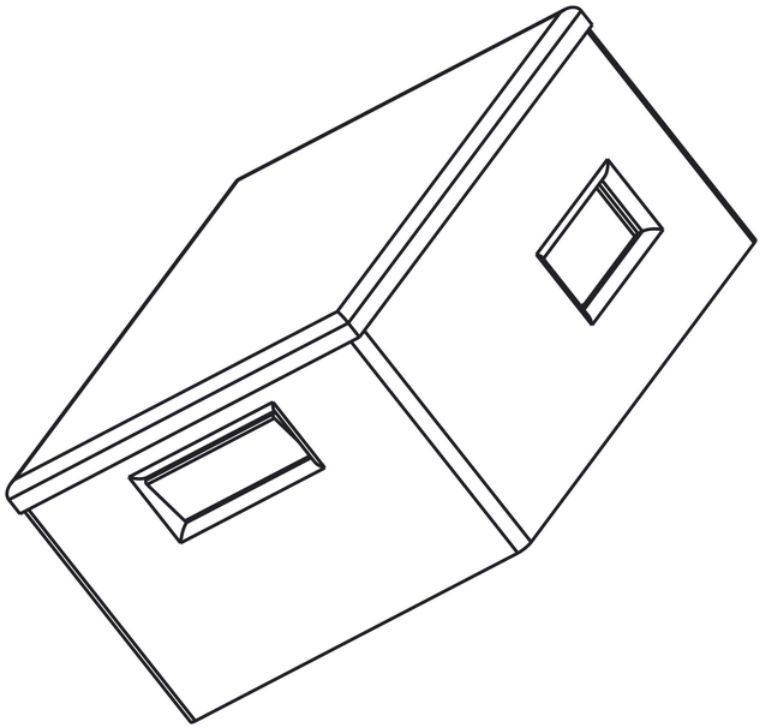

Drawn By: Timothy J Wilson	Material: PLA	MACQUARIE UNIVERSITY	
Student ID: 42868068	General Tolerance: ±0.1		
Date: 28/09/2017	Drafting Standard: AS 1100	Arduino Case	
Checked By: RDW	Projection:	Size: A4	Drawing No.: 7
Date: 28/09/2017		Scale: 1:1	Sheet: 1

Top View A

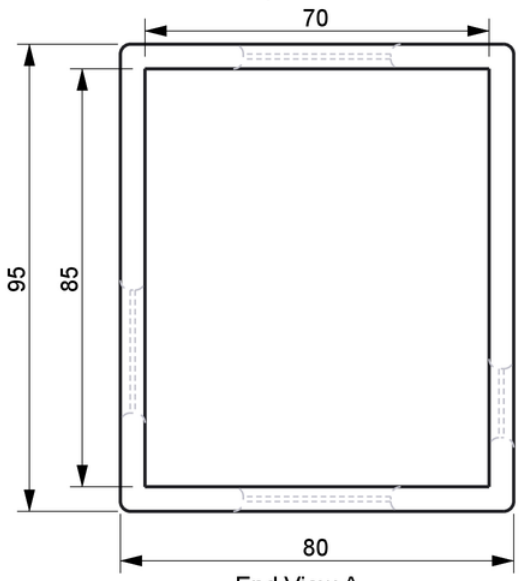

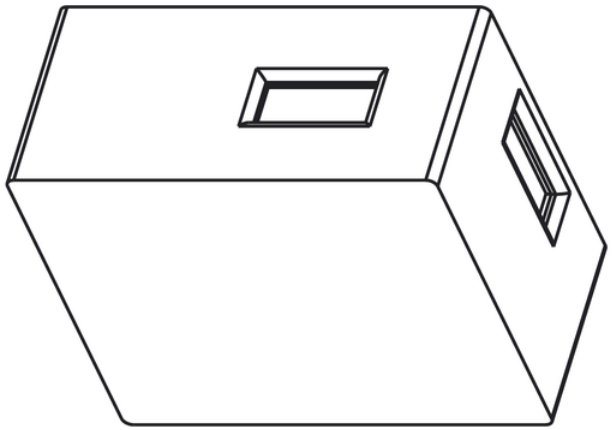

End View A

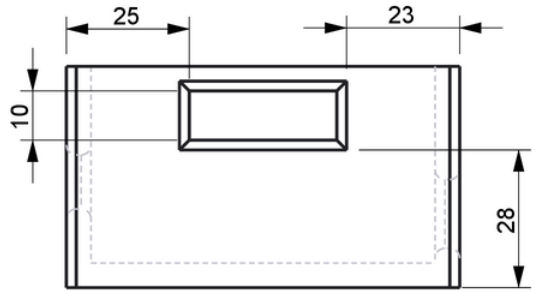

Left View A

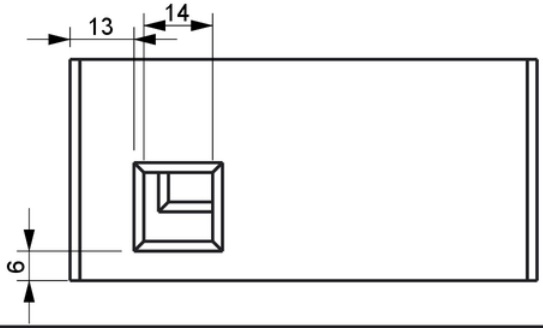

Drawn By:	Timothy J Wilson	Material:	PLA	MACQUARIE UNIVERSITY	
Student ID:	42868068	General Tolerance:	±0.1		
Date:	28/09/2017	Drafting Standard:	AS 1100	Arduino Case	
Checked By:	RDW	Projection:		Size: A4	Drawing No.: 7
Date:	28/09/2017			Scale: 4:5	Sheet: 2

Top View A

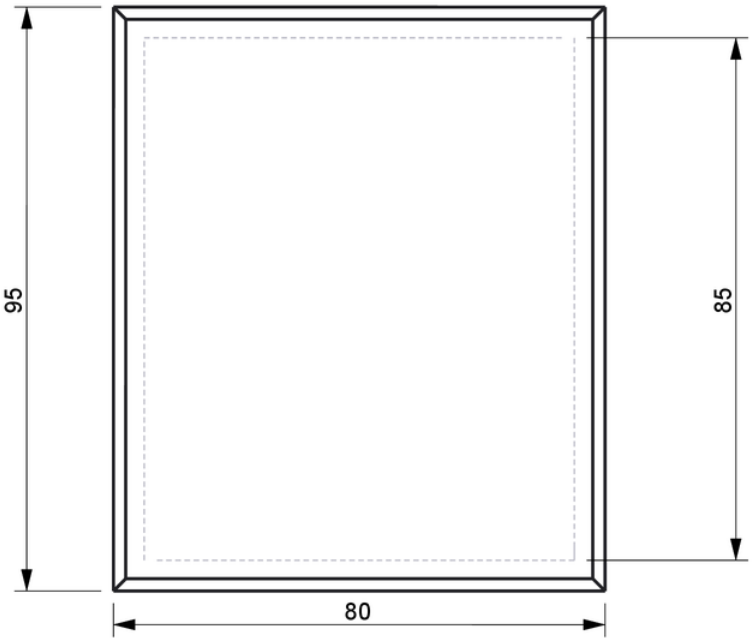

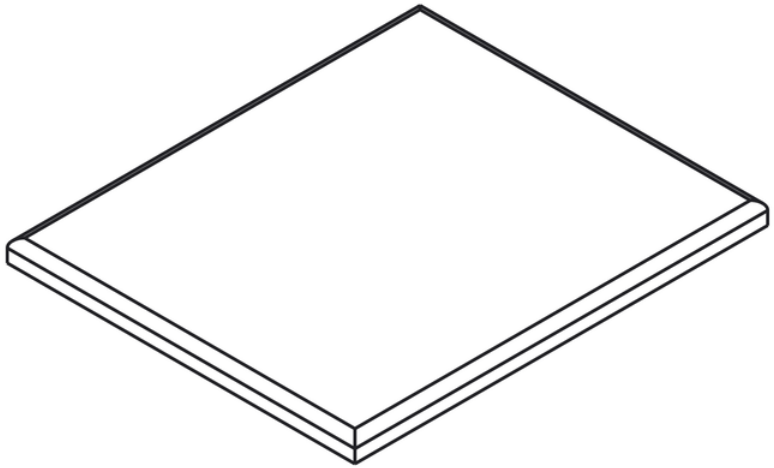

End View A

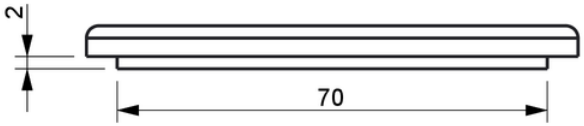

Drawn By:	Timothy J Wilson	Material:	PLA	MACQUARIE UNIVERSITY	
Student ID:	42868068	General Tolerance:	±0.1		
Date:	28/09/2017	Drafting Standard:	AS 1100	Case Lid	
Checked By:	RDW	Projection:		Size: A4	Drawing No.: 7
Date:	28/09/2017			Scale: 1:1	Sheet: 3

CHAPTER SEVEN

RESULTS

STRETCH AREA PERCENTAGE

To calculate the stretch percentage of the silicone, during the stretching operation the change in sheet surface area was calculated. The initial unstretched area was compared with the stretched area. The stretched area was calculated by determining the change in length between the stretching wells and the silicone support frame. During theses calculations the following assumptions where made;

1. There is uniform stretch across the whole surface
2. The force is uniformly applied to the silicone surface
3. There is no resistance between the stretching wells and the silicone sheet at the point of contact

These assumptions allowed for the calculations to be simplified giving approximate values for the stretch percentages. Based on these assumptions, the true stretch values should be very similar to the calculated ones.

Item	Formula	Value	Units
Stepper motor		200.00	Steps per Rotation
		1.80	Degrees per step
Stretching Range		6.00	mm
Upstretched Dimension			
X		130.00	mm
Y		86.00	mm
Upstretched Area	X ×Y = A	11180.00	mm^2
Stretched Dimension			
X*		133.64	mm
Y*		93.64	mm
Stretched Area	X* × Y* =A*	12513.14	mm^2
Percentage Change	=(ΔA -1) × 100	11.92	%
Steps in stretching range	200 × 6	1200.00	Steps
Percentage Change per step	11.924 / 1200	0.01	%
Screw Pitch		1.27	mm
		0.00635	mm per step
Total rotation over stretching range		4.72	Rotation
Total Steps in stretching range		944.88	

TABLE 2 STRETCH AREA PERCENTAGE TABLE

ACCELEROMETER RESULTS

The accelerometer was set to only measure the movement in the Z-axis and then compared to the recorded velocity with the theoretical velocity of 0.1 mm/s when the bed was traveling up and -0.01 mm/s when the bed was traveling down. The data was recorded and then graphed to show the trend and confirm that the velocity profile of the recorded data closely matched the theoretical values. The experiment was conducted three times. The following results were recorded with the raw data in Appendix D.

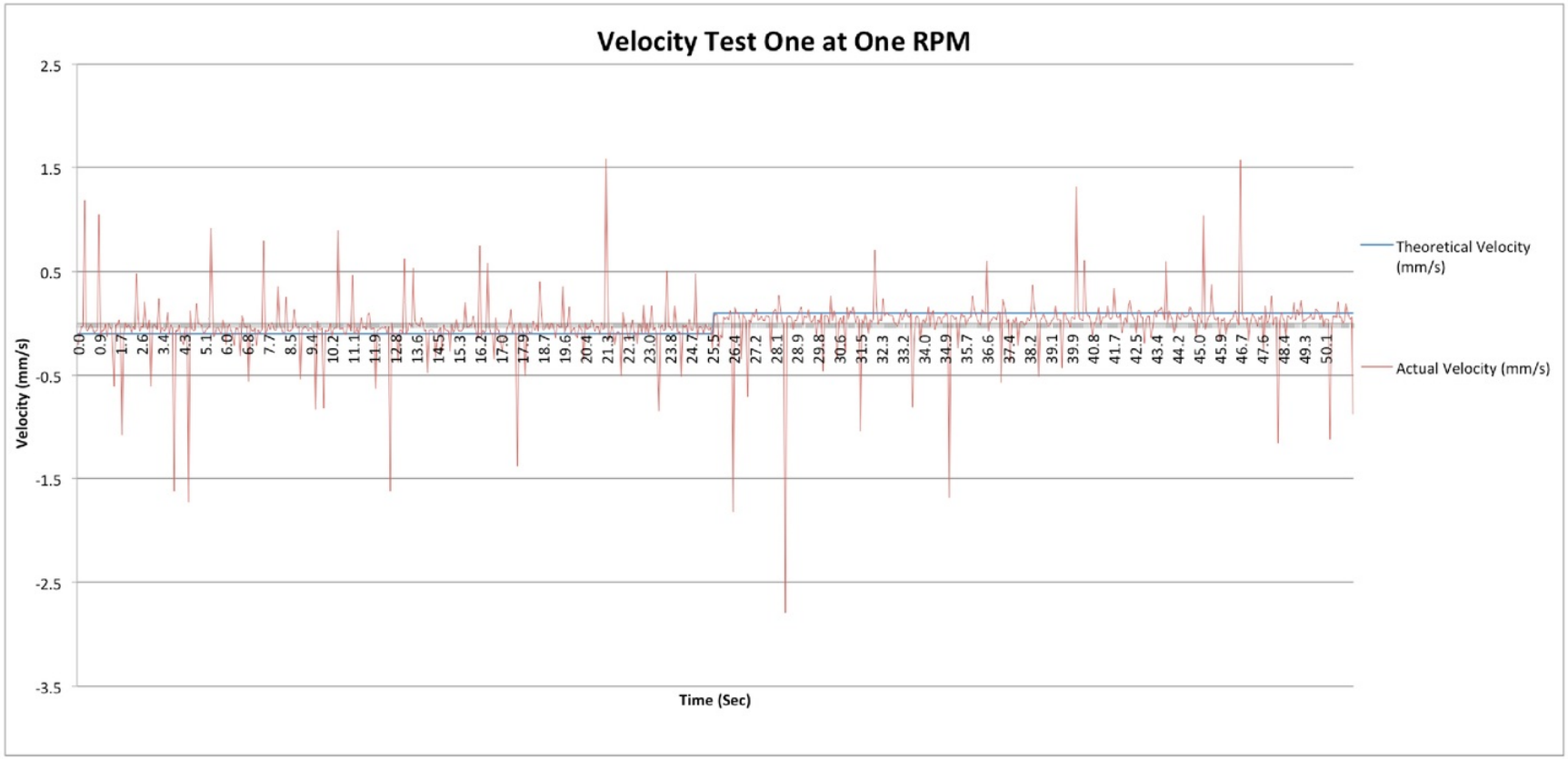

GRAPH 1 VELOCITY GRAPH TEST ONE

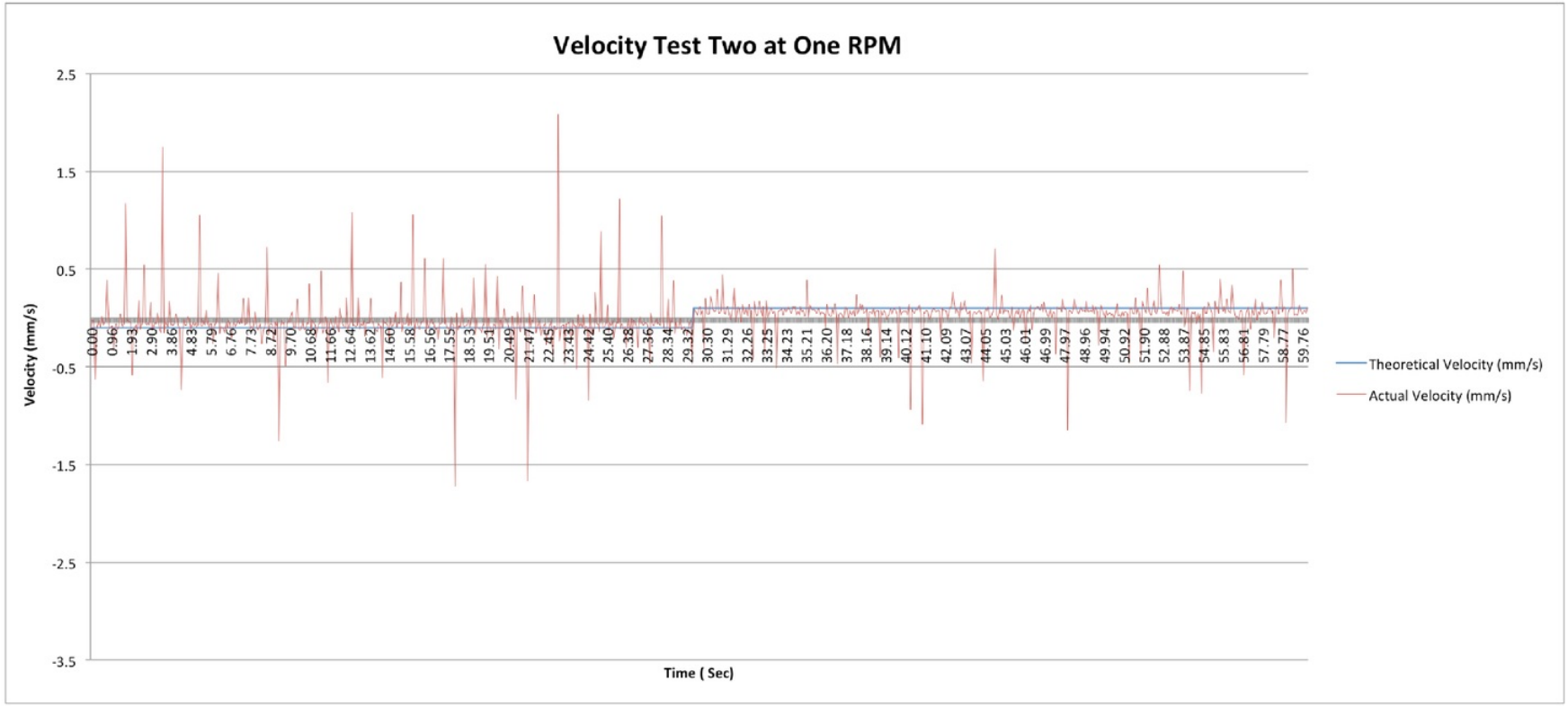

GRAPH 2 VELOCITY GRAPH TEST TWO

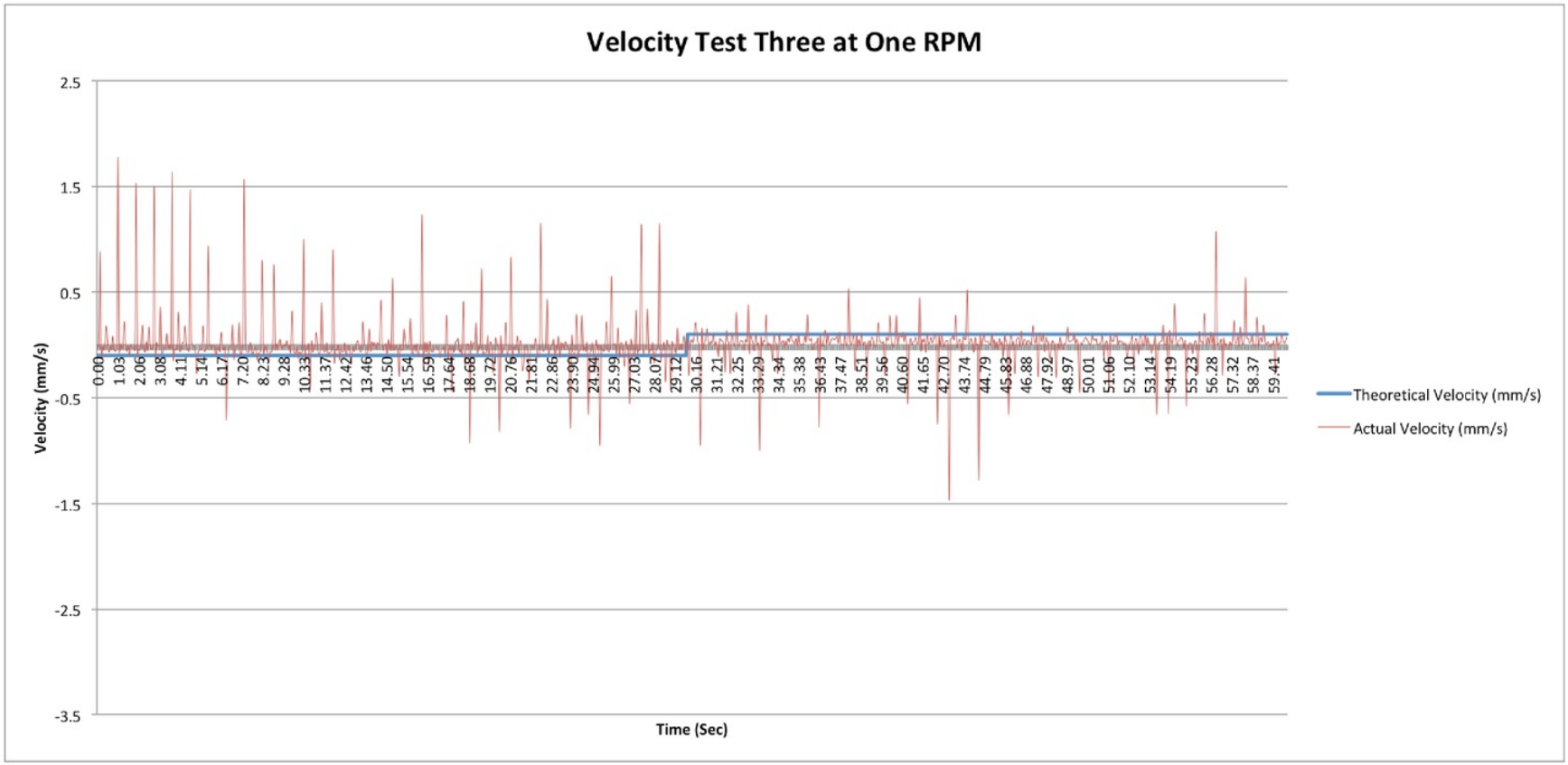

GRAPH 3 VELOCITY GRAPH TEST THREE

TENSILE STRESS TEST

To help determine if the device could produce repeatable and predictable results, the upper surface of the silicone sheet was subjected to a tensile stress test. This was achieved by placing the upper stretching plate, stretching wells, motors and the silicone sheet assembly into the tensile stress test apparatus. The tensile stress (g/mm^2) on the upper section of the sheet was calculated by using the strain gauge inside the Acaia Lunar scales. The force applied to the scales was used to determine the stress applied to the silicone sheet. The force applied to the scales was recorded every 50 steps while inside the stretching range. The scale indicated weight was then divided by the total surface area of the stretching wells to determine the tensile stress in g/mm^2. Results can be found in Appendix E.

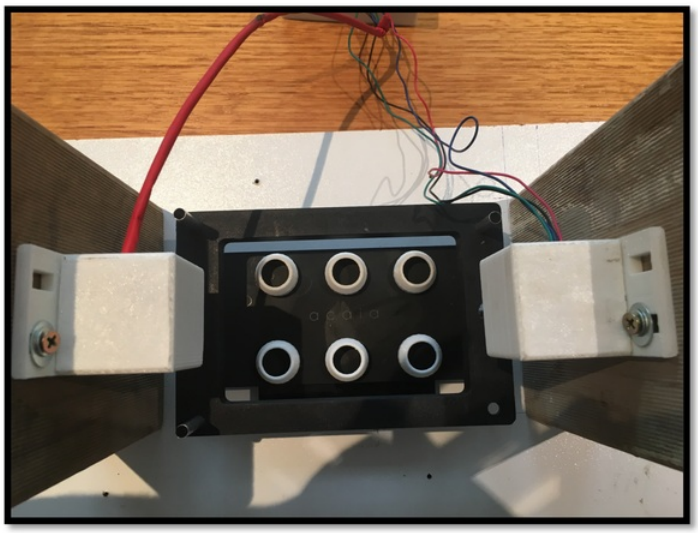

IMAGE 6 STRESS TESTING APPARATUS

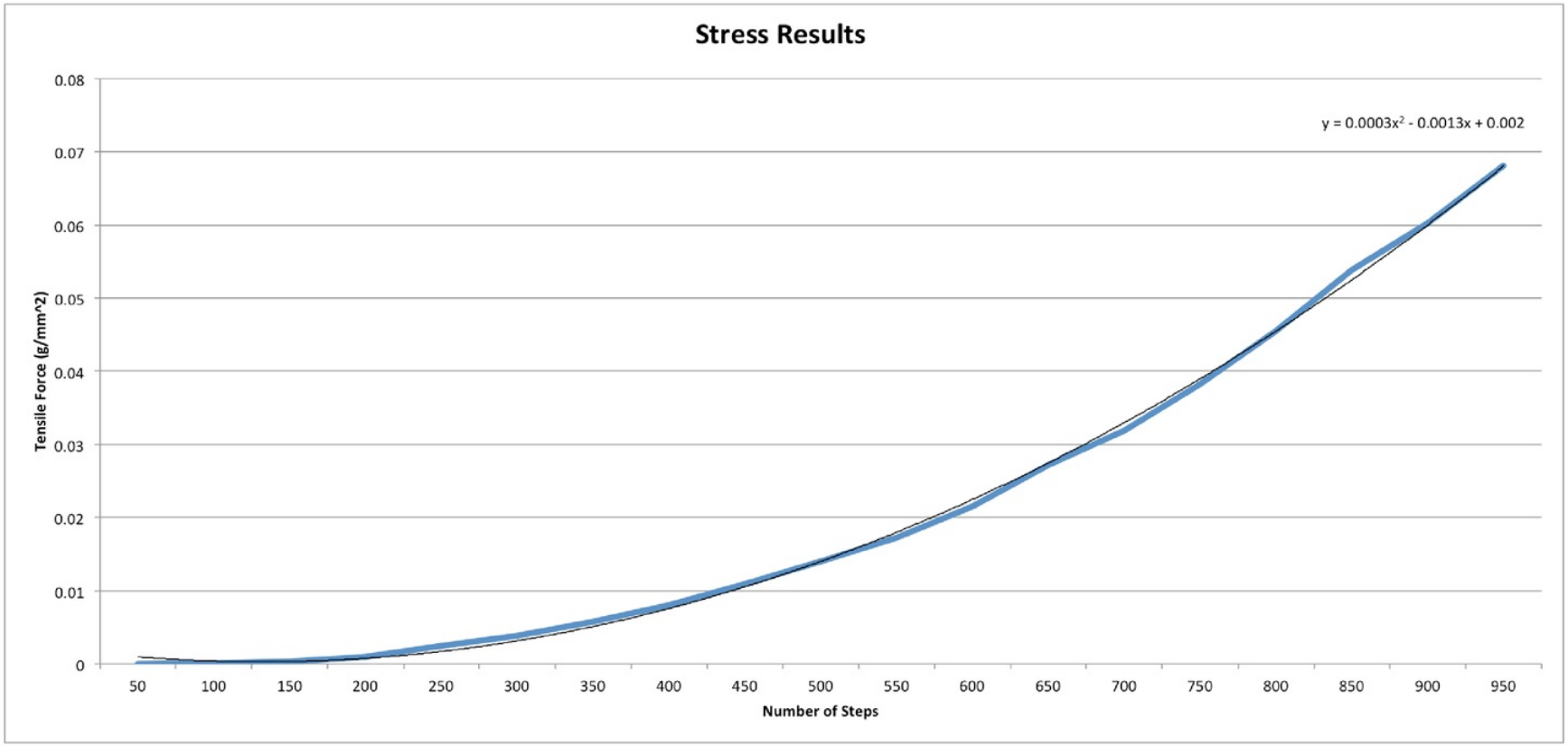

GRAPH 4 AVERAGE STRESS GRAPH

CHAPTER EIGHT

DISCUSSION

EVALUATION OF RESULTS

ACCELEROMETER

The cell-stretching device was fitted with a three-axis Adafruit accelerometer that took acceleration reading approximately every 0.06-second. These reading were used to show that the device did follow the theoretical velocity curve.

The motors were set to operate at the stretching speed of 0.11 mm/s, which was determined, based on research from similar devices to be the required stretching speeds. The motors took 100 steps down while in the 6 mm stretching range and then returned to their original position. This process took approximately 1 minute.

The accelerometer takes reading in the X, Y and Z planes, and for this reason it was critical the device and the accelerometer were perfectly leveled before testing commenced. If they were not the reading in the desired Z-axis would be impacted, as some of the movement would be occurring in the X and Y-axis. The accelerometer was attached with a thin layer of non-conductive adhesive. The accelerometer was leveled to ensure the velocity in the Z direction was recorded. The accelerometer was attached as close to the right hand side lead screw and lead nut as possible to help minimize lateral movement of the stretching plate as it travelled.

The accelerometer was controlled though the Arduino Mega and supporting code. This code was built around the accelerometers internal functions. The accelerometer algorithm for acceleration records the movement in three axis. The Z-axis component includes a gravity constant. The formula is;

$$Acc = \sqrt{(event.acceleration.x)^2 + (event.acceleration.y)^2 + (event.acceleration.z)^2} - g$$

This formula gives the velocity for the upper stretching plate. The time interval was calculated using the Arduinos internal oscillating clock. The internal clock on an Arduino calculates time in: seconds, mili-seconds or micro-seconds. To make the calculations micro-seconds were used, hence the time counter as in the order of millions. The internal oscillating clock is a 16 bit digital timer which starts recording time from initial power up. The timer was set to be a continuous count up time. To calculate the actual run time, the start time was subtracted from current time and then divided by 1 000 000 to give time in seconds. The time allowed for the actual velocities to be calculated (Arduino-info.wikispaces.com, 2017).

After conducting the experiment three times the resulting data was graphed in the results section. The recorded velocities were compared to the theoretical velocity of 0.1000 mm/s. After converting the motor RPM to a straight-line velocity, the speed was calculated to be 0.1108 mm/s. The theoretical velocity blue line was plotted on the same axis as the actual velocity.

The data shows that the actual velocity trends similarly to the theoretical velocity trend. The trends start at- 0.1mm/s at 30 seconds move to positive 0.1 mm/s. The negative velocity is the upper stretching plate moving in the stretch direction. The positive 0.1mm/s is the upper stretch plate moving back to its start position. A stepper motor is continuously cycling from zero speed to full speed with each step. The graphs have some outliers known as noise. The outliers are the result of the accelerometer measuring data, every 0.06 seconds, however the motor during some of those measurements is not at full acceleration. With the motor moving at one RPM the time between each step is greatly exaggerated and so the chance of the accelerometer taking a reading while the motor is in a stationary position is vastly increased which accounts for the large outliers which occur in all three of the graphs. Overall the graphs follow the trend of the velocity curve but have a lot of static interference, which is shown by the erratic movement of the result points as they follow the curve.

The average of the accelerometer reading for the first 30 second of the graphs were approximately –0.0564 mm/s. For the subsequent 30 second the readings on average were 0.0542 mm/s. The accelerometer readings on average for both directions were 0.05 mm/s below theoretical velocity of 0.1mm/s. This velocity issues can by resolved by increasing the shaft speed from 1 RPM to 2 RPMS. The accelerometer also took approximately 900 reading in the 1 minute test time, and because of this high number of reading some of the extreme outlier are less significant on the overall results of the experiment. The experiment still shows that the upper stretching plate moves at a relatively uniform velocity.

To run the accelerometer it required its own individual Arduino controlling board and independent laptop. This was due to the accelerometer requiring access to controlling pins, which are covered by an Arduino shield when it is attached to the Arduino. This could be avoided by using an Arduino Mega, because the shield does not cover the required pins. Further work is required to combine to remove the need for using two computers to run both sets of code, which would have streamlined the process.

Overall the results from the accelerometer test confirm that the device does move consistently during both static and dynamic testing.

STRETCH PERCENTAGE

The calculations for stretch percentage were based around the knowledge that the silicone sheet would be stretched in the Z-axis by a maximum of 6 mm. The 6 mm is found because the stretching wells protrude 12 mm above the lip the silicone support sits on and the total width of the silicone support is 6 mm. The result gives a 6 mm stretching area. The distances from the edge of the stretching well to the edge of the silicone support were also required to make the calculations. With this information and using the Cosine rule the necessary calculation to determine the increase in the length of the silicone was calculated.

The device is fitted with two ¼ inch BSW (British Standard Withworth) course thread lead screws, which have a pitch of 1.27 millimeters (Md Metric, 2015). From this the number of rotations and steps in the stretching range were calculated to be 4.72 rotations and 945 steps respectively for the full stretching range. With this information the progressive stretch percentages can be calculate. Due to the symmetry of the device the same level of stretch is assumed on all sides of the stretching area. The changes in the surface areas of the silicone sheets were calculated and so the total stretch percentage (change in surface area) was calculated. The total change in stretch was 12 percent, which can be increased by increasing the height of stretching wells or by reducing the height of the silicone support assembly. 12 percent stretch is far greater than the required stretch percentage as most brain cells are only stretched 50 to 100 micrometers in distance (Salvador, Neuhaus and Foerster, 2013). 50 to 100 microns is equivalent to approximately 20 which is approximately 40 degrees of 1 revolution.

This approach for calculating the stretch percentage relied on three assumptions;

1. There is uniform stretch across the whole surface
2. The force is uniformly applied to the silicone surface
3. There is no resistance between the stretching wells and the silicone sheet at the point of contact

Assumption one and two are linked and if one is true the other must also be true. The assumption that there is no resistance between the stretching wells and the silicone sheet is made to help simplify the mathematical calculation. All efforts were made to help reduce the coefficient of friction between stretching wells and the silicone sheet including sanding the tops of the wells with 1200 grit size in microns wet and dry and a Teflon lubricant was placed on top of each of the wells during the testing to further reduce the friction.

The original concept was to have the stretching wells machined out of PTFE due to its very low coefficient of friction and to help reduce the friction between the silicone sheet and the wells as much as possible. Due to time constraints this was not practical and the developed PLA substitutes with Teflon lubricant functioned as a replacement. The Teflon lubricant helped to reduce the friction between the stretching wells and the silicone sheet as much as possible, making assumption three a reasonable and practical assumption.

The results of the calculated stretch yields were consistent with theoretical predictions.

TENSILE STRESS TEST

To help determine if the device applied a predictable and expected amount of force to the stretching wells though the silicone sheet, tensile stress tests forces were simulated using a set of high precision scale to determine the forces applied. The device was disassembled and then re-assembled on the stress testing apparatus, as this allowed the set of high precision scales and the supporting plate to be placed below the stretching wells. Acaia Lunar scales were used which were calibrated prior to testing and measure to 0.1 g increments. The test recorded the force applied to the scales every 50 steps while inside the stretching range. This was repeated three times.

The results of the test showed that the force applied by the upper stretching plate onto the stretching well was a predictable force typically elastic, which follow a quadratic function. This elasticated force comes from the silicone-stretching sheet imparting force on the stretching wells and is not a linear or exponential function but a gradually increasing quadratic function. The increase in tensile force is characterized by the function.

$$y = 0.0003x^2 - 0.0013x + 0.002$$

The measured results of the test almost perfectly follows the curve of this quadratic. The results show a predictable and repeatable force was imparted onto the stretching wells. This test has further shown the reliability, functionality and readiness of the device for the use with live cells in laboratory conditions.

EVALUATION OF DEVICE

During the development of this device a range of issues and problems were required to be overcome to ensure that the device functioned to the desired level of operability and consistency.

PRINTING PARAMETERS

One of the primary issues with the initial stages of the devices development was determining the best parameters to use during the printing operations. During the 3D printing of the device, many parts were printed with differing 3D fills, layer heights and printing speed. This was primarily because some of the parts required a higher level of accuracy or increased strength compared to other parts. The lower and upper stretching beds were examples of this, they required a high level of accuracy in printing which achieved a small layer height, and high strength, which is correlated to an increased level of internal fill. Compared to the motor covers and the Arduino case, which required lower levels of accuracy and strength and so could have larger layer heights and reduced, fill quantities. During the design process each part had to be individually evaluated to determine the structural importance and impact that changing the layer height, extrusion heat and fill percentage would have on the component.

The ability to modify how the devices parts were printed allowed for many parts to be printed in minimal time and help to expedite the assembly process. The ability to individualize printing parameters also allowed for parts that required modifications to be quickly remade to meet these new parameters. This included reprinting the original stretching wells, motors supports and the case lid when the type of motor was changed and better designs were established.

BOWING

For the majority of the parts, 15 percent internal fill with four solid outer layers was sufficient and provided structural integrity. However some parts bowed and warped during printing. Bowing became a major issue while printing longer vertical section of the device especially while printing the motor supports. 3D components are printed directly onto the printed bed. The bowing and warping occurs because the bed temperature of 60 degrees is the glass

transition temperature of PLA. The glass transition temperature is the point where the plastic starts to transition from a hard glassy like plastic to a soft malleable substance and so the removal from the hot bed at the temperature caused the part to bend and then reset in its new shape.

After many conversations with Joel Raco and the supplier from Bilby3D who supply Macquarie University's 3D printing material it was decided that the bed temperature could be lowered to 55 degrees. 55 degrees would be ample to ensure that the produce would adhere to the bed during print whiles allowing removal and minimizing bowing post removal. This meant that the parts would not enter the glass transition phase after they had been printed and so stayed in their desired shape.

Hence the part improved were printed with minimal bowing and warping. This enabled the device to be set square and leveled allowing for an even force distribution and parts to be secured perpendicular to each other.

POLYTETRAFLUOROETHYLENE

When stretching cells by such small margins, friction and points of contact become crucial to the success of the cell stretching device. To help overcome the friction, the stretching wells were originally designed to be manufactured using PTFE. PTFE is a well know very low friction product, which is easily machined and turned, but due to its very high Young's Modulus and very low glass transition temperate, PTFE cannot be 3D printed. To machine these parts by hand would have been a very time consuming and costly process.

It was decided that the PTFE could be replaced with PLA substitute. The PLA stretching well would then be covered with a silicone membrane to help reduce the friction between the cell and the stretching membrane. The original device developed by Samer Toume, Amit Gefen and Daphne Weihs had PTFE stretching well which directly contacted the cell membrane. When deciding which material would act as a suitable replacement for the PTFE the choice was between two material; ABS and PLA both of which are 3D printable and simple to use. The key contributing factors were the Coefficient of Friction, Young's Modulus and Glass transition Temperature.

	Young's Modulus (MPa)	Glass Transition Temperature (°C)	Density (g/cm^3)	Biodegradable	Elongation Percentage* (%)	Coefficient of Friction* (μs)
PLA	37	60	1.3	Yes	6	0.2
ABS	27	105	1.2	No	50	0.8
PTFE	45	-100	2.3	No	650	0.04

TABLE 3 MATERIALS PROPERTIES TABLE

Up to the stated percentage under ideal conditions
(Brydson, 2001), (Harper, 2000), (Rae and Dattelbaum, 2004), (Khun and Liu, 2013), (Wang and Mano, 2007)

As is shown in the table above when PLA and ABS are compared, the Young's Modules of the PLA is much high than the ABS, which allows for an increased level of strength in the materials but also allows for the volume of fill to be reduced during the printing phase and still achieved the required level of strength. The lower glass transition temperature of 60 degrees compared to the 105 degrees of the ABS also means that less energy is required to print products made from PLA and because the products do not require a heated printing bed, they are less likely to warp and bend during printing. Further more, PLA is also biodegradable. The major disadvantage of using PLA in some application can be the lack of flexibility in the material. In the case of this project, this is not a disadvantage but a benefit, as the device requires rigidity. They key aspect of coefficient of friction also highly favors the PLA over the ABS as the PLA has four time less dynamic friction than ABS.

These factors made PLA the clear choice between the two products, but still the level of friction was far higher than the PTFE. To help further reduce the level of friction, the tops of the wells where coated with a dry PTFE lubricant.

DRIVE MOTORS

The device was originally designed to operate using two independently driven brushless DC motors with attached encoders. The motors needed the encoders attached so that the number of rotations the motor turned could be known and from this lead screw feed rate could be

calculated. The DC motors required a highly geared gearbox to be attached to the top of each motor to slow down the shaft speed to an appropriate RPM. After some initial testing and attempting to get the device to function using the DC motors, it was decided that the motors needed to be exchanged for a similar sized stepper motor. The primary issues with the encoders on the DC motors was they spun to fast for the Arduino to keep count of their current position, which meant that some of the time the motors would spin the require distances but other times the encoder would lose track of the number of steps and spin indefinitely. Absolute motor control is an essential requirement of the project and therfore the DC motors were no longer used. Two DC brushless motors powered the original device designed by Toume, Gefen and Weihs with encoders with an unknown gear reduction.

Exchanging the two DC motors for two NEMA 14 stepper motor solved this counting and control issue. The NEMA 14 stepper motors are small stepper motors typically used in 3D printing application. They are 200 step, 5 v direct driven stepper motors with both macro and micro step control where each step is 1/200 of 360 degrees or 1.8 degrees.

Without the motor change the cell-stretching device would not have worked adequately. The motor change allowed for accurate motor control of the upper stretching plate. The motors are wired in lock step, which ensure they move together and because of their shape developing an air tight enclosure was straightforward. The stepper motor coding was simpler and more efficient than the DC motor coding.

ARDUINO CODING

The device is controlled though open source Arduino hardware and software. The Arduino code was found on the Arduino open source website. The accelerometer was attached to the upper stretching plate. The basic code to operate the Adafruit accelerometer is provided with the accelerometer chip, and this code displays movement in the X, Y and Z axis which does not translate directly to a velocity change.

The Arduino was required to be coded to allow access to the internal oscillating clock to record time. The accelerometer code was modified to record position readings in the Z direction and ignore the gravity constant. The overall movement had to be combined to give a to velocity change over time. This coding could be further refined to calibrate the movement of the device against known standards.

The change from DC motors to Stepper motors and accompanying code allowed for absolute motor position and lead screw feed control.

LEAD SCREW

The lead screw provides the driving force for the upper stretching plate within the cell stretching apparatus. Initially a nylon lead screw was used. The nylon lead was too flexible and prone to uneven movement due to the nature of the soft material when it passed though the lead nut. The key advantage of the nylon lead screw was that due to the materials soft nature it was readily available and it was designed to attach to the motor shaft and the lead nut. The nylon lead screw did not prevent the upper stretching plate from flexing as it exerted force down onto the silicone sheet. The flexing of the nylon lead screw caused inconsistent movement as the upper stretching bed moved up and down the lead screws.

Replacing the nylon lead screw with a machined 6 mm steel lead screw rectified this issue. This provided a ridged point of contact and a smooth thread for the lead nut to move up and down. The steel lead screw had the thread machined off the upper and lower portions of it to allow for it be inserted into a machined hole in the bottom of the lower stretching bed. The upper section of the thread was machined to provide a parallel area. A PTFE collar was machined to connect the lead screw to the motor shaft. The original lead nut was also replaced with a larger brass collar, which was machined to have two horizontal groves cut into either side that accommodated cut outs in the upper stretching plate. The brass collar to upper stretching plate cut out was machined to have a small amount of clearance such that the brass collar did not influence the smooth operation of the upper stretching plate.

The accuracy and rigidity of the lead screw helped to improve and reduce the uneven movement in the upper stretching plate which was displaced when it was in motion.

SILICONE SHEET

Forming and setting the initial silicone required a number of iteration so that the silicone sheet case was the desired thickness and consistency. Originally the silicone mixture had a total volume of 20 grams, which was found to be too thin and did not provide uniform coverage. The volume was then increased to 30 grams, which provided an appropriately thick silicone sheet but excess silicone mixture overflowed the mould, which required trimming.

25 grams of silicone mixture was established as the required quantity for an appropriate sheet. The upper silicone support structure was upended into the setting mixture to form the retaining peg holes in the silicone sheet. The silicone sheet was trimmed to size using a sharp knife and secured into place.

UPPER STRETCHING PLATE MOVEMENT

After assembling the device and confirming the movement of the upper stretching plate, it was established that the stretching plate did not move uniformly. The upper stretching plate wobbled about the device longitudinal axis as it was in motion. The wobbling movement of upper stretching plate would potentially not apply even force over the whole surface of the silicone sheet and thus make the stretching tests non-uniform which meant the device would not meet the project objective. Furthermore this would make it difficult to measure the feed rate of the upper stretching plate.

The device required modification to minimize the wobble effect. Several alternatives were considered these included.

- Four motor and lead screw drive system
    - The four motors lead screw diving system potentially involved a motor and lead screw assembly in each corner of the device, which allowed for precision in the driving of the upper stretching plate. The advantage of this system is the increased level of accuracy. The disadvantage of this method is that the system does not replicate the original device and so does not comply with the design brief.
- 3D printed guiding walls
    - The 3D printed wall method used a series of supporting 3D printed walls to prevent the wobbling movement of the upper stretching plate. The walls would have been secured to the lower stretching bed. The advantage of this method was that it is simple to assemble and develop. The disadvantages were the reduction in visibility of the cell and equally as importantly, it is unlike that low cost 3D print could meet the required capability and the component accuracy to ensure smooth operation of the upper stretching plate

- Four guiding pegs
    - The guiding pags method involved providing alignment pegs and guides between the upper stretching plate and lower stretching plate. The steel guiding method entailed machining four perfectly vertical holes in each of the corners of the upper and lower stretching plates and the prevision of pegs and guides with suitable tolerances. The holes would have precision machined steel pegs (piano wire) inserted into the lower stretching plate and aluminium guide tube inserted into the upper stretching plate. The advantage of this was that the parts required to perform this are readily available and machined to suitable tolerance, which are ideal for this application. The disadvantage of this was that for the use of all four holes, the drilling had to be perfectly vertical and aligned.

After discussions with academics it was established that the four guiding pegs method was the most suitable given the suitability, time and cost consideration.

Four 6 mm diameter holes were machined in the corners of the device though both the upper and lower stretching plates. Four 70 mm piano wire pegs were secured into the holes in the lower stretching plate to act as guides for the aluminium guide tubes. The aluminium guide tubes were attached to the upper stretching plate. The piano wire and guide tubes ensured the upper and lower stretching plate moved in a coplaner relationship.

The four guiding peg impacted the device by altering the overall aesthetics however the four guiding pegs allowed the upper and lower stretching plates to move in coplanar and highly controllable motion. This also gave the device six points of contact between the two stretching plates.

DEVICE GEOMETRY

3D Print can produce rigid and accurate components. For the device to operative successfully, i.e. due to a very small stretching range less than 100 microns, the device needs to be both rigid and assembled to a high degree of accuracy.

The device design could be further modified to improve both the rigidity and the accuracy during assembly. The motor alignment was an important consideration in the device. It was observed that a misalignment of the motors and lead nut caused the nut to jam, which resulted in inconsistent forces applied to the upper stretching plate. The development of a test rig helped to establish if the motors, lead screw and base components did initially line up.

Ultimately ensuring that the device had surfaces which where perpendicular to each other enabled the product to function in the desired way.

During the assembly of the device and during the accelerometer testing it was important that the device was leveled in relation to the lower stretching plate, because the accelerometer measures movement in three axis and if the device is not leveled in relation to the lower stretching plate, the velocity will not be a true representation of the velocity of the upper stretching plate but a component of the velocity that the upper stretching plate is traveling.

To minimize the impact of leveling the device during the velocity-testing phase, the device was placed in the test assembly rig was pre-leveled. The leveled device allowed the accelerometer to be attached to the leveled surface of the upper stretching plate and provide results in only the Z-axis. Leveling further helped to aid the smooth motion of the upper stretching plate.

CELL BED

During the initial assembly and development of the project it was established that trying to acquire live cells for testing was beyond the available scope of the project. Access to a cell bed was constrained by time, cost and cell bed availability; time being the most prevalent. The result of not having access to the cell bed meant that it was difficult to confirm the correct functioning of the device. This was disappointing as the objective from the outset had been to test the device with live cells, and if the modifications to the design by Toume, Gefen and Weihs, 2016 were successful in making the device more accurate and capable of being used inside an incubator. The silicone proxy for the cell bed allowed for multiple iteration of the device to occur with no incurred additional cost.

As an alternative to testing the device with live cells, the device underwent extensive theoretical and practical examination to show that it was operating in the required way and had the finite movement control necessary to operate and provide accurate result.

INCUBATOR ENVIRONMENT

During the development of the device, Dr. Cheng and I discussed the requirement of the device to operate inside a cell incubator. An incubator grows cells at 37 degrees and 95 percent humidity. Operation of the device inside and incubator would require the electronic components of the device to be capable of with standing the incubator conditions. The motor data sheets specify that the motors are capable of operating up to 65 DegC. The Arduino hardware could be easily located external to the incubator, eliminating incubator conditions.

Stepper motor covers where developed and fitted to provide mechanical protection when operating the device.

ARDUINO HARDWARE CASING

Developing a casing for the Arduino hardware was a time consuming task, as the original designed push tab system did not provide the desired level of flexibility. PLA is approximate 5 percent flexible. The push tabs were originally sized at 3 mm thick and were reprinted 1 mm thick. Even rhen, the tabs would crack and break well before they flex far enough to enable the lid to be released.

After multiple iterations of lid printing it was decided that a tab system was not going to be an appropriate way to secure the lid to the Arduino casing. The lid system was redesigned to use an interference fit with a 1 millimeter lip eliminating the requirement for a flexible tab.

INCREASED COST

The development of the device had a number of iterations, which added to the cost of the project. The components, which were modified, include the stepper motors in lieu of DC motors, the Accelerometer and the Arduino Mega. The new parts accounted for around two hundred dollars with the majority of that being accounted for by the two new stepper motors. Each stepper motor was $45.

The overall base price for the device re-engineered excluding re-purchased components was AU $246 when compared to the actual build price of AU $416.

MODIFICATIONS TO SAMER TOUME, AMIT GEFEN AND DAPHNE WEIHS DESIGN

The objective of this project was to replicate the research conducted by Samer Toume, Amit Gefen and Daphne Weihs in their 2016 research article “Printable Low-Cost, Sustained And Dynamic Cell Stretching Apparatus”. After device assembly, testing and further development, the device that was developed was very similar to the design by Samer Toume, Amit Gefen and Daphne Weihs. The prototype developed for this project has a number of difference features to the cell stretching apparatus developed by Samer Toume, Amit Gefen and Daphne Weihs. The device has the same basic components and appearance but enhancements to improve the coplanar operation and motion control.

Samer Toume, Amit Gefen and Daphne Weihs powered their device though two DC brushless motors, which in this device were replaced with two NEMA 14 stepper motors. The DC motors allowed for a smooth movement between one direction and another but lacked the same degree of control, which is found using stepper motors. The DC motors also required the use of encoders to determine how many rotations the lead screw shaft had taken. DC

motors are still an appropriate motor for this task, however the selected DC motors and control system did not provide the required lead screw control. Stepper motor was selected and coupled with the Arduino hardware, though this the necessary lead screw control was achieved.

Samer Toume, Amit Gefen and Daphne Weihs cell stretching apparatus used PTFE stretching wells, which was the original intention for this device also. The PTFE, which was replaced by the current PLA wells, and has a lower coefficient of friction and so reduce the force required to stretch the cells. The original PTFE wells are a better long-term choice over the current PLA substitutes. Samer Toume, Amit Gefen and Daphne Weihs cell stretching apparatus does not have a silicone-stretching sheet and the accompanying support structure. The original document does not specify how the cells are grown or connected to the stretching apparatus, and so the silicone sheet and supporting structure were developed as a proxy for the cell bed.

Samer Toume, Amit Gefen and Daphne Weihs cell stretching apparatus was also not designed with protective casing so that it could be placed in an incubator for extended periods of time. The development of these mechanical protections gives the device some more practical uses and enables it to operate in different environments when compared to Samer Toume, Amit Gefen and Daphne Weihs cell stretching apparatus.

The modifications that have made to the original cell stretching apparatus have been an improvement.

OVERALL EVALUATION

Despite not having tested this cell stretching device with live cells I believe that this has been a successful experiment and thesis paper. The device has completed all of its necessary test and performed to the required levels of accuracy and consistency of data, which supports this claim. The device is not exactly the same as Samer Toume, Amit Gefen and Daphne Weihs original apparatus but achieves the same objectives and achieves the same from and fit to apply force to the cells. Overall I am very pleased with the outcomes of the project.

The use of 3D printing for the body components of this device has allowed for a very flexible design, which is simply, quickly and efficiently modified to suit device development. For this reason along with the accuracy and rigidity requirements discussed previously I believe that this has been a successful thesis project and shows the importance and place that low cost 3D printed medical equipment has in the future in the biomedical industry.

CHAPTER TEN

CONCLUSION

This project has shown that it is possible to build a modified Samer Toume, Amit Gefen and Daphne Weihs low cost cell stretching device for less than $500. The project also establishes that 3D printed device coupled with the digital controls has the necessary consistency and accuracy for cell stretching. The modifications which were made to Samer Toume, Amit Gefen and Daphne Weihs cell stretching apparatus have enhanced the device capabilities.

This project outlines modifications to the prototype developed by Samer Toume, Amit Gefen and Daphne Weihs. The cell stretching device was assembled, tested and modified resulting in a device which met the objectives of this project.

The project shows the legitimacy of the work conducted by Samer Toume, Amit Gefen and Daphne Weihs with enhancements including capabilities to operate in an incubator environment. I believe that this has been successful and has met all of the project objectives. This research paper confirms that low cost cell stretching is accessible to small biomechanical laboratories.

CHAPTER ELEVEN

FUTURE WORKS

The PLA stretching wells should be replaced with PTFE low resistance plastic wells as proposed by Samer Toume, Amit Gefen and Daphne Weihs. The PTFE has a much lower coefficient of friction and a smoother contact point with the silicone sheet or cell bed. PTFE would reduce the impact of catching and sticking between the silicone and stretching wells, which could cause uneven stretching.

The device could be redesigned to incorporate a cube-like supporting structure. The cube supporting structure would increase the strength and rigidity of the device helping to minimize the flexibility, which is found in the motor supports. The cube could have modified motor supports and an upper supporting frame, which would brace the top of the device. A cube structure would allow the same form, fit and function but improve the overall rigidity. This increased rigidity would help to eliminate motor miss alignment and improve the uniform driving force.

This supporting cube could be coupled with four corners driving motors and lead screws, rather than the two centralized motors. This four motor system would remove the need for the four guiding pegs and aluminium guide tubes. Furthermore the use of the four motor system and the cube supporting structure would eliminate any wobble which occurs as the upper stretching bed is lowered onto the silicone sheet.

The PLA parts including the motor support could be re-printed with higher-level internal fill. The chosen fill level and PLA 3D printed material resulted in some of the parts not being entirely straight and true which made alignments difficult. If the parts had an increased fill percentages, this could reduce the issues and increase the strength of the entire device making it more rigid. The increased fill, cube supporting structure and four motors system coupled together would increase the devices accuracy and ridged.

The operational coding for the device could also be improved to make it more intuitive. The human machine interface (HMI) could be improved to be more operator friendly. The current control software requires the user to modify the code to operate the device. The HMI could also integrate the coding for the accelerometer providing a single user interfaces. The four motor system coupled with modified coding would allow for the device to not only be used to apply an even force to the cell bed but an uneven force, which could help in future research.

Once all of these modifications are made, live cell testing should occur on the device. Live cell testing was unfortunately unobtainable during this project but was the ultimate objective and the purpose of this device.

When these tasks are completed, 3D printed low cost medical apparatuses will be more commonly used in medical laboratories worldwide.

REFERENCES

1. Anzalone, G., Chenlong Zhang, Wijnen, B., Sanders, P. and Pearce, J. (2013). A Low-Cost Open-Source Metal 3-D Printer. IEEE Access, 1, pp.803-810.

2. Arduino.cc. (2017). Arduino - Home. [Online] Available at: https://www.arduino.cc/ [Accessed 26 Oct. 2017].

3. Arduino-info.wikispaces.com. (2017). arduino-info - Timers-Arduino. [online] Available at: https://arduino-info.wikispaces.com/Timers-Arduino [Accessed 21 Aug. 2017].

4. Bax, B. and Müssig, J. (2008). Impact and tensile properties of PLA/Cordenka and PLA/flax composites. Composites Science and Technology, 68(7-8), pp.1601-1607.

5. Biswas, S. and Vijayan, K. (1992). Friction and wear of PTFE — a review. Wear, 158(1-2), pp.193-211.

6. Brydson, J. (2001). Plastics materials. 7th ed. Oxford: Butterworth-Heinemann.

7. Burris, D. and Sawyer, W. (2006). A low friction and ultra low wear rate PEEK/PTFE composite. Wear, 261(3-4), pp.410-418.

8. Fisher, D. and Gould, P. (2012). Open-Source Hardware Is a Low-Cost Alternative for Scientific Instrumentation and Research. Modern Instrumentation, 01(02), pp.8-20.

9. Foo, C, Chai, G and Seah, L. (2007) "Mechanical properties of Nomex material and Nomex honeycomb structure", *Composite Structures*, vol. 80, no. 4, pp. 588-594.

10. Goyanes, A., Buanz, A., Basit, A. and Gaisford, S. (2014). Fused-filament 3D printing (3DP) for fabrication of tablets. International Journal of Pharmaceutics, 476(1-2), pp.88-92.

11. Harper, C. (2000). Modern plastics handbook. New York: McGraw-Hill.

12. Hamad, K., Kaseem, M., Yang, H., Deri, F. and Ko, Y. (2015). Properties and medical applications of polylactic acid: A review. Express Polymer Letters, 9(5), pp.435-455.

13. Huang, L., Mathieu, P. and Helmke, B. (2010). A Stretching Device for High-Resolution Live-Cell Imaging. Annals of Biomedical Engineering, 38(5), pp.1728-1740.

14. Hunt, E., Zhang, C., Anzalone, N. and Pearce, J. (2015). Polymer recycling codes for distributed manufacturing with 3-D printers. Resources, Conservation and Recycling, 97, pp.24-30.

15. Kamble, H., Barton, M., Jun, M., Park, S. and Nguyen, N. (2016). Cell stretching devices as research tools: engineering and biological considerations. Lab Chip, 16(17), pp.3193-3203.

16. Kaspar, D., Seidl, W., Neidlinger-Wilke, C., Ignatius, A. and Claes, L. (2000). Dynamic cell stretching increases human osteoblast proliferation and CICP synthesis but decreases osteocalcin synthesis and alkaline phosphatase activity. Journal of Biomechanics, 33(1), pp.45-51.

17. Khun, N. and Liu, E. (2013). Thermal, mechanical and tribological properties of polycarbonate/acrylonitrile-butadiene-styrene blends. Journal of Polymer Engineering, 33(6).

18. King, D., Babasola, A., Rozario, J. and Pearce, J. (2014). Mobile Open-Source Solar-Powered 3-D Printers for Distributed Manufacturing in Off-Grid Communities. *Challenges in Sustainability*, 2(1).

19. Lipsa, R., Tudorachi, N. and Vasile, C. (2010). Poly(α-hydroxyacids) in biomedical applications: synthesis and properties of lactic acid polymers. e-Polymers, 10(1).

20. Lötters, J., Olthuis, W., Veltink, P. and Bergveld, P. (1997). The mechanical properties of the rubber elastic polymer polydimethylsiloxane for sensor applications. Journal of Micromechanics and Microengineering, 7(3), pp.145-147.

21. Mathew, A., Oksman, K. and Sain, M. (2005). Mechanical properties of biodegradable composites from poly lactic acid (PLA) and microcrystalline cellulose (MCC). Journal of Applied Polymer Science, 97(5), pp.2014-2025.

22. Md Metric. (2015). MARYLAND METRICS THREAD DATA CHARTS. [online] Available at: https://mdmetric.com/tech/thddat8.htm [Accessed 26 Sep. 2017].

23. Mpkb.org. (2017). Differences between in vitro, in vivo, and in silico studies (MPKB). [online] Available at: https://mpkb.org/home/patients/assessing_literature/in_vitro_studies [Accessed 2 Aug. 2017].

24. NILSSON. E and NILSSON. A. (2002). "Prediction And Measurement Of Some Dynamic Properties Of Sandwich Structures With Honeycomb And Foam Cores", *Journal of Sound and Vibration*, vol. 251, no. 3, pp. 409-430.

25. "Official Flashforge Store | Creator X Dual Extrusion 3D Printer". Flashforge-usa.com. N.p., 2017. Web. 13 August 2017

26. Oksman, K., Skrifvars, M. and Selin, J. (2003). Natural fibers as reinforcement in polylactic acid (PLA) composites. Composites Science and Technology, 63(9), pp.1317-1324.

27. Pearce, J. (2012). Building Research Equipment with Free, Open-Source Hardware. Science, 337(6100), pp.1303-1304.

28. Playground.arduino.cc. (2017). Arduino Playground - RotaryEncoders. [online] Available at: http://playground.arduino.cc/Main/RotaryEncoders#Libraries [Accessed 26 Aug. 2017].

29. Pouzada, A., Ferreira, E. and Pontes, A. (2006). Friction properties of moulding thermoplastics. Polymer Testing, 25(8), pp.1017-1023.

30. Rae, P. and Dattelbaum, D. (2004). The properties of poly(tetrafluoroethylene) (PTFE) in compression. Polymer, 45(22), pp.7615-7625.

31. Saharudin. M. (2016). "Development of tilt-rotor unmanned aerial vehicle (UAV): material selection and structural analysis on wing design", *IOP Conference Series: Materials Science and Engineering*, vol. 152.

32. Salvador, E., Neuhaus, W. and Foerster, C. (2013). Stretch in Brain Microvascular Endothelial Cells (cEND) as an In Vitro Traumatic Brain Injury Model of the Blood Brain Barrier. US National Library of Medicine, (80).

33. Senatov, F., Niaza, K., Zadorozhnyy, M., Maksimkin, A., Kaloshkin, S. and Estrin, Y. (2016). Mechanical properties and shape memory effect of 3D-printed PLA-based porous scaffolds. Journal of the Mechanical Behavior of Biomedical Materials, 57, pp.139-148.

34. Shapiro, A., Gray, M., Schaffer, J., Wright, J. and Venegas, J. (1994). Cell stretching Method. US5348879 A.

35. Store.arduino.cc. (2017). Arduino Mega 2560 Rev3. [online] Available at: https://store.arduino.cc/usa/arduino-mega-2560-rev3 [Accessed 26 Oct. 2017].

36. Toume, S., Gefen, A. and Weihs, D. (2016). Printable low-cost, sustained and dynamic cell stretching apparatus. Journal of Biomechanics, 49(8), pp.1336-1339.

37. Tymrak, B., Kreiger, M. and Pearce, J. (2014). Mechanical properties of components fabricated with open-source 3-D printers under realistic environmental conditions. Materials & Design, 58, pp.242-246.

38. Wang, Y. and Mano, J. (2007). Biodegradable poly(L-lactic acid)/poly(butylene succinate-co-adipate) blends: Miscibility, morphology, and thermal behavior. Journal of Applied Polymer Science, 105(6), pp.3204-3210.

39. Wang, J. and Thampatty, B. (2006). An Introductory Review of Cell Mechanobiology. Biomechanics and Modeling in Mechanobiology, 5(1), pp.1-16.

40. Wang, J., Yang, G. and Li, Z. (2005). Controlling Cell Responses to Cyclic Mechanical Stretching. Annals of Biomedical Engineering, 33(3), pp.337-342.

41. Wittbrodt, B. and Pearce, J. (2015). The effects of PLA color on material properties of 3-D printed components. Additive Manufacturing, 8, pp.110-116.

42. Wohlers, T. (2014). Tracking Global Growth in Industrial-Scale Additive Manufacturing. 3D Printing and Additive Manufacturing, 1(1), pp.2-3.

43. Zhang, C., Anzalone, N., Faria, R. and Pearce, J. (2013). Open-Source 3D-Printable Optics Equipment. PLoS ONE, 8(3), p.e59840.

APPENDIX A

INITIAL TEST CODE OF LED LIGHT TEST

```
int leadPin = 13;

void setup()
{

    pinMode(leadPin, OUTPUT);

}

void loop()
{

    digitalWrite(leadPin, HIGH);
    delay(5000);
    digitalWrite(leadPin, LOW);
    delay(5000);
    digitalWrite(leadPin, HIGH);
    delay(3000);
    digitalWrite(leadPin, LOW);
    delay(1000);
    digitalWrite(leadPin, HIGH);
    delay(10000);
```

```
}
```

End Code.

APPENDIX B

STEPPER MOTOR CODE

```
#include <AFMotor.h>

AF_Stepper motorAlpha(200, 2);  // Steps in Motor, Phase



void setup() {
  Serial.begin(9600);
  Serial.println("Stepper test!");

  motorAlpha.setSpeed(10);  // RPM
  Serial.println("Motor Speed = 10 ");
}

void loop() {
  /*
  Serial.println("Single coil steps Forward");
  motorAlpha.step(1000, FORWARD, SINGLE);

  Serial.println("Single coil steps Backward");
  motorAlpha.step(1000, BACKWARD, SINGLE);

  Serial.println("Single coil steps Stop");
  motorAlpha.setSpeed(0);

*/
```

```
  Serial.println("Micrsostep steps Up");
 //motorAlpha.step(2000, FORWARD, MICROSTEP);  // No. of Steps, Direction, Type


  Serial.println("Micrsostep steps Down");
  motorAlpha.step(200, BACKWARD, MICROSTEP);


  Serial.println("Micrsostep steps Stop");
  motorAlpha.setSpeed(0);

}
```

APPENDIX C

ACCELEROMETER CODE

```
#include <Wire.h>
#include <Adafruit_MMA8451.h>
#include <Adafruit_Sensor.h>
#include <AFMotor.h>

AF_Stepper motorAlpha(200, 2);

Adafruit_MMA8451 mma = Adafruit_MMA8451();

// Mathematical Constants
double pi = 3.14159265358979323846264338327;

//clock
float myClock = -1;
float now;
float cycleTime = 3000000 * 2; //us
float startTime = -1;
// Velocity time relationship variables
float maxVelocity = 2; // mm/s
float velocity = maxVelocity * sin((2 * pi) / (cycleTime) * (micros())); // mm/s

float mmaXo;
float mmaYo;
float mmaZo;
float a; // Theoretical acceleration
float acc; // Actual acceleration
```

```
float g;
float t;

// Sine wave
const float A = 0.1; // Max velocity
const float B = pi / 2; // Coefficient of t
const float T = 2 * pi / B; // Peroid of oscillation
const float F = 1 / T; // Frequency of oscillation
const float C = 0; // x axis offset
const float D = 0; // y axis offset
boolean oscillate = true;

void setup(void) {
  Serial.begin(9600);

 motorAlpha.setSpeed(10);  // RPM

 Serial.println("Accelerometer");

 if (! mma.begin()) {
  Serial.println("Couldnt start");
  while (1);
 }
 Serial.println("MMA8451 found!");

 mma.setRange(MMA8451_RANGE_2_G);

 Serial.print("Range = "); Serial.print(2 << mma.getRange());
 Serial.println("G");
  // Set initial acceleration values to eliminate acceleration due to the Earth
```

```
  mma.read();
  sensors_event_t event;
  mma.getEvent(&event);
  mmaXo = event.acceleration.x;
  mmaYo = event.acceleration.y;
  mmaZo = event.acceleration.z;
  g = sqrt(pow(event.acceleration.x, 2) + pow(event.acceleration.y, 2) +
pow(event.acceleration.z, 2));
  Serial.println("Inital acceleration values due to gravity.");
  Serial.print("X: \t"); Serial.print(mmaXo); Serial.print("\t");
  Serial.print("Y: \t"); Serial.print(mmaYo); Serial.print("\t");
  Serial.print("Z: \t"); Serial.print(mmaZo); Serial.print("\t");
  Serial.println("m/s^2 ");
  Serial.print("Gravity: \t"); Serial.print(g); Serial.print("\t");
  Serial.println("m/s^2");
// End setup
  Serial.println("------------------------------------------------------------");
  delay(500);
}

void loop() {
 // Clock reset
  if (myClock == -1) {
    myClock = micros();
    startTime = micros();
  }
// Actual time, Velocity, Acceleration
  t = micros() * pow(10, -6);
  velocity = A;// mm/s
  a = A * B * cos(B * t);
```

```
 mma.read();
 //Serial.println("Acceleration");

 //Serial.print("\t Time:\t"); Serial.print(micros()); Serial.print("\t");
 //Serial.print("X:\t"); Serial.print(mma.x); Serial.print("\t");
 //Serial.print("\tY:\t"); Serial.print(mma.y); Serial.print("\t");
 //Serial.print("\tZ:\t"); Serial.print(mma.z); Serial.print("\t");

 //Serial.println(" ");

 /* Get a new sensor event */
 sensors_event_t event;
 mma.getEvent(&event);

acc = sqrt(pow(event.acceleration.x, 2) + pow(event.acceleration.y, 2) +
pow(event.acceleration.z, 2)) - g;

 /* Display the results (acceleration is measured in m/s^2) */
 Serial.print("\t Time:\t"); Serial.print(micros()); Serial.print("\t");
 //Serial.print("X: \t"); Serial.print(event.acceleration.x); Serial.print("\t");
 //Serial.print("Y: \t"); Serial.print(event.acceleration.y); Serial.print("\t");
 Serial.print("Z: \t"); Serial.print(event.acceleration.z); Serial.print("\t");
 Serial.print("\tacc:\t");Serial.print(acc); Serial.print("\t");
 //Serial.print("\tActual A:\t");Serial.print(a); Serial.print("\t");
 Serial.print("\tVelocity:\t");Serial.print(velocity); Serial.print("\t");
 Serial.println("mm/s^2 ");
 }
```

APPENDIX D

RESULTS

TEST ONE

Time (sec)	Theoretical Velocity (mm/s)	Actual Velocity (mm/s)
0.0	-0.1	-0.21
0.1	-0.1	-0.11
0.1	-0.1	-0.03
0.2	-0.1	-0.03
0.3	-0.1	1.19
0.3	-0.1	-0.05
0.4	-0.1	-0.08
0.5	-0.1	-0.03
0.5	-0.1	-0.01
0.6	-0.1	-0.05
0.7	-0.1	-0.09
0.7	-0.1	-0.08
0.8	-0.1	-0.06
0.9	-0.1	1.05
0.9	-0.1	-0.14
1.0	-0.1	-0.07
1.0	-0.1	-0.07
1.1	-0.1	-0.01
1.2	-0.1	-0.13
1.2	-0.1	0
1.3	-0.1	-0.05
1.4	-0.1	-0.05
1.4	-0.1	-0.61
1.5	-0.1	-0.02
1.6	-0.1	-0.02
1.6	-0.1	0.03
1.7	-0.1	-0.07
1.8	-0.1	-1.08
1.8	-0.1	-0.12
1.9	-0.1	0.01
2.0	-0.1	-0.04
2.0	-0.1	-0.02
2.1	-0.1	-0.04
2.2	-0.1	-0.09
2.2	-0.1	-0.03
2.3	-0.1	-0.06

2.4	-0.1	0.48
2.4	-0.1	0.06
2.5	-0.1	-0.08
2.6	-0.1	-0.03
2.6	-0.1	-0.04
2.7	-0.1	0.21
2.7	-0.1	0
2.8	-0.1	-0.06
2.9	-0.1	0.03
2.9	-0.1	-0.61
3.0	-0.1	-0.03
3.1	-0.1	-0.01
3.1	-0.1	-0.03
3.2	-0.1	-0.06
3.3	-0.1	0.24
3.3	-0.1	-0.09
3.4	-0.1	-0.04
3.5	-0.1	-0.08
3.5	-0.1	-0.04
3.6	-0.1	0.11
3.7	-0.1	-0.11
3.7	-0.1	-0.02
3.8	-0.1	-0.05
3.9	-0.1	-1.62
3.9	-0.1	-0.07
4.0	-0.1	-0.08
4.1	-0.1	-0.02
4.1	-0.1	-0.13
4.2	-0.1	-0.17
4.3	-0.1	-0.21
4.3	-0.1	-0.04
4.4	-0.1	-0.04
4.4	-0.1	-1.73
4.5	-0.1	0.12
4.6	-0.1	-0.05
4.6	-0.1	-0.07
4.7	-0.1	-0.07
4.8	-0.1	0.19
4.8	-0.1	0
4.9	-0.1	-0.01
5.0	-0.1	-0.02
5.0	-0.1	-0.08
5.1	-0.1	-0.1
5.2	-0.1	-0.06
5.2	-0.1	-0.05

5.3	-0.1	-0.03
5.4	-0.1	0.92
5.4	-0.1	-0.13
5.5	-0.1	-0.12
5.6	-0.1	-0.05
5.6	-0.1	-0.04
5.7	-0.1	-0.08
5.8	-0.1	-0.11
5.8	-0.1	0.03
5.9	-0.1	-0.04
6.0	-0.1	-0.21
6.0	-0.1	-0.03
6.1	-0.1	-0.01
6.1	-0.1	-0.07
6.2	-0.1	-0.1
6.3	-0.1	-0.22
6.3	-0.1	-0.05
6.4	-0.1	-0.05
6.5	-0.1	-0.09
6.5	-0.1	-0.32
6.6	-0.1	0.08
6.7	-0.1	0
6.7	-0.1	-0.04
6.8	-0.1	-0.03
6.9	-0.1	-0.56
6.9	-0.1	-0.02
7.0	-0.1	-0.07
7.1	-0.1	-0.08
7.1	-0.1	-0.05
7.2	-0.1	-0.22
7.3	-0.1	-0.06
7.3	-0.1	-0.09
7.4	-0.1	-0.06
7.5	-0.1	0.79
7.5	-0.1	-0.11
7.6	-0.1	-0.07
7.7	-0.1	-0.01
7.7	-0.1	-0.06
7.8	-0.1	0.01
7.8	-0.1	-0.03
7.9	-0.1	-0.07
8.0	-0.1	-0.06
8.0	-0.1	0.35
8.1	-0.1	-0.01
8.2	-0.1	-0.05

8.2	-0.1	-0.09
8.3	-0.1	-0.09
8.4	-0.1	0.25
8.4	-0.1	-0.07
8.5	-0.1	-0.08
8.6	-0.1	-0.07
8.6	-0.1	-0.05
8.7	-0.1	0.13
8.8	-0.1	-0.02
8.8	-0.1	-0.05
8.9	-0.1	-0.03
9.0	-0.1	-0.54
9.0	-0.1	-0.06
9.1	-0.1	-0.04
9.2	-0.1	-0.03
9.2	-0.1	-0.05
9.3	-0.1	-0.08
9.4	-0.1	-0.04
9.4	-0.1	-0.06
9.5	-0.1	-0.09
9.5	-0.1	-0.83
9.6	-0.1	0.02
9.7	-0.1	-0.06
9.7	-0.1	-0.06
9.8	-0.1	-0.05
9.9	-0.1	-0.82
9.9	-0.1	-0.07
10.0	-0.1	-0.08
10.1	-0.1	-0.07
10.1	-0.1	0
10.2	-0.1	-0.14
10.3	-0.1	-0.06
10.3	-0.1	-0.04
10.4	-0.1	-0.05
10.5	-0.1	0.89
10.5	-0.1	-0.06
10.6	-0.1	-0.05
10.7	-0.1	-0.05
10.7	-0.1	-0.1
10.8	-0.1	-0.11
10.9	-0.1	-0.01
10.9	-0.1	-0.02
11.0	-0.1	-0.08
11.1	-0.1	0.46
11.1	-0.1	-0.09

11.2	-0.1	-0.1
11.3	-0.1	-0.04
11.3	-0.1	-0.11
11.4	-0.1	0.05
11.4	-0.1	-0.05
11.5	-0.1	-0.03
11.6	-0.1	-0.06
11.6	-0.1	0.08
11.7	-0.1	0.1
11.8	-0.1	-0.06
11.8	-0.1	-0.05
11.9	-0.1	-0.05
12.0	-0.1	-0.63
12.0	-0.1	-0.06
12.1	-0.1	-0.06
12.2	-0.1	-0.05
12.2	-0.1	-0.04
12.3	-0.1	-0.05
12.4	-0.1	-0.03
12.4	-0.1	-0.09
12.5	-0.1	-0.03
12.6	-0.1	-1.62
12.6	-0.1	0.01
12.7	-0.1	-0.1
12.8	-0.1	-0.1
12.8	-0.1	-0.1
12.9	-0.1	-0.38
13.0	-0.1	-0.06
13.0	-0.1	-0.07
13.1	-0.1	-0.1
13.1	-0.1	0.62
13.2	-0.1	-0.11
13.3	-0.1	-0.07
13.3	-0.1	0
13.4	-0.1	-0.03
13.5	-0.1	0.53
13.5	-0.1	0.03
13.6	-0.1	-0.01
13.7	-0.1	-0.02
13.7	-0.1	-0.03
13.8	-0.1	0.05
13.9	-0.1	0.01
13.9	-0.1	-0.08
14.0	-0.1	-0.06
14.1	-0.1	-0.48

14.1	-0.1	-0.07
14.2	-0.1	-0.06
14.3	-0.1	-0.06
14.3	-0.1	-0.1
14.4	-0.1	-0.33
14.5	-0.1	-0.13
14.5	-0.1	-0.07
14.6	-0.1	-0.04
14.6	-0.1	-0.28
14.7	-0.1	-0.02
14.8	-0.1	-0.06
14.8	-0.1	-0.07
14.9	-0.1	-0.08
15.0	-0.1	-0.27
15.0	-0.1	-0.01
15.1	-0.1	-0.09
15.2	-0.1	-0.06
15.2	-0.1	0.04
15.3	-0.1	-0.07
15.4	-0.1	-0.08
15.4	-0.1	-0.07
15.5	-0.1	-0.04
15.6	-0.1	0.2
15.6	-0.1	-0.04
15.7	-0.1	-0.04
15.8	-0.1	-0.02
15.8	-0.1	-0.02
15.9	-0.1	0.07
16.0	-0.1	-0.02
16.0	-0.1	-0.1
16.1	-0.1	-0.14
16.2	-0.1	0.75
16.2	-0.1	-0.13
16.3	-0.1	-0.07
16.3	-0.1	-0.09
16.4	-0.1	-0.07
16.5	-0.1	0.58
16.5	-0.1	-0.04
16.6	-0.1	-0.1
16.7	-0.1	-0.1
16.7	-0.1	-0.35
16.8	-0.1	0.05
16.9	-0.1	-0.06
16.9	-0.1	-0.07
17.0	-0.1	-0.17

17.1	-0.1	-0.27
17.1	-0.1	-0.15
17.2	-0.1	-0.14
17.3	-0.1	-0.05
17.3	-0.1	-0.01
17.4	-0.1	0.13
17.5	-0.1	-0.09
17.5	-0.1	-0.01
17.6	-0.1	-0.12
17.7	-0.1	-1.38
17.7	-0.1	-0.01
17.8	-0.1	0.01
17.9	-0.1	-0.07
17.9	-0.1	-0.09
18.0	-0.1	-0.51
18.1	-0.1	-0.01
18.1	-0.1	-0.08
18.2	-0.1	-0.09
18.2	-0.1	-0.09
18.3	-0.1	0.02
18.4	-0.1	-0.07
18.4	-0.1	-0.02
18.5	-0.1	-0.08
18.6	-0.1	0.4
18.6	-0.1	0.1
18.7	-0.1	-0.06
18.8	-0.1	-0.06
18.8	-0.1	-0.02
18.9	-0.1	0
19.0	-0.1	-0.06
19.0	-0.1	0
19.1	-0.1	-0.01
19.2	-0.1	-0.06
19.2	-0.1	-0.14
19.3	-0.1	-0.01
19.4	-0.1	-0.04
19.4	-0.1	-0.04
19.5	-0.1	0.35
19.6	-0.1	-0.09
19.6	-0.1	-0.03
19.7	-0.1	-0.03
19.8	-0.1	0.16
19.8	-0.1	-0.1
19.9	-0.1	-0.06
19.9	-0.1	-0.04

20.0	-0.1	-0.12
20.1	-0.1	-0.14
20.1	-0.1	-0.02
20.2	-0.1	-0.05
20.3	-0.1	-0.07
20.3	-0.1	-0.36
20.4	-0.1	0.01
20.5	-0.1	-0.06
20.5	-0.1	-0.04
20.6	-0.1	-0.04
20.7	-0.1	0.03
20.7	-0.1	0
20.8	-0.1	-0.08
20.9	-0.1	-0.03
20.9	-0.1	-0.03
21.0	-0.1	-0.11
21.1	-0.1	0.01
21.1	-0.1	-0.06
21.2	-0.1	-0.05
21.3	-0.1	1.59
21.3	-0.1	-0.16
21.4	-0.1	-0.12
21.4	-0.1	-0.03
21.5	-0.1	-0.08
21.6	-0.1	-0.21
21.6	-0.1	-0.1
21.7	-0.1	-0.08
21.8	-0.1	-0.1
21.8	-0.1	-0.51
21.9	-0.1	0.11
22.0	-0.1	-0.03
22.0	-0.1	-0.01
22.1	-0.1	-0.12
22.2	-0.1	-0.16
22.2	-0.1	-0.03
22.3	-0.1	0.03
22.4	-0.1	-0.09
22.4	-0.1	-0.09
22.5	-0.1	-0.2
22.6	-0.1	-0.01
22.6	-0.1	-0.02
22.7	-0.1	-0.1
22.8	-0.1	0.18
22.8	-0.1	-0.1
22.9	-0.1	0

23.0	-0.1	-0.11
23.0	-0.1	-0.03
23.1	-0.1	0.17
23.1	-0.1	-0.07
23.2	-0.1	-0.04
23.3	-0.1	-0.11
23.3	-0.1	-0.85
23.4	-0.1	-0.04
23.5	-0.1	-0.02
23.5	-0.1	-0.07
23.6	-0.1	-0.06
23.7	-0.1	0.51
23.7	-0.1	-0.03
23.8	-0.1	-0.03
23.9	-0.1	-0.07
23.9	-0.1	-0.05
24.0	-0.1	0.17
24.1	-0.1	-0.01
24.1	-0.1	-0.1
24.2	-0.1	-0.08
24.3	-0.1	-0.52
24.3	-0.1	-0.02
24.4	-0.1	-0.04
24.5	-0.1	-0.02
24.5	-0.1	-0.09
24.6	-0.1	0.04
24.7	-0.1	-0.06
24.7	-0.1	-0.07
24.8	-0.1	0
24.8	-0.1	0.48
24.9	-0.1	-0.15
25.0	-0.1	-0.04
25.0	-0.1	-0.03
25.1	-0.1	-0.05
25.2	-0.1	-0.1
25.2	-0.1	-0.01
25.3	-0.1	-0.05
25.4	-0.1	-0.07
25.4	-0.1	-0.04
25.5	-0.1	-0.24
25.6	0.1	0.06
25.6	0.1	0.09
25.7	0.1	0.08
25.8	0.1	-0.23
25.8	0.1	-0.12

25.9	0.1	-0.14
26.0	0.1	0.06
26.0	0.1	0.04
26.1	0.1	0.06
26.2	0.1	0.03
26.2	0.1	0.12
26.3	0.1	0.04
26.4	0.1	-1.82
26.4	0.1	0.15
26.5	0.1	0.09
26.6	0.1	0.11
26.6	0.1	0.03
26.7	0.1	-0.35
26.7	0.1	0.09
26.8	0.1	0.06
26.9	0.1	0.02
26.9	0.1	-0.71
27.0	0.1	0.03
27.1	0.1	0.01
27.1	0.1	0.1
27.2	0.1	0.06
27.3	0.1	0.14
27.3	0.1	0.03
27.4	0.1	0.04
27.5	0.1	0.07
27.5	0.1	0.03
27.6	0.1	0.02
27.7	0.1	0.08
27.7	0.1	0.07
27.8	0.1	0.06
27.9	0.1	-0.28
27.9	0.1	0.08
28.0	0.1	0.12
28.1	0.1	0.13
28.1	0.1	0.01
28.2	0.1	0.27
28.3	0.1	0.14
28.3	0.1	0.02
28.4	0.1	-0.01
28.4	0.1	-2.79
28.5	0.1	0.05
28.6	0.1	0.07
28.6	0.1	0.07
28.7	0.1	0.05
28.8	0.1	-0.06

28.8	0.1	0.03
28.9	0.1	0.02
29.0	0.1	0.08
29.0	0.1	0.12
29.1	0.1	0.16
29.2	0.1	-0.02
29.2	0.1	0.07
29.3	0.1	0.05
29.4	0.1	0.13
29.4	0.1	0.03
29.5	0.1	0.01
29.6	0.1	0.04
29.6	0.1	0.08
29.7	0.1	-0.11
29.8	0.1	0.03
29.8	0.1	0.01
29.9	0.1	0.09
30.0	0.1	-0.46
30.0	0.1	0.08
30.1	0.1	0.08
30.1	0.1	0.07
30.2	0.1	-0.01
30.3	0.1	0.26
30.3	0.1	0.02
30.4	0.1	0.12
30.5	0.1	0.06
30.5	0.1	-0.35
30.6	0.1	0.01
30.7	0.1	0.05
30.7	0.1	0
30.8	0.1	0.08
30.9	0.1	-0.28
30.9	0.1	0.15
31.0	0.1	0.04
31.1	0.1	0.12
31.1	0.1	0.1
31.2	0.1	0.16
31.3	0.1	0.01
31.3	0.1	0.07
31.4	0.1	0.03
31.5	0.1	-1.04
31.5	0.1	0.04
31.6	0.1	-0.01
31.7	0.1	0.09
31.7	0.1	0.02

31.8	0.1	-0.1
31.8	0.1	0.04
31.9	0.1	0.01
32.0	0.1	0.04
32.0	0.1	0.71
32.1	0.1	0.2
32.2	0.1	-0.01
32.2	0.1	0.04
32.3	0.1	0.02
32.4	0.1	0.24
32.4	0.1	0.07
32.5	0.1	0.1
32.6	0.1	0.09
32.6	0.1	0.08
32.7	0.1	0.08
32.8	0.1	0.08
32.8	0.1	0.01
32.9	0.1	0
33.0	0.1	-0.03
33.0	0.1	0.01
33.1	0.1	0.1
33.2	0.1	0.03
33.2	0.1	0.07
33.3	0.1	0.14
33.4	0.1	0.08
33.4	0.1	0.05
33.5	0.1	0.1
33.5	0.1	-0.81
33.6	0.1	-0.18
33.7	0.1	0.06
33.7	0.1	0.07
33.8	0.1	0.04
33.9	0.1	-0.18
33.9	0.1	0
34.0	0.1	0.04
34.1	0.1	0
34.1	0.1	0.06
34.2	0.1	0.16
34.3	0.1	-0.03
34.3	0.1	0.09
34.4	0.1	0.12
34.5	0.1	-0.06
34.5	0.1	-0.01
34.6	0.1	0.06
34.7	0.1	0.06

34.7	0.1	0
34.8	0.1	0.06
34.9	0.1	0.06
34.9	0.1	0.11
35.0	0.1	0.06
35.0	0.1	-1.68
35.1	0.1	0.08
35.2	0.1	0.08
35.2	0.1	0.03
35.3	0.1	0.06
35.4	0.1	-0.24
35.4	0.1	0
35.5	0.1	0.1
35.6	0.1	0.06
35.6	0.1	0.08
35.7	0.1	-0.02
35.8	0.1	0.02
35.8	0.1	0.05
35.9	0.1	0.06
36.0	0.1	0.26
36.0	0.1	0.14
36.1	0.1	0.09
36.2	0.1	0.04
36.2	0.1	0.01
36.3	0.1	-0.02
36.4	0.1	0.13
36.4	0.1	0.11
36.5	0.1	0.09
36.6	0.1	0.6
36.6	0.1	-0.08
36.7	0.1	0.01
36.7	0.1	0.03
36.8	0.1	0.06
36.9	0.1	0.05
36.9	0.1	0.03
37.0	0.1	0.11
37.1	0.1	0.11
37.1	0.1	-0.57
37.2	0.1	0.23
37.3	0.1	0.13
37.3	0.1	0.01
37.4	0.1	0.04
37.5	0.1	-0.38
37.5	0.1	-0.02
37.6	0.1	0.04

37.7	0.1	0
37.7	0.1	0.06
37.8	0.1	-0.22
37.9	0.1	0
37.9	0.1	0.02
38.0	0.1	0.01
38.1	0.1	-0.02
38.1	0.1	-0.01
38.2	0.1	0.05
38.2	0.1	0.02
38.3	0.1	0.05
38.4	0.1	0.37
38.4	0.1	0.15
38.5	0.1	0.08
38.6	0.1	0.01
38.6	0.1	-0.52
38.7	0.1	0.03
38.8	0.1	0.05
38.8	0.1	0.09
38.9	0.1	0.04
39.0	0.1	0.01
39.0	0.1	-0.03
39.1	0.1	-0.01
39.2	0.1	0.02
39.2	0.1	0.05
39.3	0.1	0.17
39.4	0.1	0.03
39.4	0.1	0.04
39.5	0.1	0.03
39.6	0.1	-0.43
39.6	0.1	0.1
39.7	0.1	0.1
39.8	0.1	0.04
39.8	0.1	0.02
39.9	0.1	-0.04
39.9	0.1	0.06
40.0	0.1	0.05
40.1	0.1	0.04
40.1	0.1	1.32
40.2	0.1	0.14
40.3	0.1	0.04
40.3	0.1	0.04
40.4	0.1	0.02
40.5	0.1	0.61
40.5	0.1	0.12

40.6	0.1	0.08
40.7	0.1	0.07
40.7	0.1	0.01
40.8	0.1	-0.12
40.9	0.1	0.01
40.9	0.1	0.01
41.0	0.1	0.07
41.1	0.1	0.15
41.1	0.1	-0.02
41.2	0.1	0.06
41.3	0.1	0.05
41.3	0.1	0.07
41.4	0.1	0.17
41.5	0.1	0.05
41.5	0.1	0.04
41.6	0.1	0.06
41.7	0.1	0.34
41.7	0.1	0.11
41.8	0.1	0.05
41.8	0.1	0.05
41.9	0.1	0.09
42.0	0.1	-0.09
42.0	0.1	0
42.1	0.1	0.05
42.2	0.1	0.01
42.2	0.1	0.18
42.3	0.1	0.22
42.4	0.1	0.1
42.4	0.1	0.07
42.5	0.1	0.03
42.6	0.1	-0.1
42.6	0.1	0.12
42.7	0.1	0.12
42.8	0.1	0.05
42.8	0.1	0.06
42.9	0.1	-0.19
43.0	0.1	0.03
43.0	0.1	0.07
43.1	0.1	0.07
43.2	0.1	-0.14
43.2	0.1	0.01
43.3	0.1	0.12
43.4	0.1	0.06
43.4	0.1	0.12
43.5	0.1	0.12

43.5	0.1	0.15
43.6	0.1	0.1
43.7	0.1	0.03
43.7	0.1	0.59
43.8	0.1	0
43.9	0.1	0.12
43.9	0.1	0.07
44.0	0.1	0.03
44.1	0.1	-0.09
44.1	0.1	-0.03
44.2	0.1	0.11
44.3	0.1	0.05
44.3	0.1	0.03
44.4	0.1	0.11
44.5	0.1	0.07
44.5	0.1	0.06
44.6	0.1	0.07
44.7	0.1	0.08
44.7	0.1	0.16
44.8	0.1	0.12
44.9	0.1	0.03
44.9	0.1	0.02
45.0	0.1	-0.13
45.0	0.1	0.1
45.1	0.1	0.06
45.2	0.1	0
45.2	0.1	1.04
45.3	0.1	-0.06
45.4	0.1	0.01
45.4	0.1	0.06
45.5	0.1	0.08
45.6	0.1	0.38
45.6	0.1	0.11
45.7	0.1	0.04
45.8	0.1	0.03
45.8	0.1	0.06
45.9	0.1	-0.16
46.0	0.1	0.04
46.0	0.1	0.02
46.1	0.1	0.05
46.2	0.1	-0.11
46.2	0.1	-0.01
46.3	0.1	0
46.4	0.1	0.04
46.4	0.1	0.04

46.5	0.1	0.1
46.6	0.1	0.12
46.6	0.1	0.03
46.7	0.1	-0.02
46.7	0.1	1.57
46.8	0.1	0.11
46.9	0.1	0.04
46.9	0.1	0.03
47.0	0.1	0.05
47.1	0.1	-0.17
47.1	0.1	-0.02
47.2	0.1	0.09
47.3	0.1	0.06
47.3	0.1	0.03
47.4	0.1	-0.03
47.5	0.1	0.06
47.5	0.1	0.03
47.6	0.1	0.08
47.7	0.1	-0.27
47.7	0.1	0.17
47.8	0.1	0
47.9	0.1	0.02
47.9	0.1	0.1
48.0	0.1	0.26
48.1	0.1	-0.02
48.1	0.1	0.05
48.2	0.1	0.06
48.2	0.1	-1.16
48.3	0.1	0.01
48.4	0.1	0.11
48.4	0.1	0.05
48.5	0.1	0.02
48.6	0.1	-0.13
48.6	0.1	0.08
48.7	0.1	0.06
48.8	0.1	0.04
48.8	0.1	0.07
48.9	0.1	0.2
49.0	0.1	0.03
49.0	0.1	0.13
49.1	0.1	0.08
49.2	0.1	0.22
49.2	0.1	0.01
49.3	0.1	0.04
49.4	0.1	0.03

49.4	0.1	0.05
49.5	0.1	0.05
49.6	0.1	0.09
49.6	0.1	0.04
49.7	0.1	0.04
49.8	0.1	0.14
49.8	0.1	0.12
49.9	0.1	0.1
50.0	0.1	0.03
50.0	0.1	0.09
50.1	0.1	-0.03
50.1	0.1	0.04
50.2	0.1	0.04
50.3	0.1	0.03
50.3	0.1	-1.12
50.4	0.1	-0.06
50.5	0.1	0.07
50.5	0.1	0.07
50.6	0.1	0.05
50.7	0.1	0.21
50.7	0.1	0.05
50.8	0.1	0.06
50.9	0.1	0
50.9	0.1	0.02
51.0	0.1	0.19
51.1	0.1	0.1
51.1	0.1	0.04
51.2	0.1	0.06
51.3	0.1	-0.88

TEST TWO

Time (sec)	Theoretical Velocity (mm/s)	Actual Velocity (mm/s)
0.00	-0.1	-0.13
0.06	-0.1	-0.02
0.13	-0.1	-0.02
0.19	-0.1	-0.63
0.26	-0.1	-0.07
0.32	-0.1	-0.09
0.39	-0.1	-0.03
0.45	-0.1	-0.09
0.52	-0.1	0.02
0.58	-0.1	-0.07
0.64	-0.1	-0.05
0.71	-0.1	-0.02
0.77	-0.1	0.39
0.84	-0.1	0.04
0.90	-0.1	-0.11
0.96	-0.1	-0.09
1.03	-0.1	-0.08
1.09	-0.1	-0.33
1.16	-0.1	-0.09
1.22	-0.1	-0.06
1.29	-0.1	-0.12
1.35	-0.1	-0.08
1.42	-0.1	0.04
1.48	-0.1	-0.07
1.54	-0.1	-0.09
1.61	-0.1	-0.06
1.67	-0.1	1.17
1.74	-0.1	-0.03
1.80	-0.1	-0.03
1.87	-0.1	-0.04
1.93	-0.1	-0.04
1.99	-0.1	-0.58
2.06	-0.1	-0.12
2.12	-0.1	-0.1
2.19	-0.1	-0.07
2.25	-0.1	-0.15
2.32	-0.1	0.18
2.38	-0.1	-0.11
2.45	-0.1	-0.08
2.51	-0.1	-0.04
2.57	-0.1	0.54
2.64	-0.1	-0.05

2.70	-0.1	-0.07
2.77	-0.1	-0.05
2.83	-0.1	-0.07
2.90	-0.1	0.16
2.96	-0.1	-0.13
3.02	-0.1	-0.11
3.09	-0.1	-0.05
3.15	-0.1	-0.06
3.22	-0.1	0.05
3.28	-0.1	-0.06
3.35	-0.1	-0.13
3.41	-0.1	-0.15
3.47	-0.1	1.75
3.54	-0.1	-0.15
3.60	-0.1	-0.04
3.67	-0.1	-0.06
3.73	-0.1	-0.09
3.80	-0.1	0.17
3.86	-0.1	-0.07
3.92	-0.1	-0.06
3.99	-0.1	-0.08
4.05	-0.1	-0.05
4.12	-0.1	0.04
4.18	-0.1	-0.01
4.25	-0.1	-0.07
4.31	-0.1	-0.11
4.38	-0.1	-0.73
4.44	-0.1	-0.15
4.50	-0.1	-0.02
4.57	-0.1	-0.07
4.63	-0.1	-0.07
4.70	-0.1	0.01
4.76	-0.1	-0.01
4.83	-0.1	-0.12
4.89	-0.1	-0.08
4.95	-0.1	-0.04
5.02	-0.1	-0.08
5.08	-0.1	-0.05
5.15	-0.1	-0.09
5.21	-0.1	-0.07
5.28	-0.1	1.05
5.34	-0.1	-0.08
5.41	-0.1	-0.08
5.47	-0.1	-0.03
5.53	-0.1	-0.07

5.60	-0.1	0.08
5.66	-0.1	-0.06
5.73	-0.1	-0.1
5.79	-0.1	-0.06
5.86	-0.1	-0.06
5.92	-0.1	-0.26
5.99	-0.1	-0.06
6.05	-0.1	-0.07
6.11	-0.1	-0.02
6.18	-0.1	0.46
6.24	-0.1	-0.16
6.31	-0.1	-0.09
6.37	-0.1	-0.1
6.44	-0.1	-0.1
6.50	-0.1	-0.15
6.56	-0.1	-0.04
6.63	-0.1	-0.1
6.69	-0.1	-0.03
6.76	-0.1	-0.05
6.82	-0.1	-0.2
6.89	-0.1	-0.07
6.95	-0.1	-0.05
7.02	-0.1	-0.09
7.08	-0.1	-0.06
7.15	-0.1	-0.03
7.21	-0.1	-0.06
7.28	-0.1	-0.01
7.34	-0.1	-0.05
7.41	-0.1	0.2
7.47	-0.1	-0.07
7.54	-0.1	-0.05
7.60	-0.1	-0.06
7.67	-0.1	0.21
7.73	-0.1	-0.11
7.80	-0.1	-0.09
7.86	-0.1	-0.11
7.93	-0.1	-0.07
8.00	-0.1	0.06
8.06	-0.1	-0.09
8.13	-0.1	-0.13
8.19	-0.1	-0.1
8.26	-0.1	-0.06
8.32	-0.1	-0.26
8.39	-0.1	-0.12
8.45	-0.1	-0.1

8.52	-0.1	-0.01
8.58	-0.1	0.72
8.65	-0.1	-0.17
8.72	-0.1	-0.06
8.78	-0.1	-0.06
8.85	-0.1	-0.07
8.91	-0.1	-0.22
8.98	-0.1	-0.04
9.04	-0.1	-0.08
9.11	-0.1	-0.04
9.17	-0.1	-1.26
9.24	-0.1	-0.09
9.30	-0.1	-0.03
9.37	-0.1	-0.06
9.44	-0.1	-0.04
9.50	-0.1	-0.49
9.57	-0.1	-0.06
9.63	-0.1	-0.03
9.70	-0.1	-0.04
9.76	-0.1	0.02
9.83	-0.1	0.06
9.89	-0.1	-0.1
9.96	-0.1	-0.1
10.02	-0.1	-0.02
10.09	-0.1	0.19
10.15	-0.1	-0.12
10.22	-0.1	-0.13
10.28	-0.1	-0.07
10.35	-0.1	-0.02
10.42	-0.1	-0.12
10.48	-0.1	-0.12
10.55	-0.1	-0.05
10.61	-0.1	-0.06
10.68	-0.1	0.35
10.74	-0.1	-0.14
10.81	-0.1	-0.02
10.87	-0.1	-0.05
10.94	-0.1	-0.07
11.01	-0.1	-0.2
11.07	-0.1	-0.12
11.14	-0.1	-0.06
11.20	-0.1	-0.05
11.27	-0.1	0.48
11.33	-0.1	-0.16
11.40	-0.1	-0.12

11.46	-0.1	0.01
11.53	-0.1	-0.04
11.59	-0.1	-0.66
11.66	-0.1	-0.06
11.72	-0.1	-0.01
11.79	-0.1	-0.07
11.86	-0.1	-0.12
11.92	-0.1	-0.08
11.99	-0.1	0.02
12.05	-0.1	-0.09
12.12	-0.1	-0.14
12.18	-0.1	0.1
12.25	-0.1	0.01
12.31	-0.1	-0.06
12.38	-0.1	-0.09
12.44	-0.1	-0.1
12.51	-0.1	0.21
12.57	-0.1	-0.12
12.64	-0.1	-0.08
12.70	-0.1	-0.02
12.77	-0.1	1.08
12.83	-0.1	-0.08
12.90	-0.1	-0.07
12.97	-0.1	-0.09
13.03	-0.1	-0.07
13.10	-0.1	0.21
13.16	-0.1	-0.11
13.23	-0.1	-0.06
13.29	-0.1	-0.08
13.36	-0.1	-0.03
13.42	-0.1	-0.19
13.49	-0.1	-0.05
13.56	-0.1	-0.05
13.62	-0.1	-0.05
13.69	-0.1	0.2
13.75	-0.1	0
13.82	-0.1	-0.04
13.88	-0.1	-0.1
13.95	-0.1	-0.12
14.01	-0.1	-0.14
14.08	-0.1	-0.05
14.14	-0.1	-0.08
14.21	-0.1	-0.09
14.27	-0.1	-0.61
14.34	-0.1	-0.02

14.41	-0.1	-0.05
14.47	-0.1	-0.05
14.54	-0.1	-0.08
14.60	-0.1	-0.21
14.67	-0.1	0.01
14.73	-0.1	-0.09
14.80	-0.1	-0.08
14.86	-0.1	-0.03
14.93	-0.1	0.06
14.99	-0.1	-0.1
15.06	-0.1	-0.04
15.12	-0.1	-0.06
15.19	-0.1	0.37
15.25	-0.1	-0.14
15.32	-0.1	-0.05
15.39	-0.1	-0.06
15.45	-0.1	-0.06
15.52	-0.1	0.05
15.58	-0.1	-0.08
15.65	-0.1	-0.01
15.71	-0.1	-0.08
15.78	-0.1	1.06
15.84	-0.1	-0.21
15.91	-0.1	-0.08
15.97	-0.1	-0.01
16.04	-0.1	-0.07
16.11	-0.1	-0.12
16.17	-0.1	-0.04
16.24	-0.1	-0.04
16.30	-0.1	-0.02
16.37	-0.1	0.61
16.43	-0.1	-0.16
16.50	-0.1	-0.02
16.56	-0.1	-0.1
16.63	-0.1	-0.05
16.70	-0.1	-0.01
16.76	-0.1	-0.06
16.83	-0.1	-0.05
16.89	-0.1	-0.12
16.96	-0.1	-0.1
17.02	-0.1	-0.22
17.09	-0.1	-0.05
17.15	-0.1	-0.06
17.22	-0.1	-0.05
17.28	-0.1	0.61

17.35	-0.1	-0.06
17.42	-0.1	-0.02
17.48	-0.1	-0.1
17.55	-0.1	-0.1
17.61	-0.1	-0.16
17.68	-0.1	0.01
17.74	-0.1	-0.06
17.81	-0.1	-0.07
17.87	-0.1	-1.72
17.94	-0.1	0.05
18.00	-0.1	-0.13
18.07	-0.1	-0.08
18.13	-0.1	-0.09
18.20	-0.1	0.1
18.26	-0.1	-0.07
18.33	-0.1	-0.09
18.40	-0.1	-0.08
18.46	-0.1	-0.07
18.53	-0.1	-0.02
18.59	-0.1	-0.1
18.66	-0.1	-0.05
18.72	-0.1	0.01
18.79	-0.1	0.41
18.85	-0.1	-0.17
18.92	-0.1	-0.02
18.98	-0.1	-0.1
19.05	-0.1	-0.1
19.12	-0.1	-0.12
19.18	-0.1	-0.15
19.25	-0.1	-0.06
19.31	-0.1	-0.08
19.38	-0.1	0.55
19.44	-0.1	-0.21
19.51	-0.1	0
19.57	-0.1	-0.08
19.64	-0.1	-0.1
19.70	-0.1	-0.19
19.77	-0.1	-0.06
19.84	-0.1	-0.08
19.90	-0.1	-0.12
19.97	-0.1	0.43
20.03	-0.1	-0.32
20.10	-0.1	-0.02
20.16	-0.1	-0.04
20.23	-0.1	-0.1

20.29	-0.1	0.09
20.36	-0.1	-0.02
20.42	-0.1	-0.02
20.49	-0.1	-0.06
20.56	-0.1	-0.11
20.62	-0.1	-0.33
20.69	-0.1	0.02
20.75	-0.1	-0.08
20.82	-0.1	-0.12
20.88	-0.1	-0.83
20.95	-0.1	0.06
21.01	-0.1	-0.09
21.08	-0.1	-0.14
21.14	-0.1	-0.03
21.21	-0.1	0.33
21.27	-0.1	-0.1
21.34	-0.1	-0.13
21.41	-0.1	-0.12
21.47	-0.1	-1.67
21.54	-0.1	0.05
21.60	-0.1	-0.1
21.67	-0.1	-0.02
21.73	-0.1	-0.04
21.80	-0.1	0.24
21.86	-0.1	-0.15
21.93	-0.1	-0.1
21.99	-0.1	-0.04
22.06	-0.1	-0.03
22.12	-0.1	-0.18
22.19	-0.1	-0.13
22.25	-0.1	-0.07
22.32	-0.1	-0.05
22.39	-0.1	-0.27
22.45	-0.1	-0.17
22.52	-0.1	-0.09
22.58	-0.1	-0.05
22.65	-0.1	-0.03
22.71	-0.1	-0.41
22.78	-0.1	-0.08
22.84	-0.1	-0.12
22.91	-0.1	-0.11
22.98	-0.1	2.08
23.04	-0.1	-0.23
23.11	-0.1	-0.09
23.17	-0.1	-0.07

23.24	-0.1	-0.07
23.30	-0.1	-0.47
23.37	-0.1	-0.06
23.43	-0.1	-0.06
23.50	-0.1	-0.04
23.57	-0.1	-0.14
23.63	-0.1	-0.24
23.70	-0.1	-0.02
23.76	-0.1	-0.08
23.83	-0.1	-0.08
23.89	-0.1	-0.52
23.96	-0.1	0.03
24.02	-0.1	-0.09
24.09	-0.1	-0.05
24.15	-0.1	-0.1
24.22	-0.1	0.03
24.28	-0.1	-0.12
24.35	-0.1	-0.09
24.42	-0.1	-0.1
24.48	-0.1	-0.84
24.55	-0.1	0.04
24.61	-0.1	-0.08
24.68	-0.1	-0.18
24.74	-0.1	-0.09
24.81	-0.1	0.26
24.87	-0.1	-0.06
24.94	-0.1	-0.06
25.00	-0.1	-0.14
25.07	-0.1	0.88
25.13	-0.1	-0.02
25.20	-0.1	-0.1
25.27	-0.1	-0.09
25.33	-0.1	-0.05
25.40	-0.1	0.13
25.46	-0.1	-0.15
25.53	-0.1	-0.05
25.59	-0.1	-0.08
25.66	-0.1	-0.03
25.72	-0.1	-0.2
25.79	-0.1	-0.12
25.85	-0.1	-0.04
25.92	-0.1	-0.05
25.99	-0.1	1.22
26.05	-0.1	-0.11
26.12	-0.1	-0.06

26.18	-0.1	-0.11
26.25	-0.1	-0.09
26.31	-0.1	-0.3
26.38	-0.1	-0.13
26.44	-0.1	-0.01
26.51	-0.1	-0.11
26.58	-0.1	0
26.64	-0.1	-0.2
26.71	-0.1	-0.02
26.77	-0.1	-0.04
26.84	-0.1	-0.09
26.90	-0.1	-0.3
26.97	-0.1	-0.07
27.03	-0.1	0.01
27.10	-0.1	-0.05
27.16	-0.1	-0.08
27.23	-0.1	-0.05
27.29	-0.1	-0.05
27.36	-0.1	-0.06
27.43	-0.1	-0.1
27.49	-0.1	-0.46
27.56	-0.1	0.05
27.62	-0.1	-0.05
27.69	-0.1	-0.08
27.75	-0.1	-0.04
27.82	-0.1	-0.01
27.88	-0.1	-0.06
27.95	-0.1	-0.05
28.01	-0.1	-0.08
28.08	-0.1	1.04
28.15	-0.1	0.03
28.21	-0.1	-0.09
28.28	-0.1	-0.15
28.34	-0.1	-0.11
28.41	-0.1	0.19
28.47	-0.1	-0.13
28.54	-0.1	-0.03
28.60	-0.1	-0.04
28.67	-0.1	0.38
28.73	-0.1	-0.16
28.80	-0.1	-0.04
28.86	-0.1	-0.1
28.93	-0.1	-0.1
29.00	-0.1	0
29.06	-0.1	-0.12

29.13	-0.1	-0.1
29.19	-0.1	-0.09
29.26	-0.1	-0.12
29.32	-0.1	-0.18
29.39	-0.1	-0.1
29.45	-0.1	-0.05
29.52	-0.1	-0.02
29.58	-0.1	-0.47
29.65	0.1	-0.02
29.71	0.1	0.09
29.78	0.1	0.06
29.84	0.1	0.03
29.91	0.1	0.09
29.98	0.1	0.12
30.04	0.1	0.03
30.11	0.1	0.08
30.17	0.1	-0.32
30.24	0.1	0.2
30.30	0.1	0.05
30.37	0.1	0.04
30.43	0.1	0.04
30.50	0.1	0.22
30.56	0.1	0.15
30.63	0.1	0.09
30.70	0.1	0.06
30.76	0.1	0.08
30.83	0.1	0.29
30.89	0.1	0.05
30.96	0.1	0.05
31.02	0.1	0.08
31.09	0.1	0.44
31.15	0.1	0.05
31.22	0.1	0.04
31.29	0.1	0.09
31.35	0.1	0.12
31.42	0.1	0.04
31.48	0.1	-0.02
31.55	0.1	0.07
31.61	0.1	0.09
31.68	0.1	0.31
31.74	0.1	-0.04
31.81	0.1	0.06
31.87	0.1	0.11
31.94	0.1	0.09
32.00	0.1	-0.04

32.07	0.1	0.14
32.13	0.1	0.04
32.20	0.1	0.04
32.26	0.1	0.1
32.33	0.1	0.02
32.40	0.1	0.14
32.46	0.1	0
32.53	0.1	0.08
32.59	0.1	-0.42
32.66	0.1	0.17
32.72	0.1	0.05
32.79	0.1	0.02
32.85	0.1	0.05
32.92	0.1	0.17
32.99	0.1	0.06
33.05	0.1	0.02
33.12	0.1	0.12
33.18	0.1	-0.38
33.25	0.1	0.18
33.31	0.1	0
33.38	0.1	0.05
33.44	0.1	0.07
33.51	0.1	0.1
33.57	0.1	0.05
33.64	0.1	0.07
33.71	0.1	0.03
33.77	0.1	-0.51
33.84	0.1	0.06
33.90	0.1	0.08
33.97	0.1	0.08
34.03	0.1	0.1
34.10	0.1	0.03
34.16	0.1	0.09
34.23	0.1	0.06
34.30	0.1	0.1
34.36	0.1	0.11
34.43	0.1	0.08
34.49	0.1	0.05
34.56	0.1	0.12
34.62	0.1	0.1
34.69	0.1	0.12
34.75	0.1	0.03
34.82	0.1	0.07
34.88	0.1	0.03
34.95	0.1	0.12

35.02	0.1	0.06
35.08	0.1	0.08
35.15	0.1	0.02
35.21	0.1	0.06
35.28	0.1	0.39
35.34	0.1	0.01
35.41	0.1	0.13
35.47	0.1	0.09
35.54	0.1	0.08
35.61	0.1	0.09
35.67	0.1	0.08
35.74	0.1	0.05
35.80	0.1	0.09
35.87	0.1	0.09
35.93	0.1	0.03
36.00	0.1	0.06
36.06	0.1	0.05
36.13	0.1	0.04
36.20	0.1	-0.1
36.26	0.1	0.14
36.33	0.1	0.05
36.39	0.1	0.02
36.46	0.1	0.02
36.52	0.1	0.1
36.59	0.1	0.04
36.65	0.1	0.15
36.72	0.1	0.02
36.78	0.1	-0.47
36.85	0.1	0.03
36.91	0.1	0.05
36.98	0.1	0.04
37.05	0.1	0
37.11	0.1	0.01
37.18	0.1	0.11
37.24	0.1	0.09
37.31	0.1	0
37.37	0.1	0.08
37.44	0.1	0.05
37.50	0.1	0.03
37.57	0.1	0.08
37.63	0.1	0.02
37.70	0.1	0.24
37.77	0.1	0.04
37.83	0.1	0.07
37.90	0.1	0.15

37.96	0.1	0.08
38.03	0.1	0.13
38.09	0.1	0.05
38.16	0.1	0.06
38.22	0.1	0.09
38.29	0.1	-0.19
38.35	0.1	0.06
38.42	0.1	0.06
38.49	0.1	0.04
38.55	0.1	0.1
38.62	0.1	0.01
38.68	0.1	0.06
38.75	0.1	0.08
38.81	0.1	0.07
38.88	0.1	-0.4
38.94	0.1	0.08
39.01	0.1	0.03
39.07	0.1	0.08
39.14	0.1	0.05
39.21	0.1	-0.01
39.27	0.1	0.01
39.34	0.1	0.04
39.40	0.1	0.09
39.47	0.1	0.04
39.53	0.1	0.09
39.60	0.1	0.09
39.66	0.1	0.08
39.73	0.1	0.03
39.79	0.1	-0.41
39.86	0.1	0.12
39.93	0.1	0.03
39.99	0.1	0.06
40.06	0.1	0.07
40.12	0.1	0.06
40.19	0.1	0.07
40.25	0.1	0.03
40.32	0.1	0.14
40.38	0.1	-0.94
40.45	0.1	0.1
40.52	0.1	0.07
40.58	0.1	0.05
40.65	0.1	0.09
40.71	0.1	0.08
40.78	0.1	0.12
40.84	0.1	0.13

40.91	0.1	0.04
40.97	0.1	-1.08
41.04	0.1	0.06
41.10	0.1	0.05
41.17	0.1	0.08
41.24	0.1	0.07
41.30	0.1	-0.01
41.37	0.1	0.01
41.43	0.1	0.05
41.50	0.1	0.09
41.56	0.1	0.09
41.63	0.1	0.06
41.69	0.1	0.07
41.76	0.1	0.08
41.82	0.1	0.07
41.89	0.1	-0.23
41.95	0.1	0.1
42.02	0.1	0.08
42.09	0.1	0.08
42.15	0.1	0.07
42.22	0.1	-0.01
42.28	0.1	0.06
42.35	0.1	0.11
42.41	0.1	0.1
42.48	0.1	0.27
42.54	0.1	0.15
42.61	0.1	0.05
42.67	0.1	0.09
42.74	0.1	0.06
42.81	0.1	0
42.87	0.1	0.16
42.94	0.1	0.08
43.00	0.1	0.1
43.07	0.1	0.18
43.13	0.1	0.08
43.20	0.1	0.04
43.26	0.1	0.05
43.33	0.1	0.07
43.39	0.1	-0.46
43.46	0.1	0.03
43.53	0.1	0.06
43.59	0.1	0.06
43.66	0.1	0.04
43.72	0.1	0.06
43.79	0.1	0.08

43.85	0.1	0.04
43.92	0.1	0.06
43.98	0.1	-0.64
44.05	0.1	0.06
44.11	0.1	0.09
44.18	0.1	0.07
44.25	0.1	0.11
44.31	0.1	0
44.38	0.1	0.02
44.44	0.1	0.06
44.51	0.1	0.06
44.57	0.1	0.71
44.64	0.1	0.03
44.70	0.1	-0.01
44.77	0.1	0.09
44.83	0.1	0.05
44.90	0.1	0.23
44.96	0.1	0.04
45.03	0.1	0.09
45.10	0.1	0.07
45.16	0.1	0.08
45.23	0.1	0.07
45.29	0.1	0
45.36	0.1	0.05
45.42	0.1	0.11
45.49	0.1	-0.13
45.55	0.1	0.03
45.62	0.1	0.08
45.68	0.1	0.04
45.75	0.1	0.1
45.81	0.1	0
45.88	0.1	0.06
45.95	0.1	0.09
46.01	0.1	0.06
46.08	0.1	-0.25
46.14	0.1	0.03
46.21	0.1	0.09
46.27	0.1	0.07
46.34	0.1	0.13
46.40	0.1	-0.12
46.47	0.1	0.05
46.53	0.1	0.1
46.60	0.1	0.1
46.66	0.1	0.12
46.73	0.1	0.11

46.79	0.1	0.08
46.86	0.1	0.14
46.93	0.1	0.06
46.99	0.1	0.16
47.06	0.1	0.09
47.12	0.1	0.05
47.19	0.1	0.01
47.25	0.1	0.02
47.32	0.1	0.09
47.38	0.1	0.01
47.45	0.1	0.06
47.52	0.1	0.04
47.58	0.1	-0.37
47.65	0.1	0.11
47.71	0.1	0.09
47.78	0.1	0.1
47.84	0.1	0.06
47.91	0.1	0.19
47.97	0.1	0.1
48.04	0.1	0.09
48.10	0.1	0.06
48.17	0.1	-1.14
48.24	0.1	0.08
48.30	0.1	0.07
48.37	0.1	0.05
48.43	0.1	0.1
48.50	0.1	0.19
48.56	0.1	0.12
48.63	0.1	0.07
48.69	0.1	0.04
48.76	0.1	0.09
48.82	0.1	0.11
48.89	0.1	0.07
48.96	0.1	0.08
49.02	0.1	0.06
49.09	0.1	0.17
49.15	0.1	0.07
49.22	0.1	0.06
49.28	0.1	0.08
49.35	0.1	0.06
49.41	0.1	0.13
49.48	0.1	0.04
49.55	0.1	0.11
49.61	0.1	0.06
49.68	0.1	-0.28

49.74	0.1	-0.01
49.81	0.1	0.13
49.87	0.1	0.08
49.94	0.1	0.04
50.00	0.1	0
50.07	0.1	0.08
50.13	0.1	0.03
50.20	0.1	0.05
50.26	0.1	0.05
50.33	0.1	0.03
50.39	0.1	0.04
50.46	0.1	0
50.53	0.1	0.06
50.59	0.1	0.15
50.66	0.1	0.02
50.72	0.1	0.03
50.79	0.1	0.01
50.85	0.1	0.06
50.92	0.1	0.02
50.98	0.1	0.06
51.05	0.1	0.06
51.11	0.1	0.04
51.18	0.1	-0.46
51.24	0.1	0.1
51.31	0.1	0.1
51.38	0.1	0.05
51.44	0.1	0.04
51.51	0.1	0.21
51.57	0.1	0.04
51.64	0.1	0.1
51.70	0.1	0.04
51.77	0.1	-0.43
51.83	0.1	0.17
51.90	0.1	0.13
51.97	0.1	0.09
52.03	0.1	0.05
52.10	0.1	0.31
52.16	0.1	0.12
52.23	0.1	0.04
52.29	0.1	0.03
52.36	0.1	0.1
52.42	0.1	0.18
52.49	0.1	0.06
52.56	0.1	0.04
52.62	0.1	0.11

52.69	0.1	0.54
52.75	0.1	0.15
52.82	0.1	0.08
52.88	0.1	0.05
52.95	0.1	0.06
53.01	0.1	0.03
53.08	0.1	0.06
53.15	0.1	0.02
53.21	0.1	0.09
53.28	0.1	0.11
53.34	0.1	0.05
53.41	0.1	0.1
53.47	0.1	0.08
53.54	0.1	0.08
53.60	0.1	0.07
53.67	0.1	0.14
53.73	0.1	0.07
53.80	0.1	0.03
53.87	0.1	0.48
53.93	0.1	-0.09
54.00	0.1	0.01
54.06	0.1	0.09
54.13	0.1	0.09
54.19	0.1	-0.74
54.26	0.1	0.01
54.32	0.1	0.06
54.39	0.1	0.04
54.45	0.1	0.06
54.52	0.1	-0.06
54.58	0.1	0.05
54.65	0.1	-0.02
54.71	0.1	0.04
54.78	0.1	-0.77
54.85	0.1	0.09
54.91	0.1	0.12
54.98	0.1	0.05
55.04	0.1	0.05
55.11	0.1	0.16
55.17	0.1	0.11
55.24	0.1	0.09
55.30	0.1	0.05
55.37	0.1	-0.35
55.44	0.1	0.17
55.50	0.1	0.09
55.57	0.1	0.11

55.63	0.1	0.05
55.70	0.1	0.4
55.76	0.1	0.13
55.83	0.1	0.07
55.89	0.1	0.12
55.96	0.1	0.05
56.02	0.1	0.19
56.09	0.1	0.07
56.16	0.1	0.06
56.22	0.1	0.05
56.29	0.1	0.34
56.35	0.1	0.12
56.42	0.1	0.03
56.48	0.1	0.01
56.55	0.1	0.02
56.61	0.1	-0.01
56.68	0.1	0.07
56.74	0.1	0.08
56.81	0.1	0.03
56.88	0.1	-0.58
56.94	0.1	0.01
57.01	0.1	0.07
57.07	0.1	0.11
57.14	0.1	0.04
57.20	0.1	-0.11
57.27	0.1	0.09
57.33	0.1	0.03
57.40	0.1	0.03
57.46	0.1	0.19
57.53	0.1	-0.02
57.59	0.1	0.06
57.66	0.1	0.03
57.73	0.1	0.09
57.79	0.1	0.16
57.86	0.1	0.05
57.92	0.1	0.04
57.99	0.1	0.05
58.05	0.1	0.07
58.12	0.1	0.1
58.18	0.1	0.09
58.25	0.1	0.05
58.31	0.1	0.07
58.38	0.1	-0.2
58.44	0.1	0.11
58.51	0.1	0.11

58.58	0.1	0.04
58.64	0.1	0.09
58.71	0.1	0.39
58.77	0.1	0.06
58.84	0.1	0.11
58.90	0.1	0.1
58.97	0.1	-1.07
59.03	0.1	0.02
59.10	0.1	0.08
59.17	0.1	0.1
59.23	0.1	0.11
59.30	0.1	0.5
59.36	0.1	0.03
59.43	0.1	0.04
59.49	0.1	0.03
59.56	0.1	0.03
59.62	0.1	0.13
59.69	0.1	0.08
59.76	0.1	0.04
59.82	0.1	0.07
59.89	0.1	0.08
59.95	0.1	0.05
60.02	0.1	0.11

TEST THREE

Time (sec)	Theoretical Velocity (mm/s)	Actual Velocity (mm/s)
0.00	-0.1	0
0.06	-0.1	-0.02
0.13	-0.1	0.88
0.19	-0.1	-0.13
0.26	-0.1	-0.02
0.32	-0.1	-0.05
0.39	-0.1	0.02
0.45	-0.1	0.18
0.51	-0.1	0.03
0.58	-0.1	-0.07
0.64	-0.1	-0.01
0.71	-0.1	-0.04
0.77	-0.1	0.08
0.83	-0.1	-0.05
0.90	-0.1	-0.06
0.96	-0.1	-0.03
1.03	-0.1	1.78
1.09	-0.1	-0.07
1.16	-0.1	0.01
1.22	-0.1	-0.03
1.28	-0.1	0
1.35	-0.1	0.22
1.41	-0.1	-0.02
1.48	-0.1	-0.06
1.54	-0.1	-0.01
1.60	-0.1	-0.1
1.67	-0.1	0
1.73	-0.1	-0.03
1.80	-0.1	-0.03
1.86	-0.1	-0.05
1.93	-0.1	1.53
1.99	-0.1	-0.11
2.06	-0.1	-0.04
2.12	-0.1	-0.05
2.18	-0.1	-0.02
2.25	-0.1	0.19
2.31	-0.1	-0.01
2.38	-0.1	-0.07
2.44	-0.1	0.03
2.50	-0.1	-0.05
2.57	-0.1	0.17
2.63	-0.1	-0.01

2.70	-0.1	-0.04
2.76	-0.1	-0.03
2.83	-0.1	1.5
2.89	-0.1	-0.15
2.95	-0.1	0.02
3.02	-0.1	-0.01
3.08	-0.1	0
3.15	-0.1	0.36
3.21	-0.1	-0.08
3.28	-0.1	-0.07
3.34	-0.1	-0.03
3.40	-0.1	0
3.47	-0.1	0.11
3.53	-0.1	-0.03
3.60	-0.1	0
3.66	-0.1	-0.03
3.73	-0.1	1.64
3.79	-0.1	-0.14
3.85	-0.1	-0.04
3.92	-0.1	-0.04
3.98	-0.1	-0.04
4.05	-0.1	0.31
4.11	-0.1	-0.06
4.18	-0.1	-0.04
4.24	-0.1	0.02
4.30	-0.1	0.02
4.37	-0.1	0.18
4.43	-0.1	0
4.49	-0.1	-0.03
4.56	-0.1	-0.06
4.62	-0.1	1.47
4.69	-0.1	0.03
4.75	-0.1	0
4.82	-0.1	-0.01
4.88	-0.1	-0.04
4.95	-0.1	-0.27
5.01	-0.1	-0.08
5.07	-0.1	-0.05
5.14	-0.1	-0.04
5.20	-0.1	-0.04
5.27	-0.1	0.18
5.33	-0.1	-0.06
5.40	-0.1	-0.04
5.46	-0.1	-0.02
5.52	-0.1	0.94

5.59	-0.1	-0.01
5.65	-0.1	0
5.72	-0.1	-0.04
5.78	-0.1	0
5.85	-0.1	-0.01
5.91	-0.1	-0.11
5.98	-0.1	-0.04
6.04	-0.1	-0.02
6.10	-0.1	-0.06
6.17	-0.1	0.12
6.23	-0.1	-0.01
6.30	-0.1	-0.05
6.36	-0.1	-0.02
6.43	-0.1	-0.71
6.49	-0.1	-0.15
6.56	-0.1	-0.04
6.62	-0.1	-0.02
6.68	-0.1	0
6.75	-0.1	0.19
6.81	-0.1	-0.13
6.88	-0.1	-0.04
6.94	-0.1	-0.02
7.00	-0.1	0
7.07	-0.1	0.21
7.13	-0.1	-0.1
7.20	-0.1	-0.07
7.26	-0.1	0
7.32	-0.1	1.57
7.39	-0.1	0.04
7.45	-0.1	-0.07
7.52	-0.1	-0.07
7.58	-0.1	-0.03
7.65	-0.1	0.02
7.71	-0.1	-0.08
7.78	-0.1	-0.08
7.84	-0.1	-0.03
7.91	-0.1	-0.02
7.97	-0.1	-0.14
8.04	-0.1	-0.08
8.10	-0.1	-0.07
8.17	-0.1	-0.05
8.23	-0.1	0.8
8.30	-0.1	-0.08
8.37	-0.1	-0.01
8.43	-0.1	-0.04

8.50	-0.1	-0.07
8.56	-0.1	-0.17
8.63	-0.1	-0.06
8.69	-0.1	-0.07
8.76	-0.1	-0.01
8.82	-0.1	0.76
8.89	-0.1	-0.04
8.96	-0.1	0.01
9.02	-0.1	-0.05
9.09	-0.1	0.02
9.15	-0.1	0.05
9.21	-0.1	-0.03
9.28	-0.1	-0.01
9.35	-0.1	0
9.41	-0.1	-0.01
9.48	-0.1	0.04
9.54	-0.1	-0.03
9.61	-0.1	-0.01
9.67	-0.1	-0.07
9.74	-0.1	0.32
9.80	-0.1	-0.05
9.87	-0.1	-0.08
9.93	-0.1	-0.08
10.00	-0.1	-0.02
10.07	-0.1	-0.13
10.13	-0.1	-0.06
10.20	-0.1	-0.09
10.26	-0.1	-0.05
10.33	-0.1	1
10.39	-0.1	-0.17
10.46	-0.1	-0.03
10.52	-0.1	-0.03
10.59	-0.1	0.01
10.65	-0.1	-0.42
10.72	-0.1	0.03
10.78	-0.1	-0.07
10.85	-0.1	-0.04
10.91	-0.1	0.01
10.98	-0.1	0.12
11.04	-0.1	-0.01
11.11	-0.1	-0.1
11.17	-0.1	-0.05
11.24	-0.1	0.4
11.31	-0.1	-0.02
11.37	-0.1	-0.07

11.44	-0.1	-0.06
11.50	-0.1	0.02
11.57	-0.1	-0.11
11.63	-0.1	-0.07
11.70	-0.1	-0.07
11.76	-0.1	-0.05
11.83	-0.1	0.9
11.89	-0.1	-0.16
11.96	-0.1	-0.04
12.03	-0.1	-0.05
12.09	-0.1	0
12.16	-0.1	-0.14
12.22	-0.1	-0.03
12.29	-0.1	-0.07
12.35	-0.1	-0.06
12.42	-0.1	0.02
12.48	-0.1	-0.1
12.55	-0.1	-0.05
12.61	-0.1	-0.01
12.68	-0.1	-0.06
12.75	-0.1	-0.18
12.81	-0.1	-0.02
12.88	-0.1	-0.06
12.94	-0.1	-0.04
13.01	-0.1	0.01
13.07	-0.1	0.04
13.14	-0.1	-0.01
13.20	-0.1	-0.07
13.27	-0.1	-0.06
13.33	-0.1	0.22
13.40	-0.1	0.02
13.46	-0.1	-0.04
13.53	-0.1	-0.1
13.59	-0.1	-0.05
13.66	-0.1	0.15
13.72	-0.1	-0.06
13.79	-0.1	0.03
13.85	-0.1	0
13.92	-0.1	0.02
13.98	-0.1	-0.04
14.05	-0.1	0.02
14.11	-0.1	0
14.18	-0.1	0.02
14.24	-0.1	0.42
14.31	-0.1	0.03

14.37	-0.1	-0.05
14.44	-0.1	0
14.50	-0.1	0.01
14.57	-0.1	-0.1
14.63	-0.1	0.05
14.70	-0.1	-0.03
14.76	-0.1	-0.05
14.83	-0.1	0.63
14.89	-0.1	-0.05
14.96	-0.1	-0.03
15.02	-0.1	-0.01
15.09	-0.1	-0.04
15.15	-0.1	-0.3
15.22	-0.1	0
15.28	-0.1	-0.05
15.35	-0.1	-0.04
15.42	-0.1	0.15
15.48	-0.1	0.04
15.54	-0.1	-0.02
15.61	-0.1	-0.03
15.68	-0.1	0.02
15.74	-0.1	0.25
15.80	-0.1	-0.08
15.87	-0.1	-0.09
15.94	-0.1	0
16.00	-0.1	-0.06
16.07	-0.1	0.01
16.13	-0.1	-0.1
16.20	-0.1	-0.04
16.26	-0.1	0
16.33	-0.1	1.23
16.39	-0.1	-0.18
16.46	-0.1	0.02
16.52	-0.1	-0.07
16.59	-0.1	0.02
16.65	-0.1	-0.19
16.72	-0.1	0.03
16.78	-0.1	-0.05
16.85	-0.1	-0.07
16.91	-0.1	-0.04
16.98	-0.1	-0.02
17.05	-0.1	-0.01
17.11	-0.1	-0.03
17.18	-0.1	-0.04
17.24	-0.1	-0.12

17.31	-0.1	-0.03
17.37	-0.1	-0.03
17.44	-0.1	-0.02
17.50	-0.1	-0.08
17.57	-0.1	0.28
17.64	-0.1	-0.12
17.70	-0.1	-0.01
17.77	-0.1	-0.01
17.83	-0.1	-0.44
17.90	-0.1	-0.02
17.96	-0.1	-0.07
18.03	-0.1	0.03
18.09	-0.1	0.03
18.16	-0.1	0.06
18.22	-0.1	-0.07
18.29	-0.1	-0.04
18.35	-0.1	-0.09
18.42	-0.1	0.41
18.48	-0.1	-0.17
18.55	-0.1	-0.04
18.61	-0.1	0.01
18.68	-0.1	0
18.74	-0.1	-0.93
18.81	-0.1	0.03
18.87	-0.1	-0.03
18.94	-0.1	0.02
19.00	-0.1	0.01
19.07	-0.1	0.21
19.13	-0.1	-0.08
19.20	-0.1	-0.01
19.26	-0.1	-0.03
19.33	-0.1	0.72
19.39	-0.1	-0.09
19.46	-0.1	-0.06
19.53	-0.1	-0.07
19.59	-0.1	-0.07
19.66	-0.1	0.09
19.72	-0.1	-0.1
19.79	-0.1	0.03
19.85	-0.1	0
19.92	-0.1	-0.26
19.98	-0.1	-0.19
20.05	-0.1	0.06
20.11	-0.1	0.01
20.18	-0.1	-0.04

20.24	-0.1	-0.82
20.31	-0.1	0.07
20.37	-0.1	-0.08
20.44	-0.1	-0.03
20.50	-0.1	-0.03
20.57	-0.1	0.21
20.63	-0.1	-0.1
20.70	-0.1	-0.06
20.76	-0.1	0
20.83	-0.1	0.83
20.90	-0.1	-0.14
20.96	-0.1	-0.02
21.03	-0.1	-0.04
21.09	-0.1	-0.01
21.16	-0.1	0.08
21.22	-0.1	-0.08
21.29	-0.1	0.04
21.35	-0.1	0
21.42	-0.1	-0.24
21.48	-0.1	-0.17
21.55	-0.1	-0.01
21.61	-0.1	0
21.68	-0.1	-0.05
21.74	-0.1	-0.33
21.81	-0.1	-0.02
21.88	-0.1	0
21.94	-0.1	-0.03
22.01	-0.1	-0.01
22.07	-0.1	0.06
22.14	-0.1	-0.04
22.20	-0.1	-0.12
22.27	-0.1	-0.1
22.33	-0.1	1.15
22.40	-0.1	0.09
22.46	-0.1	-0.06
22.53	-0.1	-0.05
22.59	-0.1	-0.03
22.66	-0.1	0.43
22.72	-0.1	-0.09
22.79	-0.1	-0.05
22.86	-0.1	-0.02
22.92	-0.1	0
22.99	-0.1	0.05
23.05	-0.1	-0.12
23.12	-0.1	-0.01

23.18	-0.1	-0.03
23.25	-0.1	0.08
23.31	-0.1	-0.12
23.38	-0.1	0.02
23.44	-0.1	0.01
23.51	-0.1	-0.04
23.57	-0.1	0.03
23.64	-0.1	0.01
23.70	-0.1	-0.02
23.77	-0.1	-0.03
23.83	-0.1	-0.79
23.90	-0.1	0.08
23.96	-0.1	-0.06
24.03	-0.1	-0.09
24.09	-0.1	-0.05
24.16	-0.1	0.29
24.22	-0.1	-0.12
24.29	-0.1	-0.05
24.35	-0.1	-0.05
24.42	-0.1	0.28
24.48	-0.1	-0.05
24.55	-0.1	-0.02
24.62	-0.1	-0.06
24.68	-0.1	0.02
24.75	-0.1	-0.66
24.81	-0.1	-0.1
24.88	-0.1	-0.05
24.94	-0.1	0.02
25.01	-0.1	-0.07
25.07	-0.1	-0.26
25.14	-0.1	0.04
25.20	-0.1	-0.03
25.27	-0.1	0
25.33	-0.1	-0.95
25.40	-0.1	-0.01
25.46	-0.1	-0.04
25.53	-0.1	-0.06
25.60	-0.1	0
25.66	-0.1	0.22
25.72	-0.1	-0.03
25.79	-0.1	-0.07
25.86	-0.1	0
25.92	-0.1	0.65
25.99	-0.1	0
26.05	-0.1	0

26.12	-0.1	0.01
26.18	-0.1	-0.08
26.25	-0.1	0.16
26.31	-0.1	-0.12
26.38	-0.1	0.02
26.44	-0.1	0.02
26.51	-0.1	-0.06
26.57	-0.1	-0.2
26.64	-0.1	0.03
26.70	-0.1	-0.04
26.77	-0.1	-0.01
26.83	-0.1	-0.56
26.90	-0.1	0.05
26.96	-0.1	-0.01
27.03	-0.1	-0.09
27.09	-0.1	-0.11
27.16	-0.1	0.33
27.22	-0.1	-0.08
27.29	-0.1	-0.04
27.36	-0.1	-0.05
27.42	-0.1	1.14
27.49	-0.1	0
27.55	-0.1	-0.09
27.62	-0.1	-0.02
27.68	-0.1	0
27.75	-0.1	0.34
27.81	-0.1	-0.08
27.88	-0.1	-0.04
27.94	-0.1	-0.05
28.01	-0.1	0.02
28.07	-0.1	-0.17
28.14	-0.1	-0.08
28.20	-0.1	-0.03
28.27	-0.1	-0.03
28.34	-0.1	1.15
28.40	-0.1	-0.15
28.47	-0.1	-0.07
28.53	-0.1	-0.02
28.60	-0.1	0.02
28.66	-0.1	-0.35
28.73	-0.1	0.04
28.79	-0.1	-0.01
28.86	-0.1	-0.02
28.92	-0.1	-0.42
28.99	-0.1	0.03

29.05	-0.1	0
29.12	-0.1	-0.03
29.18	-0.1	-0.08
29.25	-0.1	0.16
29.31	-0.1	0
29.38	-0.1	-0.04
29.44	-0.1	0.01
29.51	-0.1	-0.04
29.57	-0.1	0.08
29.64	-0.1	0
29.70	-0.1	-0.04
29.77	0.1	0.05
29.83	0.1	-0.29
29.90	0.1	0.02
29.96	0.1	0.05
30.03	0.1	0.02
30.10	0.1	0.08
30.16	0.1	0.21
30.23	0.1	0.15
30.29	0.1	0.03
30.36	0.1	0
30.42	0.1	-0.95
30.49	0.1	0.14
30.55	0.1	-0.04
30.62	0.1	0.02
30.68	0.1	0.05
30.75	0.1	0.15
30.81	0.1	0.04
30.88	0.1	0
30.95	0.1	0.03
31.01	0.1	0.02
31.08	0.1	0.11
31.14	0.1	-0.03
31.21	0.1	0.03
31.27	0.1	-0.02
31.34	0.1	-0.11
31.40	0.1	0.06
31.47	0.1	0.04
31.53	0.1	0.04
31.60	0.1	0.01
31.66	0.1	-0.26
31.73	0.1	0.13
31.79	0.1	0.04
31.86	0.1	0.02
31.92	0.1	-0.27

31.99	0.1	0.11
32.05	0.1	0.08
32.12	0.1	-0.01
32.18	0.1	0.03
32.25	0.1	0.31
32.32	0.1	0.01
32.38	0.1	-0.01
32.45	0.1	0.04
32.51	0.1	0.04
32.58	0.1	0.03
32.64	0.1	-0.05
32.71	0.1	0.05
32.77	0.1	0.03
32.84	0.1	0.38
32.90	0.1	-0.08
32.97	0.1	0.08
33.03	0.1	0.05
33.10	0.1	0.01
33.16	0.1	-0.05
33.23	0.1	0.11
33.29	0.1	-0.01
33.36	0.1	0.02
33.42	0.1	-1
33.49	0.1	0.07
33.56	0.1	-0.01
33.62	0.1	0.04
33.69	0.1	0.03
33.75	0.1	0.29
33.82	0.1	-0.01
33.88	0.1	0.02
33.95	0.1	-0.01
34.01	0.1	0
34.08	0.1	-0.15
34.14	0.1	0.09
34.21	0.1	0.02
34.27	0.1	0.01
34.34	0.1	-0.27
34.40	0.1	0.1
34.47	0.1	0.02
34.53	0.1	0.01
34.60	0.1	0.04
34.66	0.1	-0.02
34.73	0.1	0.04
34.79	0.1	0
34.86	0.1	0.06

34.92	0.1	0.03
34.99	0.1	0.1
35.05	0.1	0.05
35.12	0.1	0.03
35.19	0.1	0.01
35.25	0.1	0.06
35.32	0.1	-0.01
35.38	0.1	0.1
35.45	0.1	0.01
35.51	0.1	0
35.58	0.1	0
35.64	0.1	0
35.71	0.1	0.08
35.77	0.1	0.03
35.84	0.1	0.29
35.90	0.1	0.05
35.97	0.1	0.04
36.03	0.1	0.06
36.10	0.1	-0.04
36.16	0.1	0
36.23	0.1	0.02
36.29	0.1	0.02
36.36	0.1	0.06
36.43	0.1	-0.78
36.49	0.1	0.08
36.56	0.1	-0.01
36.62	0.1	-0.01
36.69	0.1	0.07
36.75	0.1	0.14
36.82	0.1	0.01
36.88	0.1	0.09
36.95	0.1	0.01
37.01	0.1	0.03
37.08	0.1	0.06
37.14	0.1	0.06
37.21	0.1	0.05
37.28	0.1	0.06
37.34	0.1	0.08
37.41	0.1	0.02
37.47	0.1	0.12
37.54	0.1	0.01
37.60	0.1	0
37.67	0.1	-0.01
37.73	0.1	0.09
37.80	0.1	-0.01

37.86	0.1	0.03
37.93	0.1	0.53
37.99	0.1	0.03
38.06	0.1	0
38.12	0.1	0.06
38.19	0.1	0.09
38.25	0.1	-0.24
38.32	0.1	0.09
38.38	0.1	-0.01
38.45	0.1	0.05
38.51	0.1	0
38.58	0.1	0.11
38.65	0.1	0
38.71	0.1	0.03
38.78	0.1	0.02
38.84	0.1	-0.33
38.91	0.1	0.01
38.97	0.1	0.04
39.04	0.1	-0.01
39.10	0.1	0.07
39.17	0.1	0.05
39.23	0.1	-0.01
39.30	0.1	-0.01
39.36	0.1	0.05
39.43	0.1	0.21
39.49	0.1	0.05
39.56	0.1	0.02
39.62	0.1	0.02
39.69	0.1	0.03
39.76	0.1	-0.29
39.82	0.1	0.07
39.89	0.1	0.04
39.95	0.1	0.07
40.02	0.1	0.28
40.08	0.1	0.08
40.15	0.1	-0.01
40.21	0.1	-0.02
40.28	0.1	0.06
40.34	0.1	0.28
40.41	0.1	0.01
40.47	0.1	0.08
40.54	0.1	0.08
40.60	0.1	0.07
40.67	0.1	0.12
40.74	0.1	0.03

40.80	0.1	0.09
40.87	0.1	0.02
40.93	0.1	-0.56
41.00	0.1	-0.05
41.06	0.1	0.06
41.13	0.1	0
41.19	0.1	0.03
41.26	0.1	0.03
41.32	0.1	0.07
41.39	0.1	0.01
41.45	0.1	0.01
41.52	0.1	0.45
41.59	0.1	-0.05
41.65	0.1	0.05
41.72	0.1	0.03
41.78	0.1	0.06
41.85	0.1	-0.07
41.91	0.1	0.11
41.98	0.1	0.01
42.04	0.1	0.03
42.11	0.1	0.07
42.17	0.1	0.02
42.24	0.1	0.06
42.30	0.1	0.11
42.37	0.1	0.04
42.44	0.1	-0.75
42.50	0.1	0.08
42.57	0.1	-0.02
42.63	0.1	0.1
42.70	0.1	0.04
42.76	0.1	-0.02
42.83	0.1	0.03
42.89	0.1	0.04
42.96	0.1	0.04
43.02	0.1	-1.47
43.09	0.1	0.06
43.15	0.1	0.06
43.22	0.1	0.09
43.28	0.1	0.05
43.35	0.1	0.28
43.42	0.1	-0.02
43.48	0.1	0.01
43.55	0.1	0.05
43.61	0.1	0.01
43.68	0.1	-0.06

43.74	0.1	0.08
43.81	0.1	0.05
43.87	0.1	0.05
43.94	0.1	0.52
44.00	0.1	0.01
44.07	0.1	0.02
44.13	0.1	0.06
44.20	0.1	0
44.27	0.1	-0.07
44.33	0.1	0.07
44.40	0.1	0
44.46	0.1	0.01
44.53	0.1	-1.28
44.59	0.1	0.09
44.66	0.1	-0.01
44.72	0.1	0.04
44.79	0.1	0.1
44.85	0.1	0.03
44.92	0.1	0.03
44.98	0.1	0.03
45.05	0.1	0.01
45.11	0.1	0
45.18	0.1	0.11
45.24	0.1	0.01
45.31	0.1	0.05
45.38	0.1	-0.03
45.44	0.1	0.03
45.51	0.1	-0.04
45.57	0.1	0.06
45.64	0.1	0
45.70	0.1	0.03
45.77	0.1	-0.12
45.83	0.1	0.08
45.90	0.1	0.04
45.96	0.1	0
46.03	0.1	-0.66
46.09	0.1	0.01
46.16	0.1	0.1
46.22	0.1	-0.01
46.29	0.1	0.03
46.35	0.1	-0.27
46.42	0.1	0.04
46.48	0.1	0.06
46.55	0.1	0.07
46.61	0.1	-0.01

46.68	0.1	0.13
46.74	0.1	0
46.81	0.1	0.05
46.88	0.1	0.05
46.94	0.1	0
47.01	0.1	0.04
47.07	0.1	0.04
47.14	0.1	0.01
47.20	0.1	0
47.27	0.1	0.18
47.33	0.1	0.05
47.40	0.1	0.02
47.46	0.1	0.08
47.53	0.1	-0.3
47.59	0.1	0.1
47.66	0.1	0.08
47.73	0.1	0.03
47.79	0.1	0.1
47.86	0.1	-0.06
47.92	0.1	0.07
47.99	0.1	0.03
48.05	0.1	0.03
48.12	0.1	-0.13
48.18	0.1	-0.05
48.25	0.1	0.04
48.31	0.1	0.02
48.38	0.1	0
48.44	0.1	-0.31
48.51	0.1	0.01
48.57	0.1	-0.03
48.64	0.1	0.07
48.70	0.1	0.01
48.77	0.1	-0.04
48.83	0.1	0.01
48.90	0.1	0.01
48.97	0.1	0.05
49.03	0.1	0.17
49.10	0.1	0.03
49.16	0.1	0.03
49.23	0.1	0.04
49.29	0.1	0.05
49.36	0.1	0.11
49.42	0.1	0.01
49.49	0.1	0.05
49.55	0.1	0

49.62	0.1	-0.45
49.69	0.1	0.02
49.75	0.1	0
49.82	0.1	0.03
49.88	0.1	0.05
49.95	0.1	0.07
50.01	0.1	0.05
50.08	0.1	0.03
50.14	0.1	0
50.21	0.1	0.01
50.27	0.1	0.09
50.34	0.1	0.05
50.40	0.1	0.04
50.47	0.1	0.06
50.54	0.1	0
50.60	0.1	0
50.66	0.1	0.01
50.73	0.1	0.03
50.80	0.1	0.08
50.86	0.1	-0.11
50.93	0.1	-0.01
50.99	0.1	0.04
51.06	0.1	0
51.12	0.1	-0.44
51.19	0.1	0.08
51.25	0.1	0.04
51.32	0.1	0.03
51.38	0.1	0.08
51.45	0.1	0.08
51.51	0.1	0.11
51.58	0.1	0
51.64	0.1	0.04
51.71	0.1	0.03
51.77	0.1	0.03
51.84	0.1	0
51.91	0.1	0.02
51.97	0.1	0
52.04	0.1	-0.12
52.10	0.1	-0.04
52.16	0.1	0.01
52.23	0.1	0.03
52.30	0.1	0.08
52.36	0.1	-0.2
52.43	0.1	0
52.49	0.1	0.06

52.56	0.1	0.01
52.62	0.1	-0.09
52.69	0.1	0.08
52.75	0.1	0.08
52.82	0.1	0
52.88	0.1	-0.01
52.95	0.1	0.1
53.01	0.1	0
53.08	0.1	0.07
53.14	0.1	0.01
53.21	0.1	0
53.27	0.1	-0.08
53.34	0.1	-0.01
53.40	0.1	0.01
53.47	0.1	0.08
53.53	0.1	-0.66
53.60	0.1	-0.06
53.66	0.1	0.02
53.73	0.1	0.03
53.79	0.1	0.04
53.86	0.1	0.19
53.93	0.1	0
53.99	0.1	0
54.06	0.1	0.08
54.12	0.1	-0.65
54.19	0.1	0.13
54.25	0.1	0.05
54.32	0.1	0.01
54.38	0.1	0.08
54.45	0.1	0.39
54.51	0.1	0.06
54.58	0.1	-0.01
54.64	0.1	0.04
54.71	0.1	0.05
54.77	0.1	0.07
54.84	0.1	0.05
54.91	0.1	-0.03
54.97	0.1	0.04
55.04	0.1	-0.58
55.10	0.1	-0.02
55.17	0.1	0
55.23	0.1	0.02
55.30	0.1	0.01
55.36	0.1	-0.08
55.43	0.1	0.01

55.49	0.1	0.04
55.56	0.1	0.02
55.62	0.1	-0.28
55.69	0.1	0.12
55.75	0.1	0.03
55.82	0.1	0.03
55.88	0.1	0.01
55.95	0.1	0.3
56.01	0.1	0.08
56.08	0.1	0
56.14	0.1	0.07
56.21	0.1	0.01
56.28	0.1	0.12
56.34	0.1	0.01
56.41	0.1	0.09
56.47	0.1	-0.03
56.54	0.1	1.07
56.60	0.1	0
56.67	0.1	0.01
56.73	0.1	0.02
56.80	0.1	0.05
56.86	0.1	-0.29
56.93	0.1	0.06
56.99	0.1	0
57.06	0.1	0.01
57.13	0.1	-0.04
57.19	0.1	-0.03
57.25	0.1	0.03
57.32	0.1	0
57.39	0.1	0.05
57.45	0.1	0.23
57.52	0.1	0.02
57.58	0.1	0.02
57.65	0.1	0.08
57.71	0.1	-0.01
57.78	0.1	0.17
57.84	0.1	0.06
57.91	0.1	0
57.97	0.1	0.07
58.04	0.1	0.64
58.10	0.1	0.06
58.17	0.1	0.06
58.23	0.1	0.02
58.30	0.1	0.03
58.37	0.1	0.1

58.43	0.1	0
58.50	0.1	-0.01
58.56	0.1	0.03
58.63	0.1	0.26
58.69	0.1	-0.01
58.76	0.1	0.05
58.82	0.1	0.07
58.89	0.1	0.03
58.95	0.1	0.19
59.02	0.1	0.05
59.08	0.1	0
59.15	0.1	0.03
59.21	0.1	0.02
59.28	0.1	-0.02
59.34	0.1	0.01
59.41	0.1	0
59.47	0.1	0.04
59.54	0.1	-0.28
59.61	0.1	0.07
59.67	0.1	0
59.74	0.1	0.02
59.80	0.1	0.02
59.87	0.1	0.1
59.93	0.1	0.03
60.00	0.1	0.02
60.06	0.1	0.04
60.13	0.1	0.07

APPENDIX E

STRAIN RESULTS

Steps	g	g	g		g/mm^2
50	0	0	0	0.00	0
100	0.5	0.7	0.6	0.60	0.000141471
150	1.6	1.4	1.4	1.47	0.000345818
200	4	3.7	4.6	4.10	0.000966719
250	9.8	9.9	11.1	10.27	0.002420727
300	16.6	16.4	16.6	16.53	0.003898314
350	24	25	24.6	24.53	0.005784594
400	33.5	34.4	34.8	34.23	0.00807171
450	46.2	46.9	45.9	46.33	0.01092471
500	58.8	59.7	59.8	59.43	0.014013494
550	72.2	73.5	74.3	73.33	0.017290907
600	88.4	93.3	92.6	91.43	0.021558618
650	112.2	117.2	116.7	115.37	0.027201741
700	133.2	136.5	136.1	135.27	0.031893865
750	158.3	164.4	163.5	162.07	0.038212905
800	187.5	196.3	195.7	193.17	0.045545822
850	223.5	231.2	231.1	228.60	0.053900474
900	249.9	259.6	257.6	255.70	0.06029025
950	283.1	292.2	291.1	288.80	0.068094737

Outer Area	1963.495408	Total well	4241.150082
Inner Area	1256.637061		
Total Area	706.8583471		

Consultation Meetings Attendance Form

Week	Date	Comments (if applicable)	Student's Signature	Supervisor's Signature
1	8/8	parts ordering		
2	15/8	parts arrived		
3	22/8	Expectations & Report		
4	29/8	Current progress & printing		
6	12/8	Design discussions & Progress Report.		
7	26/~~09~~	Accelerometer Testing		
8	3/10	presentation of finished product.		
10	17/10	Discussion about fixing wobbling.		
11	24/10	Discussion about additional testing		
12	31/10	Final meeting.		